Endovascular Optical Coherence Tomography Imaging in Cerebrovascular Disease

by

Christopher R. Pasarikovski, MD

A thesis submitted in conformity with the requirements
for the degree of Doctor of Philosophy

Institute of Medical Science
University of Toronto

Endovascular Optical Coherence Tomography Imaging in Cerebrovascular Disease

Christopher R. Pasarikovski

Doctor of Philosophy

Institute of Medical Sciences
University of Toronto

2021

Abstract

Neurointerventional surgery is a subspecialty focused on the diagnosis and treatment of vascular diseases of the central nervous system. The appeal of treating vascular diseases through minimally invasive techniques without the need for open surgery has led to continued technological innovation and device development. Endovascular optical coherence tomography (OCT) is the highest resolution intravascular imaging modality available, utilizing near-infrared light with a wavelength of approximately 1300 nm and excellent spatial resolution of 10μm is achievable. With near histologic resolution, OCT has been described as an optical biopsy modality. The adoption of endovascular OCT imaging in the evolving field of neurointerventional surgery seems instinctive. The goal of this doctoral thesis was to utilize OCT as an adjunct in the diagnosis and treatment of cerebrovascular diseases.

Towards that goal, preclinical animal and human investigations were performed. We assessed the feasibility of OCT imaging in quantifying vascular injury after endovascular thrombectomy (EVT) in a swine model. OCT was found to be feasible in assessing vascular injury after EVT with histological accuracy. Varying degrees of vessel wall injury occur after EVT, and residual luminal thrombus was present despite complete angiographic revascularization. Next, we designed a preclinical swine model of cerebral venous sinus thrombosis (CVST) with subsequent EVT and OCT imaging. OCT revealed that residual bridging cortical vein thrombus may be present despite complete sinus recanalization on angiography. This thrombus may be the etiology of poor clinical outcome despite technical success.

Establishing preclinical feasibility with novel findings of undetected residual thrombus allowed for research ethics board approval for human OCT imaging. OCT imaging in patients with basilar stroke was undertaken. OCT was safe and capable of producing cross-sectional images displaying evidence of endothelial injury and residual thrombus. OCT may guide future antithrombotic treatment for patients with demonstrated residual thrombus. OCT carries great promise in the future of neurointerventional surgery.

Acknowledgments

I must begin with expressing my sincerest gratitude to Dr. Victor Yang. When I first approached Dr. Yang in my third year of neurosurgical residency about pursuing a graduate degree, Dr. Yang welcomed me without hesitation and first described the technology of endovascular optical coherence tomography. Throughout my research period, Dr. Yang has been supportive in all regards. In the angiography suite, he took the time to teach me the fundamentals of catheter-based techniques and the endovascular management and treatment of neurosurgical diseases. The skills Dr. Yang taught me were essential in completing the work of this thesis, and preparing me for life as a neurosurgeon. There was never an idea that Dr. Yang rejected, and he always supported my curiosity. I can't imagine a better environment to learn, and Dr. Yang provided me with every tool and the mentorship needed to succeed. I feel incredibly lucky, and for this I will always be grateful.

My fiancée Samantha and my entire family deserve praise. Throughout my life and to this day my parents and two sisters have always supported me, and I could not have asked for a more caring family. Without them, I would not be a fraction of the person I am today. Samantha has tolerated years of my neurosurgical training and accommodated every aspect of my education, always remaining by my side, and for this I will be forever grateful.

Next, I must thank my Program Advisory Committee composed of Dr. Sandra Black and Dr. Alan Moody for their ongoing direction and advice throughout my research. We had countless

meetings and discussions about this research and overall thesis, and for that I am very thankful. Our lab members including Jerry Ku, Joel Ramjist, and Yuta Dobashi were present every step of the way during this research and they provided endless help. The work accomplished in this thesis would not have been possible without their support.

Dr. Leo da Costa and Dr. Ashish Kumar are endovascular neurosurgeons at Sunnybrook who always welcomed me in the angiography suite, and also took the time to teach me and expand my endovascular skills set, which was necessary to complete the preclinical animal models developed in this thesis. Thank you for the ongoing support.

Finally, the Surgeon-Scientist Training Program at the University of Toronto is the institution that allowed me to pursue a graduate degree during residency, and I am grateful for their support. None of this would have been possible without the SSTP. Furthermore, funding from organizations such as the Brain Aneurysm Foundation, CIHR, NSERC, and the American Academy of Neurological Surgeons allowed us to pursue these ambitious experiments.

Preface

The entirety of the work presented in this thesis was completed during my PhD studies under the supervision of Dr. Victor Yang. Three preclinical animal models will be discussed, along with human investigations. With respect to the preclinical models, I designed and carried out all animal experiments. I analyzed all angiographic and OCT imaging data and Dr. Julia Keith (neuropathologist) assisted with the histologic examination of harvested tissues. The animal experiments were done with endovascular technical assistance from Dr. Yang, along with support staff in the operating room for veterinary anesthesia and operating the OCT machine during image acquisition. For all human investigations, I designed the image acquisition protocol and wrote the research ethics board submissions. During OCT imaging in humans, I was present as an assistant to Dr. Yang (primary operator) in these procedures and analyzed all angiographic and OCT imaging subsequently.

Contents

List of Tables

List of Figures

Abbreviations

AIS	Acute ischemic stroke
AVM	Arteriovenous malformation
AOL	Arterial occlusive lesion
ASA	Aspirin
CAS	Carotid artery stenting
CTV	Computed tomography venography
CVS	Cerebral venous sinuses
CVST	Cerebral venous sinus thrombosis
DSA	Digital subtraction angiography
dOCT	Doppler OCT
dAVF	Dural arteriovenous fistula
EVT	Endovascular thrombectomy
FDA	Food and drug administration
GDC	Guglielmi detachable coil
H&E	Hematoxylin and eosin
IIH	Idiopathic intracranial hypertension

IJ	Internal jugular
ITA	Internal thoracic artery
IVUS	Intravascular ultrasound
LMWH	Low molecular weight heparin
MRV	Magnetic resonance venography
MRVW	Magnetic resonance vessel-wall
NASCET	North American Symptomatic Carotid Endarterectomy Trial
OCT	Optical coherence tomography
PCA	Posterior cerebral artery
SCA	Superficial cervical arteries
SNIS	Society of Neurointerventional Surgery
SSS	Superior sagittal sinus
TICI	Thrombolysis in cerebral infarction
UFH	Unfractionated heparin
WEB	Woven EndoBridge

Chapter 1: Doctoral Thesis Structure

1.1 Organization

The structure of this thesis will be that of a "paper format" as opposed to the traditional "continuous" structure of a doctoral thesis. The thesis begins with a general introduction to the field of cerebrovascular neurosurgery in Chapter 2, and subsequently provides an overview of the specific diseases studied in this research: acute ischemic stroke secondary to large vessel occlusion, and cerebral venous sinus imaging and thrombosis. An overview of optical coherence tomography is provided, focusing on the specific device used to conduct this research. Chapter 3 provides the general and disease specific motivation, hypothesis, and aims.

The remaining chapters are "self-contained" chapters with introductions, methods, results, and discussions based on published peer-reviewed manuscripts. Chapter 4 is a reformatted version of a manuscript published in *The Journal of Neurosurgery* (Pasarikovski et al. 2020) examining how endovascular optical coherence tomography was used to reveal endothelial injury during endovascular thrombectomy. Chapter 5 is a reformatted version of a manuscript published in *The American Journal of Neuroradiology* (Pasarikovski et al. 2020) displaying the feasibility of intravascular imaging in the cerebral venous sinuses. Chapter 6 builds on the findings in Chapter 5, and is based on a manuscript published in *The Journal of Neurosurgery* (Pasarikovski et al. 2020) examining a new model of cerebral venous sinus occlusion, thrombectomy, and subsequent optical coherence tomography imaging.

Chapter 7 extends the use of optical coherence tomography to basilar stroke patients undergoing endovascular thrombectomy and is adapted from a manuscript published in *The Journal of Neurosurgery* (Pasarikovski et al. 2019). This work also builds upon the preclinical feasibility outlined in Chapter 4.

Chapter 8 complements the discussion sections of Chapter 4-7, providing a general discussion and going beyond the specific goals achieved in each chapter, and addresses the broader views of optical coherence tomography imaging in cerebrovascular disease. This chapter is partially based on a perspective review manuscript published in *The Journal of Biomedical Optics* (Pasarikovski et al. 2019) and a review article published in *The Journal of Clinical Neuroscience* (Pasarikovski et al. 2020).

Chapter 2: General Introduction

This introductory chapter will first present the field of neurointerventional surgery and provide background on the specific vascular diseases addressed in this research. Next, endovascular optical coherence tomography is introduced, followed by the motivation to utilize this technology for the diagnosis and treatment of cerebrovascular diseases.

There are sections of this chapter that are reformatted from two publications in *The Journal of Biomedical Optics* and *The Journal of Clinical Neuroscience* reprinted with full permission:

Pasarikovski, C. R., Cardinell, J. & Yang, V. X. D. Perspective review on applications of optics in cerebral endovascular neurosurgery. *Journal of biomedical optics* **24**, 1-7. (2019).

Pasarikovski, C. R., Ku, J. C., Priola, S. M., da Costa, L. & Yang, V. X. D. Endovascular optical coherence tomography imaging in cerebrovascular disease. *Journal of clinical neuroscience : official journal of the Neurosurgical Society of Australasia* **80**, 30-37. (2020).

2.1 Neurointerventional Surgery

Neurointerventional surgery is the neurosurgical subspecialty focused on the diagnosis and treatment of vascular diseases of the central nervous system. This primarily includes cerebral aneurysms, arteriovenous malformations (AVM), dural arteriovenous fistulas (dAVF), carotid atherosclerotic disease and acute ischemic stroke (AIS) secondary to large vessel occlusions. The essence of this subspecialty is the use of minimally invasive catheter-based techniques with vascular access primarily through the radial and femoral arteries. In the era of evidence based medicine, several landmark trials have demonstrated the effectiveness of endovascular techniques for various cerebral vascular diseases. The ISAT trial in 2005 showed that endovascular aneurysmal embolization resulted in increased independent survival at 1-year when compared to open surgical clipping for ruptured brain aneurysms (Molyneux et al. 2005). The CREST trial in 2012 showed that carotid stenting was effective and safe when compared to surgical endarterectomy for carotid artery stenosis (Brott et al. 2010). Finally, for the management of stroke, the DAWN trial in 2018 revealed that endovascular thrombectomy was far superior to standard medical care even for patients 6-24 hours after stroke onset (Nogueira et al. 2018). The HERMES collaboration has revolutionized stroke care for patients (Goyal et al. 2016).

The appeal of treating vascular diseases through minimally invasive endovascular techniques without the need for open surgery has led to continued technological innovation and device development (Hopkins and Ecker 2008). The mounting evidence behind the effectiveness of endovascular treatments and the general desire toward minimally invasive procedures will likely

lead to even greater role for endovascular management in the future. Below we will review the specific cerebrovascular diseases researched in this thesis.

2.1.1 Arterial Ischemic Stroke

A stroke is defined as a focal neurological deficit attributed to a vascular cause. The most common form of stroke is ischemic stroke, occurring in approximately 80% of all stroke patients (Patel and White 2011). Stroke has become the third leading cause of disability in developed nations (Writing Group et al. 2016). Arterial ischemic strokes occur when there is a blockage in a blood vessel in the brain (Figure 2-1). The brain tissue that relies on the affected blood vessel becomes devoid of oxygen and will eventually expire, causing irreversible damage and loss of neurological function.

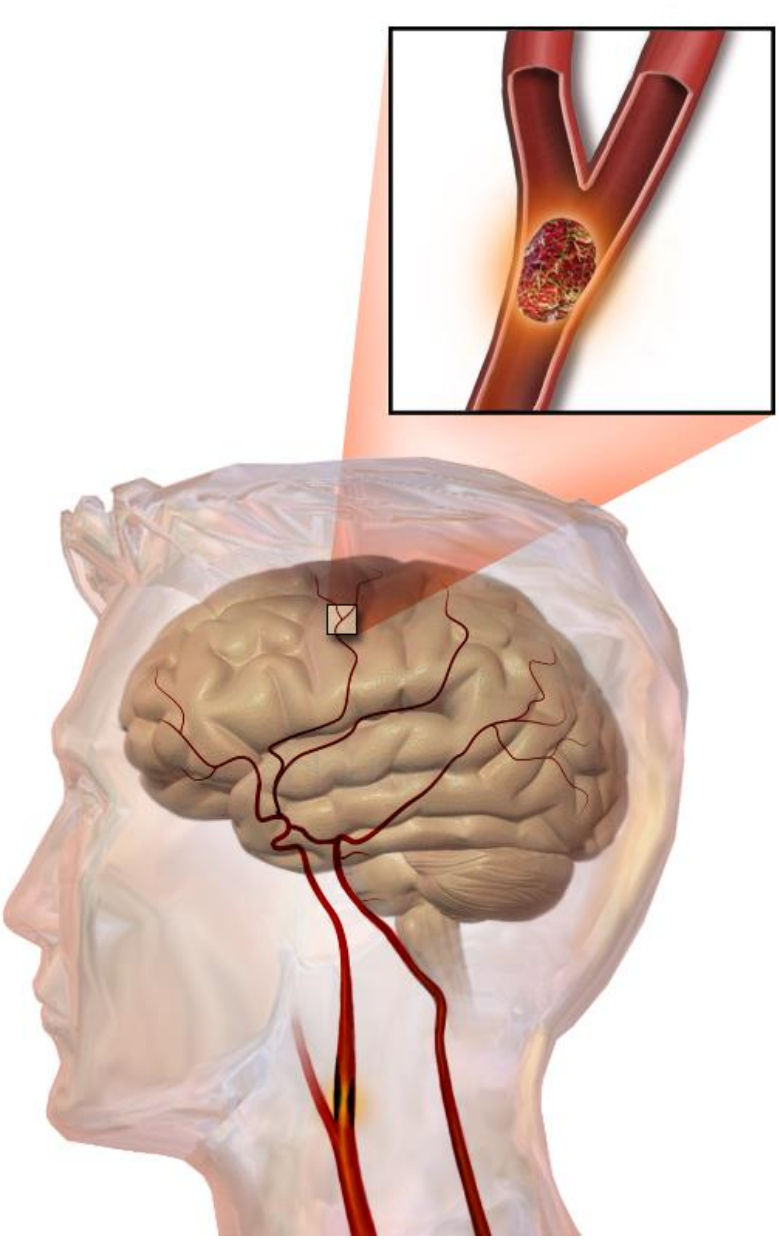

Figure 2-1: Acute Arterial Ischemic Stroke. An acute ischemic stroke occurs when a blood clot (as shown in the caption) causes a blockage in the blood vessel in the brain. The brain tissue that relies on this blood vessel will subsequently die from a lack of oxygen if the blood flow is not restored. Reprinted with permission from Blausen Medical Communications Inc.

The goal of any treatment in acute ischemic stroke is the restoration of cerebral blood flow to brain tissue at further risk of infarction. For over two decades the only proven treatment for acute ischemic stroke was the administration of intravenous alteplase within a window of 4.5 hours. More recently there has been a paradigm shift in the management of acute ischemic stroke. Five open-label randomized controlled trials have shown that intervention using second generation mechanical thrombectomy devices in patients with acute ischemic stroke secondary to proximal anterior circulation large vessel occlusion is superior to standard treatment with intravenous alteplase alone (Figure 2-2) (Berkhemer et al. 2015, Campbell et al. 2015, Goyal et al. 2015, Jovin et al. 2015, Saver et al. 2015). A meta-analysis of these trials confirmed that the rate of functional independence was significantly greater for patients treated with mechanical thrombectomy compared to standard treatment alone (Goyal, Menon et al. 2016). The current standard of care as described in the 2018 ASA/AHA guidelines recommends mechanical thrombectomy in certain patients with acute ischemic stroke secondary to proximal anterior circulation occlusion (Powers et al. 2018). It is likely that the role of mechanical thrombectomy will only continue to expand, as evident in the recent DAWN trial published in January 2018 revealing that thrombectomy was far superior to standard care even for patients 6-24 hours after stroke onset (Nogueira, Jadhav et al. 2018).

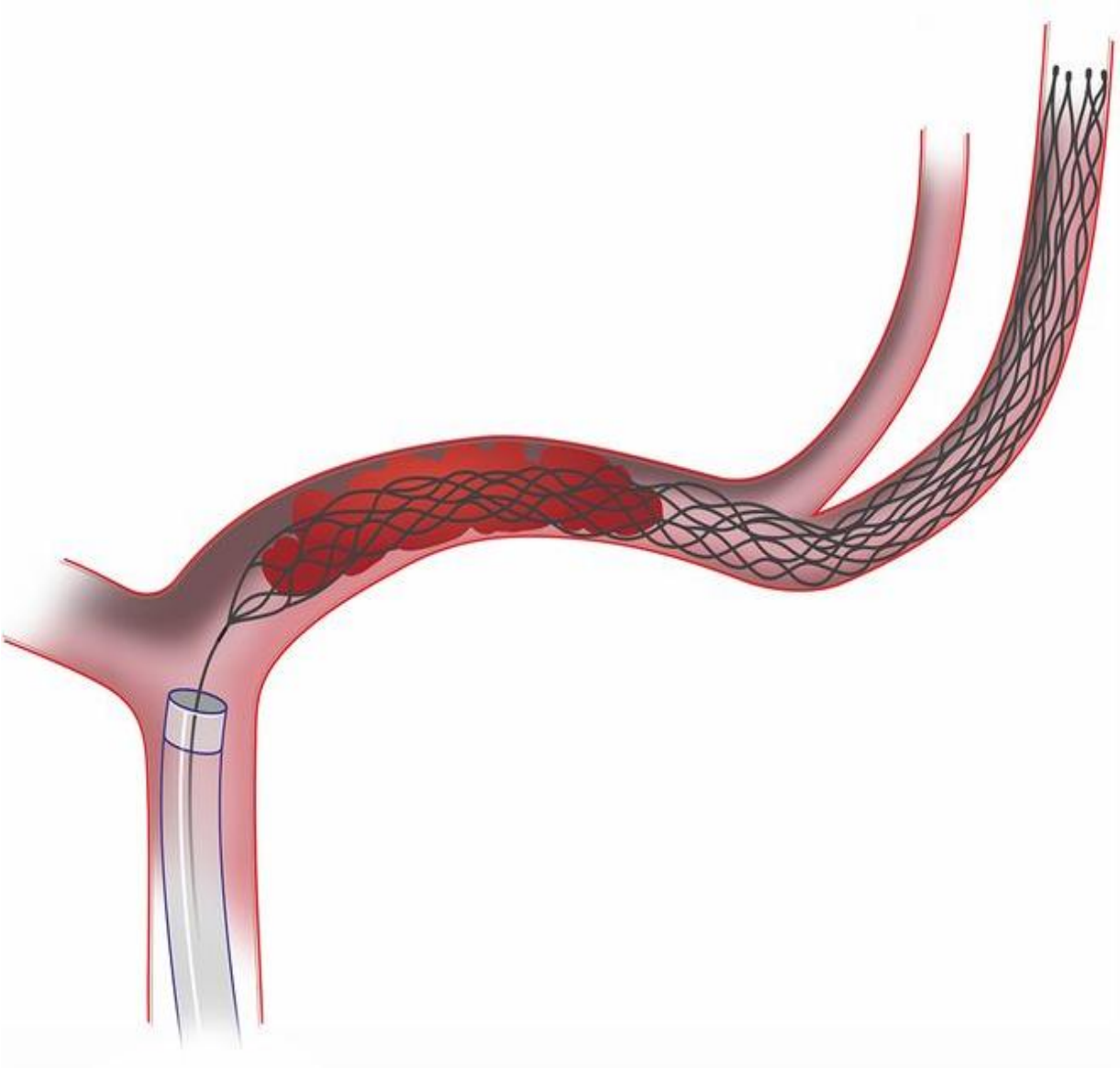

Figure 2-2: Endovascular Thrombectomy. Endovascular thrombectomy is the current standard of care for eligible patients with acute ischemic stroke secondary to large vessel occlusion in the anterior circulation. In this diagram a stent retriever is used to remove the blood clot from the blood vessel. Adapted from (Maus et al. 2019) and reprinted with permission from BMJ Publishing Group LTD.

2.1.2 Cerebral Venous Sinus Thrombosis

The cerebral venous sinuses are rigid structures located anatomically between the periosteal and meningeal layers of the dura matter. The sinuses act as reservoirs for collecting venous blood from both the deep and superficial venous system, and are lined with endothelium and elastic lamina. They lack the smooth muscle layers found in most blood vessels and have no valves. Along with the systemic venous system, thrombus can form throughout the cerebral venous sinuses or cortical veins. The incidence of Cerebral Venous Sinus Thrombosis (CVST) is approximately 15 million per year. The most common anatomic location of thrombosis is the superior sagittal sinus (SSS) accounting for 70% of all cases, followed by the transverse sinus. Anticoagulation remains the mainstay of early treatment of CVST based on randomized controlled data. However, a significant portion of patients will fail to respond to medical management and clinically deteriorate.

As described above, mechanical thrombectomy has revolutionized acute ischemic stroke treatment secondary to large vessel occlusions of the anterior circulation. Although designed to treat arterial thromboembolic disease, mechanical thrombectomy devices have also been used in CVST (Figure 2-3). In 2015 Siddiqui *et al.* conducted the largest systematic review comprising 185 patients undergoing mechanical thrombectomy for medically refractory CVST (Siddiqui et al. 2015). Overall 84% of patients had favourable outcome (mRs 0-2), however 25% of patients had no/partial recanalization of the sinus (Siddiqui, Dandapat et al. 2015). AngioJet was the most commonly used thrombectomy device in 40% of procedures. This device, along with several other devices used to treat CVST (AngioJet, Fogarty Embolectomy Device, Wires), have become

obsolete as the technology and techniques evolved considerably over the past decade. There exists limited data regarding recanalization rates and outcomes in patients with CVST undergoing thrombectomy with modern endovascular devices.

Furthermore, animal CVST models to test modern mechanical thrombectomy devices do not exist. Modern thrombectomy devices are designed for arterial thrombectomy and are not tested in the venous system, where the venous sinus wall anatomically differs considerably. Most animal CVST models surgically expose the superior sagittal sinus and thrombose the sinus via either surgical ligation, injection of thrombotic material directly into the sinus, or topical application of ferric chloride. To our knowledge, Wang *et al*. in 2010 are the only group to describe an endovascular technique to occlude the SSS in an animal model (Wang et al. 2010).

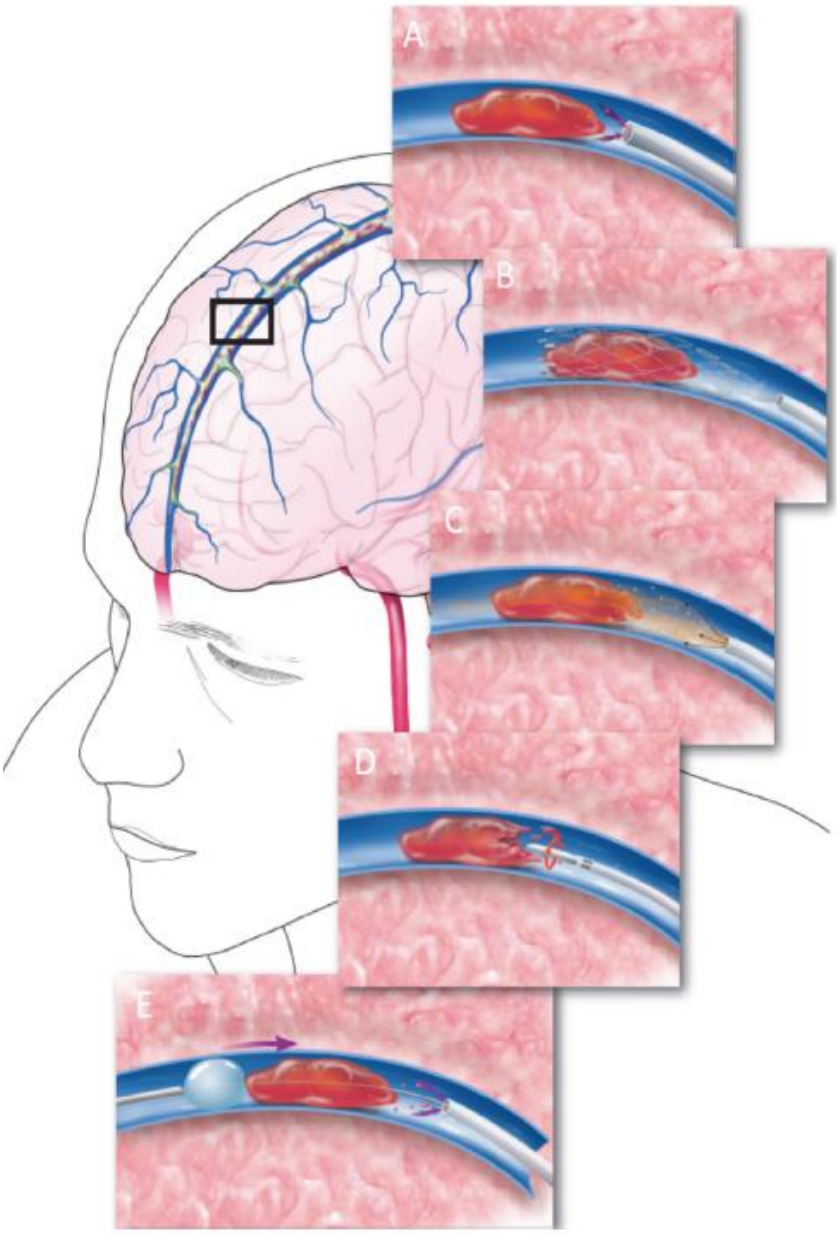

Figure 2-3: Current Thrombectomy Devices for Cerebral Venous Sinus Thrombosis. (A) Direct aspiration thrombectomy, **(B)** Stent retriever thrombectomy, **(C)** Direct thrombolysis with injection of local thrombolytics, **(D)** Clot disruption with the AngioJet catheter, and **(E)** Mechanical thrombectomy with balloon-stabilized aspiration. Adapted from (Lee et al. 2018) and reprinted with permission from BMJ Publishing Group LTD.

2.2 Optical Coherence Tomography

In 1991 a technology called optical coherence tomography (OCT) was developed by Huang *et al*. who first demonstrated the technique and its application on the human retina and coronary artery in vitro (Huang et al. 1991). The cross-sectional images generated using OCT utilize backscattered light from the vessel wall structure (Figure 2-4) (Tereshchenko et al. 2013). A swept-source laser is used with near-infrared light and a wavelength centered on 1300 nm. The underlying principal is that various biological tissues in the body have varying optical indices, and therefore different tissue layers within the vessel wall will reflect the light at different amplitudes. An optical beam splitter splits the light coming from the laser into a reference beam and a sample beam. The back-reflected light from both the sample and reference beam are combined, and will either add constructively or destructively. This intensity is then measured using a photo detector. Vessel wall spatial resolution of 10–15 μm is achievable. The depth of vessel wall penetration is approximately 3 mm. In comparison, intravascular ultrasound (IVUS) has a spatial resolution of 100 μm (approximately 10 times less resolution), and 3-Tesla MR vessel-wall imaging has a voxel size of 2.0 × 0.4 × 0.4 mm (Figure 2-5). With near histologic resolution, OCT has been described as an optical biopsy modality.

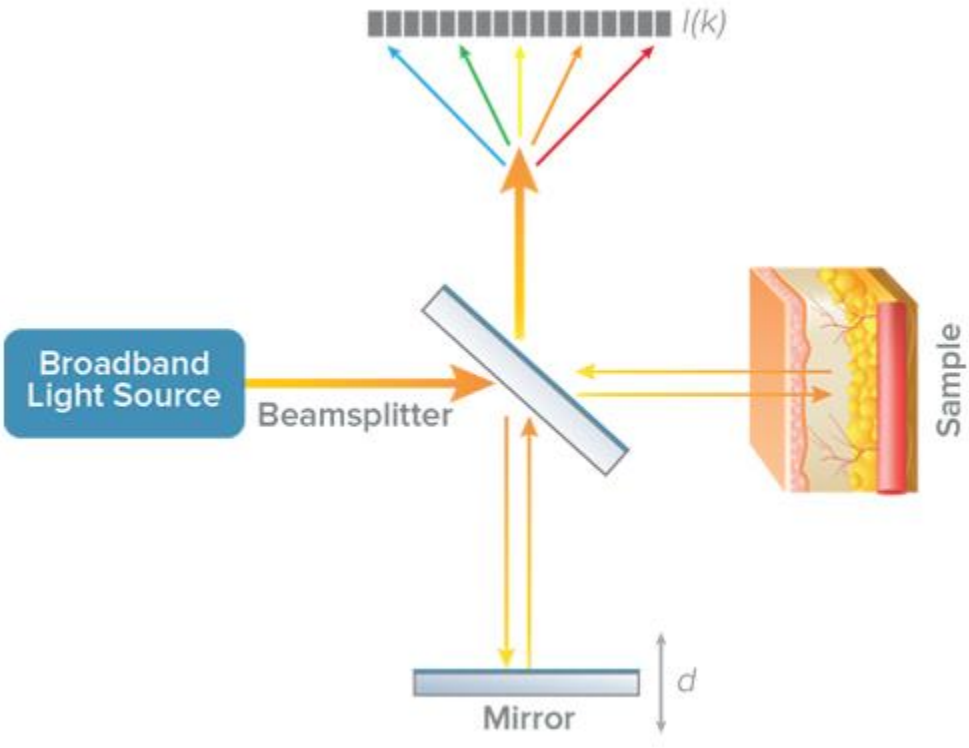

Figure 2-4: Schematic Diagram of Optical Coherence Tomography. A broadband light source is split by a beam splitter, with one beam directed towards a stationary mirror (frequency-domain optical coherence tomography) acting as the reference beam, and another toward the tissue sample.

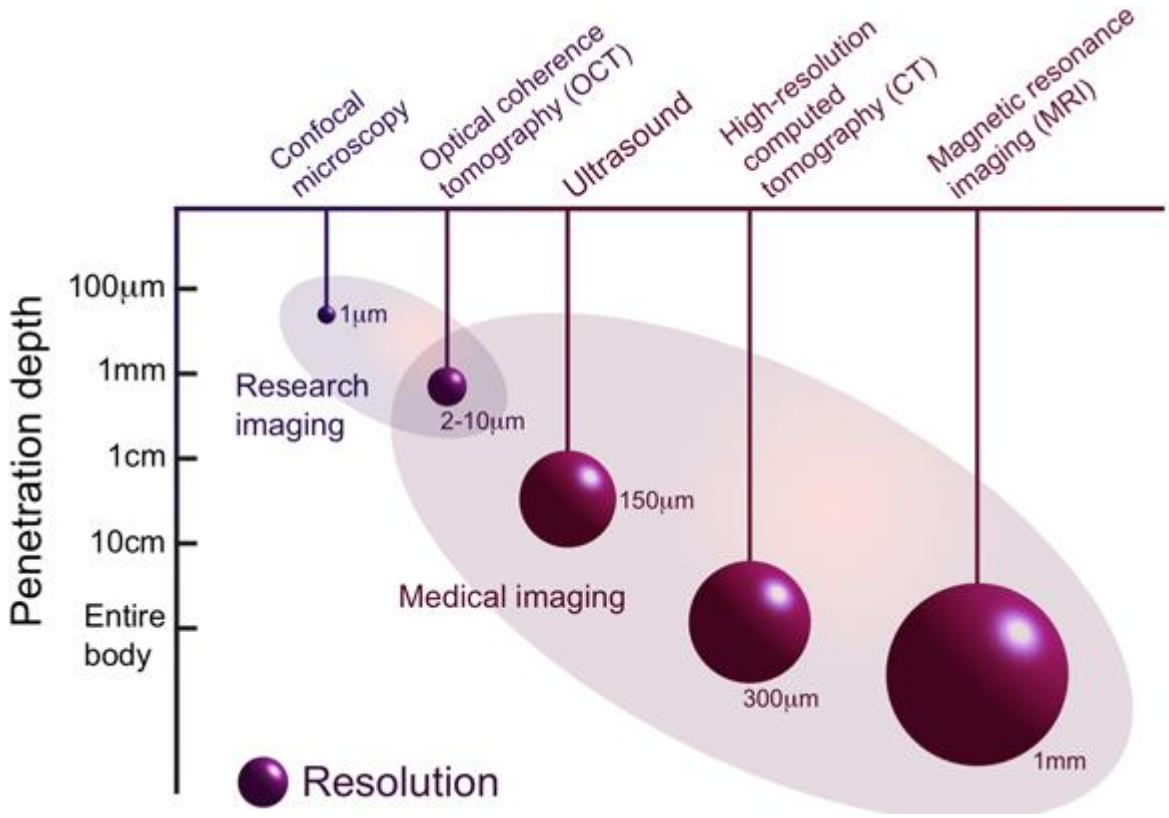

Figure 2-5: Various imaging modalities with their respective spatial resolution and depth of tissue penetration.

2.2.1 Endovascular Optical Coherence Tomography

The United States Food and Drug Administration (FDA) approved the use of endovascular OCT for the diagnosis and treatment of cardiovascular disease in 2010. The commercially available OCT catheter incorporated frequency-domain technology. Following FDA approval, the number of publications using OCT has expanded exponentially, principally in the field of interventional cardiology (Bouma et al. 2017). The unmatched spatial resolution of OCT has allowed for coronary atherosclerotic plaque composition, morphology (including plaque disruption, erosion, and thinning), neovascularization, and stent position to be studied like never before (Uemura et al. 2012). Blood vessel microanatomy such as the internal/external elastic lamina, intima, media and adventitia can be reliably visualized.

The adoption of endovascular OCT imaging in the evolving field of neurointerventional surgery seems instinctive. As observed in cardiology, the ability to visualize the luminal environment and anatomy, along with the stent-vessel interaction could be of great utility for various cerebrovascular diseases. As endovascular OCT is only FDA approved for the diagnosis and treatment of cardiovascular disease, research ethics board approval is required for all cerebrovascular OCT imaging. Clinicians first utilized OCT in patients with carotid atherosclerotic disease examining: plaque morphology, stent positioning and tissue prolapse through the stent struts after stenting (Shindo et al. 2015, Griessenauer et al. 2017, Dohad et al. 2018). Early case reports were promising and revealed free intraluminal red thrombus, fibrous cap dissections, and thin-cap fibroatheromas with underlying ulcerative plaque in certain patients. There are currently only 2 commercially available endovascular OCT catheters. The

first FDA approved OCT catheter was the Dragonfly^{TM} (St. Jude Medical, Minneapolis, MN) in 2010. The Novasight Hybrid System (Conavi Medical, Toronto, ON) dual OCT and IVUS catheter received approval in 2018. In this research, we exclusively used the ILUMIEN OPTIS system with the Dragonfly OCT catheter (Figure 2-6).

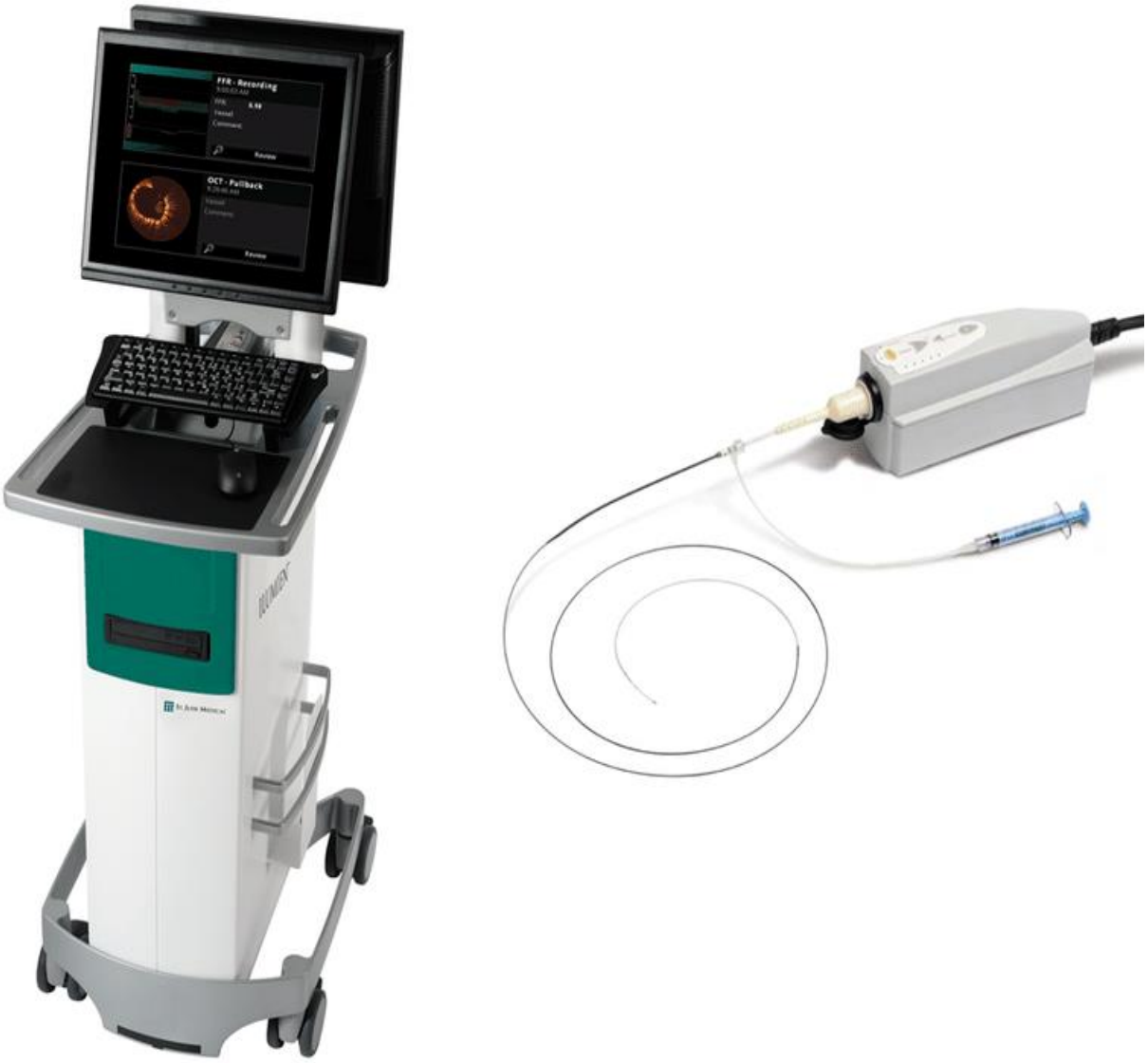

Figure 2-6: The ILUMIEN OPTIS system and Dragonfly OCT catheter. Above is the OCT system along with the docking station, and attached OCT catheter to the right. Attached to the catheter is a small blue syringe used to flush the catheter during use.

This device generates cross-sectional intraluminal images with spatial resolution of 10-20μm. The depth of tissue penetration is approximately 3mm. The catheter can be navigated to the site of interest in either a monorail fashion over a 0.014" microwire, or coaxially through a distal access catheter. To position the catheter in the region of interest, radiopaque catheter markers are used (Figure 2-7). There is one radiopaque marker located near the tip of the catheter and one marker at the lens spaced 23mm apart. The lens marker is located 50mm distal to the proximal marker. The lens motorized pullback length is 54mm.

The catheter is connected to heparinized saline flush to prevent thrombus formation within the lumen of the catheter. The following steps are generally followed for image acquisition: 1) Flush the OCT catheter with saline using the provided 5cc syringe, 2) Load an automated injection pump with 150 cc of heparinized saline. This is used to clear the blood within the vessel lumen during image acquisition. If needed you can also load the pump with a 50:50 mixture of saline and contrast or exclusively contrast, 3) Mount the catheter on a rapid exchange microwire and position such that the lens radiopaque marker is distal to the stenosis as shown above, 4) Infuse a specific rate of heparinized saline depending on the size of the blood vessel. The OCT catheter then automatically detects luminal blood-clearing and performs the motorized automated pullback of 54mm. OCT imaging frequency is 100 frames per second, with a total of 540 cross sectional images generated per pullback.

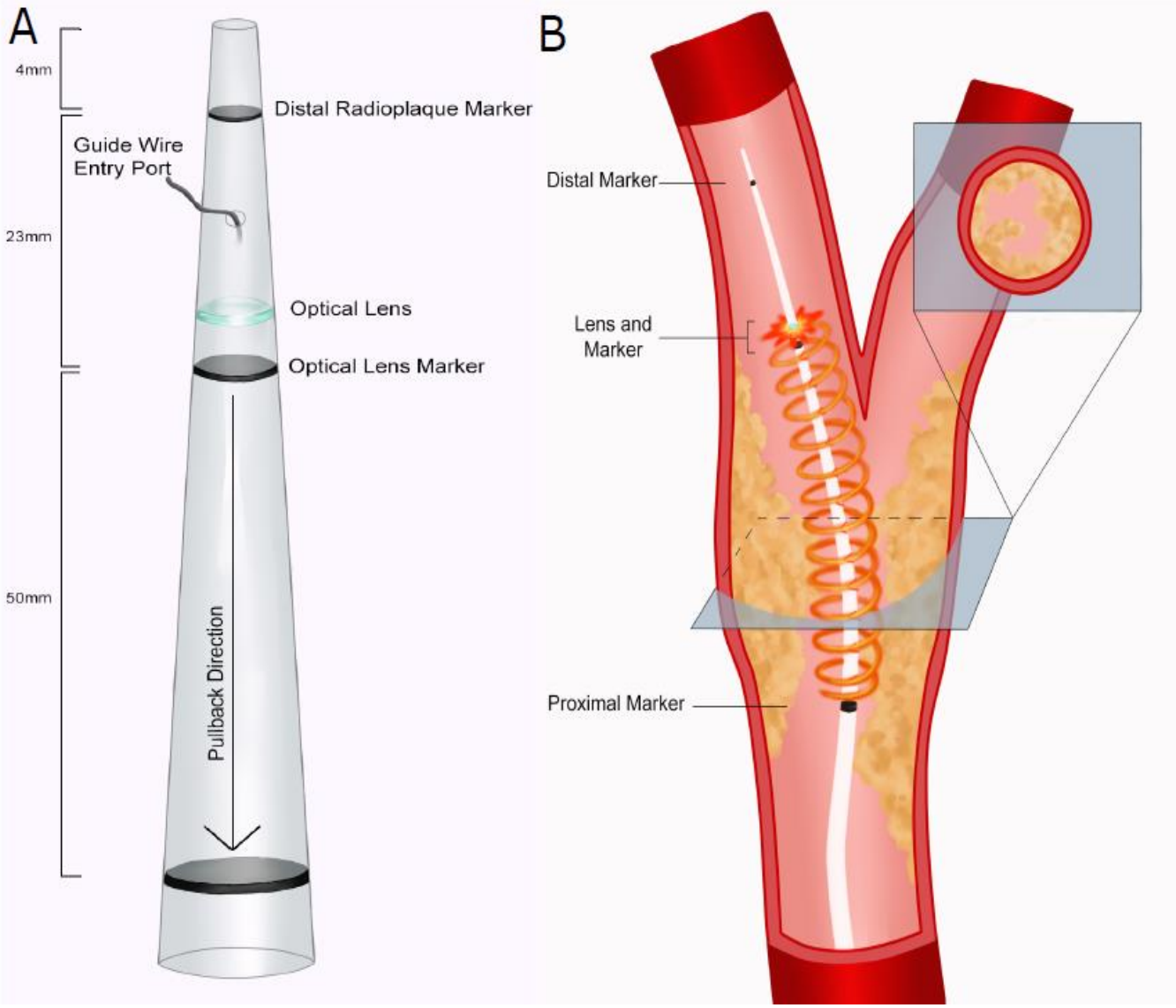

Figure 2-7: Distal OCT catheter and positioning. (**A)** There is one radiopaque marker located near the tip of the catheter and one marker at the lens spaced 23mm apart. The lens marker is located 50mm distal to the proximal marker. The lens motorized pullback length is 54mm. **(B)** In order to ensure imaging of the entire plaque, place the lens maker distal to the stenosis before starting the pump injection. Reprinted with permission from (Pasarikovski et al. 2020).

Chapter 3: Motivation, Hypothesis, and Aims

The motivation for this doctoral thesis began with the fundamental belief that the field of neurointerventional surgery will continue to expand and evolve. The ongoing innovation and device development is accelerating new treatment options, the likes of which we have not witnessed in neurosurgery. As an example, the endovascular management of cerebral aneurysms has considerably evolved over the past two decades. The Guglielmi Detachable Coil System (GDC) was the first system demonstrating efficacy for the endovascular treatment of cerebral aneurysms. However, wide-neck aneurysms could not be treated appropriately with coils, leading to the development of balloon-assisted coiling and ultimately stent-assisted coiling of aneurysms. These advances preceded the development of flow-diverting stents designed to treat wide neck aneurysms without the need for coils, revolutionizing the treatment of aneurysms. Most recently, the Woven EndoBridge (WEB) device, which is an aneurysmal intrasaccular device designed to treat wide neck aneurysms, has allowed clinicians to treat ruptured wide-neck aneurysms without the need for dual antiplatelet therapy.

Given this, the one facet of neurointerventional surgery that is currently absent is intraluminal imaging. As observed in cardiology, intraluminal imaging can be used to help understand the pathophysiology of vascular diseases (in vivo observation of coronary plaque progression over time, along with the plaque composition), aid in the diagnosis of vascular lesions (determining the degree of coronary artery stenosis, dissections, and thrombus) and used as an adjunct during treatment (evaluating for stent apposition during coronary artery stenting and the presence of

plaque prolapse through the stent). The unmatched spatial resolution of endovascular OCT makes it a natural choice for intraluminal imaging.

The general aim of this research was to utilize endovascular OCT in cerebrovascular diseases. The strategy was to begin with preclinical animal studies of OCT imaging in arterial ischemic stroke and cerebral venous sinus thrombosis. With respect to arterial stroke, the goal was to investigate for vascular injury during the thrombectomy procedure. This information is essential in order to continue to improve the devices and techniques used to perform thrombectomy. With respect to cerebral venous sinus thrombosis, the goal was to examine if OCT imaging in the venous system was possible, and next examine the luminal environment after thrombectomy to help shed light as to why these patients do not improve after treatment in certain scenarios. If feasibility could be demonstrated in these preclinical models, the next step would be human imaging for various vascular diseases. Below we will outline the motivation, hypothesis, and aims for each cerebrovascular disease studied in this thesis.

3.1 Arterial Ischemic Stroke

3.1.1 Motivation

Data is emerging pertaining to the amount of blood vessel wall injury due to the mechanical thrombectomy device during clot retrieval. The cerebral blood vessel is composed of three layers: intima, media, and adventitia. The intima layer is further composed of cerebrovascular endothelial cells supported by an internal elastic lamina. These cerebrovascular endothelial cells

are vital in regulating the permeability of the blood-brain barrier, the inflammatory response, and autoregulation of circulating cerebral blood flow. Thus it is intuitive that any iatrogenic damage caused by thrombectomy devices could cause secondary neuronal injury in stroke patients by disrupting the blood-brain barrier or inflammatory cascade.

In an effort to better characterise the iatrogenic vessel wall damage secondary to thrombectomy devices, studies have examined the vessel wall using MRI, histopathological studies examining retrieved clot, and transcranial doppler of affected vessels. Singh *et al*. showed that in 58% of clots retrieved in 48 patients contained cerebrovascular endothelial cells with no evidence of subendothelial components, suggesting that there is some endothelial damage (Singh et al. 2013). Renu *et al*. 2017 performed MRI vessel wall imaging on 60 patients after thrombectomy and found that over 50% of patients had vessel wall enhancement (hematoma/breakdown of the blood-brain barrier) and 45% had severe blood-brain barrier disruption (Renu et al. 2017). They further reported that both vessel wall enhancement and blood-brain barrier disruption was associated with increase in final patient infarct volume. Perren *et al*. in 2018 used transcranial doppler to study the affected vessel and found focal acceleration of blood after mechanical thrombectomy likely due to endothelial layer damage, as there was no evidence of stenosis or vasospasm during angiography (Perren et al. 2018). The literature is far from definitive with respect to iatrogenic vessel injury and the clinical sequel. These techniques such as Magnetic Resonance Vessel Wall (MRVW) imaging have insufficient spatial resolution to directly visualize endothelial injury, and histopathologic examinations are ex-vivo, prone to processing artifacts, and unable to provide real-time patterns of injury. Endovascular OCT may be the

technology poised to investigate iatrogenic vascular injury. OCT enables real-time imaging of all layers of the vessel wall, including defining the internal and external elastic lamina.

Furthermore, contrary to the findings in the anterior circulation, large multicenter observational studies have demonstrated poor clinical outcome despite successful recanalization of the basilar artery (Singer et al. 2015). Others have found no correlation between favourable outcome and time to recanalization (van Houwelingen et al. 2016). One notable criticism is the potential inclusion of patients with established infarcts of the brainstem for which revascularization will be futile, owing to difficulty determining the extent of ischemic core in the brainstem (Lindsberg and Strbian 2015). Nonetheless, the etiology of the difference in outcomes between the anterior and posterior circulation remains unknown. Intravascular imaging may reveal injury to the basilar artery during thrombectomy, or ongoing thrombosis of vital basilar perforators which cannot be observed with conventional angiography.

3.1.2 Hypothesis

We hypothesize that iatrogenic vascular injury occurs during endovascular thrombectomy and that there will be varying degrees of vascular injury including: endothelial denudation, intimal dissection, and edema of the tunica media. These variable degrees of injury will likely have varying clinical implications for patients and need to be characterized. Furthermore, we hypothesize that increased duration of thrombosis will cause increased vascular injury during thrombectomy, due to the toxic effects of the thrombus adjacent to the vessel endothelium.

3.1.3 Aims

1. Design a preclinical animal model of endovascular OCT imaging, deposition of autologous thrombus within a 2-3mm artery to simulate the middle cerebral artery, perform subsequent thrombectomy with a second-generation stent retriever at varying time intervals, and repeat OCT imaging investigating iatrogenic vascular injury.

2. Compare endovascular OCT imaging and histology with respect to the degree of endothelial denudation, detachment, separation of layers of the media, hemorrhage within the media, vessel dissection, and luminal thrombus.

3. If endovascular OCT is feasible in the preclinical animal model with excellent correlation with histology, proceed to human imaging in patients with basilar thrombosis to investigate the luminal environment for evidence of basilar endothelial injury or ongoing perforator thrombosis.

3.2 Cerebral Venous Sinus Thrombosis

3.2.1 Motivation

Cerebral venous sinus thrombosis (CVST) is a unique type of stroke, affecting mostly young and middle age women. The standard of care for the treatment of CVST is early anticoagulation after confirming the diagnosis with either CT or MR venography imaging. The majority of patients

with CVST will clinically improve with systemic anticoagulation, and approximately 85% of patients will fall in this category and have good outcomes (Ferro et al. 2004). However, a portion of patients will present in either a comatose state or continue to deteriorate clinically despite early anticoagulation. In these patients, it is likely that the burden of sinus and bridging cortical vein thrombus has exceeded the brains ability to compensate, leading to significant compromise of venous drainage, venous infarcts, and raised intracranial pressure. In these cases, along with treating the underlying thrombophilia, timely thrombolysis (not merely halting propagation of sinus thrombus with anticoagulation) may be beneficial.

Coutinho *et al.* in 2020 performed one of the largest randomized controlled trials in CVST treatment including 67 patients (Coutinho et al. 2020). The study was a multicenter, open-label, randomized trial and they found no difference in the degree of disability between patients undergoing endovascular treatment versus standard of care with anticoagulation. The study authors hypothesized several reasons for the inability to demonstrate the efficacy of EVT, mostly revolving around the technical aspects of the procedure. The trial did not specify which endovascular devices or techniques must be used during thrombectomy. Interestingly, they did observe that patency of the superior sagittal sinus was higher in the group of patients randomized to thrombectomy compared to anticoagulation alone. It is conceivable that large bridging cortical veins could remain thrombosed even though the sinus is patent. Patency of the sinus without patency of bridging veins (particularly if the vein drains an eloquent or large portion of the cerebral cortex) is unlikely to be beneficial. Conventional angiography cannot reliably assess patency of draining cortical veins or assess for residual thrombus due to limitations of spatial resolution. Furthermore, as Coutinho *et al*. suggested, contrary to arterial stroke research, the

pre-clinical models utilized to test various endovascular techniques and devices for CVST are absent.

3.2.2 Hypothesis

We hypothesize that a preclinical animal model with swine can be used for intravascular imaging and creating a venous thrombosis model to test various devices and techniques. Modern endovascular techniques should allow for the catheterization of the sinus with subsequent imaging, imagine-guided thrombosis, and treatment. We hypothesize that intravascular imaging can identify regions of ongoing cortical vein thrombosis despite recanalization of the sinus.

3.2.3 Aims

1. Design a preclinical animal model for cerebral venous sinus catheterization and subsequent endovascular OCT imaging of the sinus and bridging cortical veins, comparing OCT findings with histology.

2. If the above can be accomplished, proceed to a model of sagittal sinus thrombosis, subsequent endovascular thrombectomy, and OCT imaging.

Chapter 4: Optical Coherence Tomography Imaging after Endovascular Thrombectomy: Novel Method for Evaluating Vascular Injury in a Swine Model

This chapter is based on the following work, with full reprint permission from *The Journal of Neurosurgery.*

Pasarikovski, C. R. *et al.* Optical coherence tomography imaging after endovascular thrombectomy: a novel method for evaluating vascular injury in a swine model. *Journal of neurosurgery*, 1-8, doi:10.3171/2019.12.JNS192881 (2020).

4.1 Introduction

The cerebrovascular endothelium is known to play a pivotal role in regulating inflammatory pathways, permeability of the blood-brain barrier, and thrombosis (Pearson 1999). During endovascular thrombectomy (EVT) with second-generation stent retrievers, considerable chronic outward force can be delivered to the vessel wall via the stent struts or thrombus (Pierot et al. 2015). Studies evaluating for iatrogenic endothelial injury during EVT have been done by means of retrieved human thrombus, post-mortem histopathologic analysis, magnetic resonance vessel-wall (MRVW) imaging, and animal histopathologic studies (Gounis et al. 2013, Singh, Doostkam et al. 2013, Power et al. 2014).

Furthermore, damage to the endothelium may not strictly be due to the mechanical thrombectomy device. Prolonged vessel wall exposure to luminal thrombus can also cause endothelial damage (Wengrovitz et al. 1995). Reil *et al*. showed that ligated arteries with thrombus had increased endothelial damage compared to arteries with interrupted flow in the absence of thrombus (Reil et al. 2000). Various components of the thrombus can affect endothelial function and morphology (Jorgensen et al. 1986). Endovascular optical coherence tomography (OCT) imaging is the highest-resolution intravascular imaging modality currently available. This technology has traditionally been utilized in interventional cardiology, and more recently applied in neurointerventional surgery (Gounis et al. 2018). OCT utilizes near-infrared light with a wavelength of approximately 1.3μm and excellent intraluminal spatial resolution of 10-20 μm is achievable (Tearney et al. 2012).

Although studies have shown that some degree of iatrogenic endothelial injury likely occurs during EVT, whether this is clinically significant remains unknown. Before attempting to correlate vessel injury with clinical outcome, the degree of vessel wall injury should be adequately quantified, as it is likely endothelial denudation, intimal dissection, and edema of the media will have varying clinical implications. Current techniques such as MRVW imaging have insufficient spatial resolution to directly visualize endothelial injury, and histopathologic examinations are ex-vivo, prone to processing artifacts, and unable to provide real-time patterns of injury (Teng et al. 2015).

The purpose of this study is to assess the feasibility of endovascular OCT in quantifying vessel injury in real-time after EVT, correlate the OCT findings of vessel injury with histology, and imaging after EVT at varying time intervals to assess the impact of prolonged direct vessel exposure to thrombus.

4.2 Methods

All experiments were conducted in accordance with policies established by our institutional research ethics board committee. Nine vessels in three Yorkshire swine weighing 35-40kg were selected for the animal model, as they have well-developed superficial cervical arteries (SCA) similar in caliber to human middle cerebral arteries (Yuki et al. 2013). All procedures were carried out under general anesthetic with continuous hemodynamic monitoring. The animals were fed standard diets at our facility for 2 weeks before the procedure.

Technical Success Definition

Technical parameters include: 1) Navigation of the OCT catheter to the appropriate location within the vessel, 2) Clearing of luminal blood with minimal scattering artifact from red blood cells, 3) Capturing circumferential OCT images of the entire arterial lumen along the entire region of interest, 4) Identifying normal anatomic structures (intima, media, adventitia, and internal/external elastic lamina) where present, and 5) Identifying interatrial and vessel wall lesions when present. For the image acquisition to be defined as technically successful, all above criteria must be met for each pullback.

Thrombus Preparation

Autologous venous whole blood was drawn 48 hours before the procedure in circular tubes without sodium citrate (Peschillo et al. 2017). The autologous blood was left to incubate at 4º for 24 hours. The solid red clot was separated from the plasma. Before the procedure the thrombi were sectioned into 5mm X 20mm segments and stored at 37ºC.

Vessel Occlusion and Thrombectomy

An 8 French sheath was inserted into the right common femoral artery and connected to continuous saline irrigation. No heparin or other antithrombotics/thrombolytic agents were administered throughout the procedure. There is inconsistency among the major EVT trials with respect to procedural heparin administration. Kreitzer *et al*. reported that no two major EVT

trials had the same heparin EVT protocol, and therefore we did not administer antithrombotics (Kreitzer et al. 2016). First, thrombi were deposited into three arteries sequentially: 1) right SCA, 2) right internal thoracic artery (ITA), and 3) left SCA. A FlowGate (Stryker, Fremont, California) double lumen balloon guide catheter was positioned in the subclavian artery. A distal access catheter was navigated through the double lumen balloon guide into the vessel of interest and thrombus was injected slowly through the catheter under proximal balloon occlusion. If incomplete vessel occlusion was observed, thrombus injection was repeated until complete occlusion was observed.

EVT was then performed at one, three, and six hour after vessel occlusion. A FlowGate guide catheter was again positioned in the subclavian artery. A Trevo-18 microcatheter (Stryker, Fremont, California) was advanced over a microwire 3mm beyond the thrombus. A Trevo 4mm X 20mm stent retriever (Stryker, Fremont, California) was deployed for 5 minutes before retrieval. The thrombectomy devices were slowly withdrawn under proximal balloon occlusion and continued aspiration through a 60cc syringe. The goal was complete revascularization defined as thrombolysis in cerebral infarction (TICI) reperfusion grade 3 and arterial occlusive lesion (AOL) recanalization score of 3. If incomplete angiographic revascularization was observed, the procedure was repeated again up to a maximum of three attempts.

Optical Coherence Tomography Image Acquisition and Analysis

After thrombectomy OCT images were immediately obtained. The Dragonfly^{TM} OCT catheter (Abbott Vascular, Chicago, IL) was used. The following steps were sequentially followed for

image acquisition: 1) Load an automated injection pump with 150ml of saline. This is used to clear the blood within the lumen during image acquisition, 2) Mount the catheter on a rapid exchange micro-guidewire and position the device such that the optical lens radiopaque marker is distal to the segment with previous thrombus, 3) Saline infusion of 4cc per second for 6 seconds via the automated pump. The OCT catheter automatically detects luminal blood-clearing and performs the motorized automated pullback of 54mm total. OCT imaging frequency is 100 frames per second, with a total of 540 cross sectional images generated per pullback.

All cross-sectional OCT images were analyzed. The percentage of surface area was used to quantify endothelial injury, and the inner media circumference percentage was used for media layer edema/separation. The following characteristics of vascular injury were quantified: 1) Endothelial denudation, 2) Endothelial detachment and elevation from the underlying media, 3) Separation of layers of the media, 4) Hemorrhage within the media, 5) Vessel dissection, and 6) Luminal thrombus. In order to quantify the degree of residual thrombus present, the thrombus scoring system developed by Prati *et al*. was utilized (Prati et al. 2010). This scoring system is based first on the semi-quantitative assessment of the number of quadrants with residual thrombus present in each cross sectional OCT image. A value of zero is assigned if no residual thrombus is present. A value of 1, 2, 3, and 4 is assigned to each cross-sectional OCT image depending on the number of quadrants with thrombus. Subsequently all scores from each cross-section are added for a final thrombus burden total score.

Histological Analysis

After OCT imaging and the sacrifice of the animal, an approximately 4 cm segment of each affected artery was harvested. The site of the thrombus was landmarked using angiography images and marked on the external surface of the artery using tissue ink. The resected arterial segments were fixed in 10% neutral buffered formalin. After formalin fixation, the arteries were cross-sectioned into 5mm segments and embedded in paraffin. Three different levels through each of these tissue blocks were created, and 5 micrometer thick tissue sections were mounted on glass slides and stained with hematoxylin and eosin (H&E). H&E stained slides from each level of the sampled arteries were examined at 4X, 10X and 20X magnification by an experienced Neuropathologist (JK) and the same six characteristics of vascular injury were assessed (endothelial denudation, endothelial detachment, separation of layers of the media, hemorrhage within the media, dissection, and luminal thrombus). The only difference arises in the assessment of residual luminal thrombus. On histology, thrombus quantification was defined as present or absent, whereas with OCT the method by Prati *et al*. was utilized as described above (Prati, Capodanno et al. 2010). Slides were scanned by Aperio AT Turbo slide scanner (Leica Biosystems, Buffalo Grove, Illinois), and the dimensions of the luminal thrombi, mural thrombi and dissection were measured in μm. With respect to statistical analysis, Bland-Altman plots were generated using the mean difference between histology and OCT scores and a 1.96 standard deviation (SD) with respect to the various vessel wall injury characteristics.

4.3 Results

Successful revascularization (TICI/AOL grade 3) was achieved in all 9 vessels (Figure 4-1). OCT image acquisition was technically successful in all (100%) of cases. Regions beyond the thrombectomy site showed normal swine vessel anatomy, with a thin layer of endothelium and thick tunica media which constitutes most of the arterial wall, and no obvious external elastic lamina (Figure 4-2A). On OCT analysis, endothelial denudation (Figure 4-2C) was present in 65 ±16%, 87 ±8%, and 93 ±7% of the vessel surface 1, 3, and 6 hours after thrombus deposition and subsequent EVT, respectively (Table 4-1). Separation of the layers within the media was present in 5 ±15%, 49 ±11%, and 66 ±18% of the vessel 1, 3, and 6 hours after thrombus deposition and subsequent EVT, respectively. Hemorrhage was observed within the media for vessels exposed to thrombus for 6 hours only. Dissection was only present in one vessel exposed to thrombus for 6 hours (Figure 4-2D). Residual intraluminal thrombus was present in vessels at all time intervals despite complete angiographic revascularization (TICI/AOL grade 3). The residual thrombus burden score was 6.2 ±1, 4.3 ±2, and 9 ±5 in vessels 1, 3, and 6 hours after thrombus deposition and subsequent EVT, respectively (Figure 4-3A-D). The average number of EVT passes to achieve TICI/AOL grade 3 reperfusion was 1.3, 1, and 2, after 1, 3, and 6 hours respectively.

Bland-Altman analysis demonstrated good agreement between histology (Figure 4-4) and OCT images across all vessel injury characteristics (Figure 4-5). For endothelial denudation a mean difference with 1.96 and -1.96 SD (mean, [SD]) of 0.11 [0.29, -0.3] was observed, with 5% (4/73) of points outside the 95% confidence interval (Figure 4-5A). For endothelial elevation a mean difference of 0.001 [0.04, -0.04] was observed, with 4% (3/73) of points outside the 95%

confidence interval (Figure 4-5B). For separation of the media a mean difference of -0.04 [0.27, -0.36] was observed, with 8% (6/73) of points outside the 95% confidence interval (Figure 4-5C). For hemorrhage of the media a mean difference of 0.01 [0.15, -0.16] was observed, with 7% (4/59) of points outside the 95% confidence interval (Figure 4-5D).

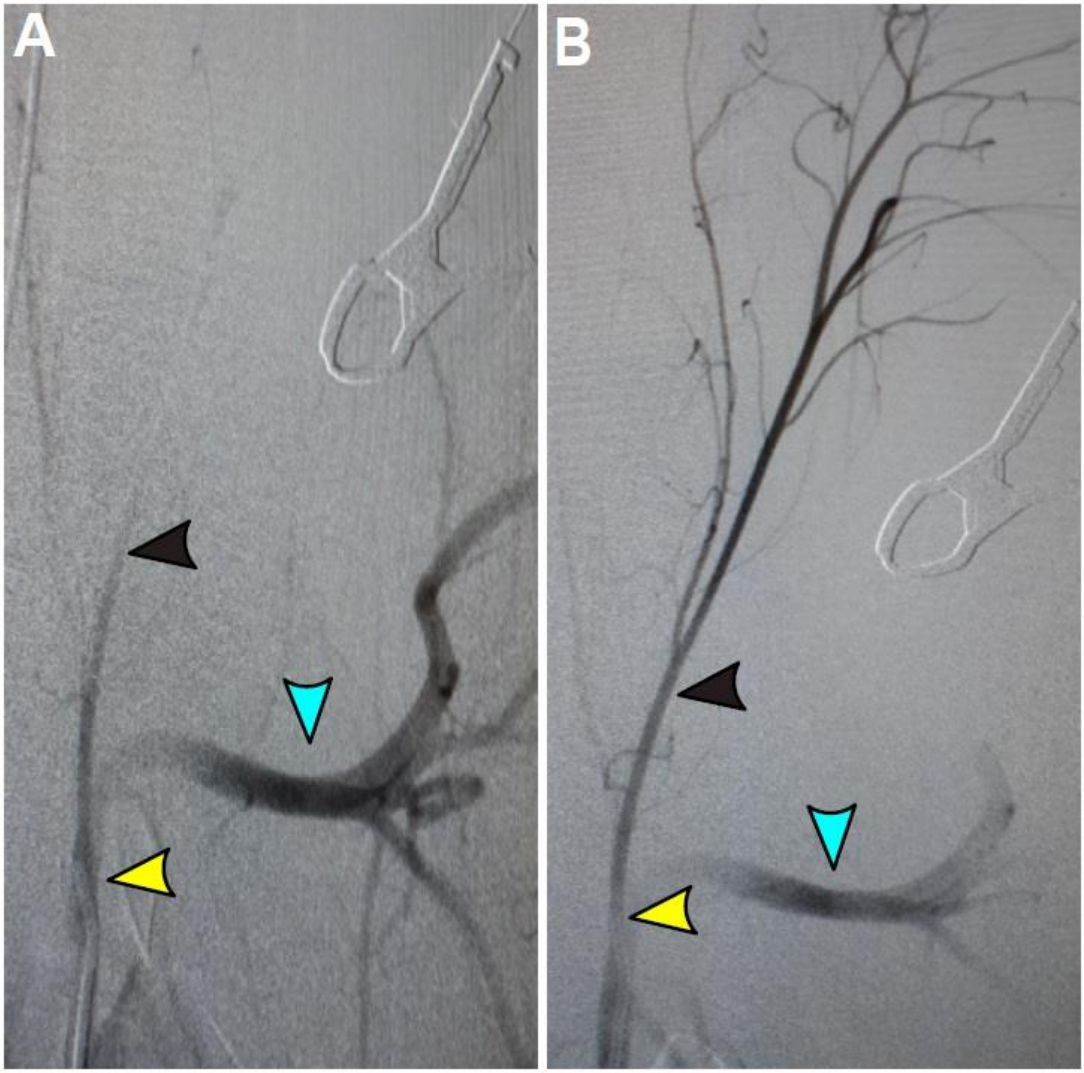

Figure 4-1: Clot Deposition and Thrombectomy. A catheter is shown in the proximal left subclavian (yellow arrow) with filling of the middle left subclavian (blue arrow). **A)** Occlusion of the proximal left superficial cervical artery (black arrow) using erythrocyte rich thrombus. **B)** The left superficial cervical artery is patent (TICI/AOL 3 revascularization) after mechanical thrombectomy (black arrow). **Abbreviations**: TICI= thrombolysis in cerebral infarction, AOL= arterial occlusive lesion.

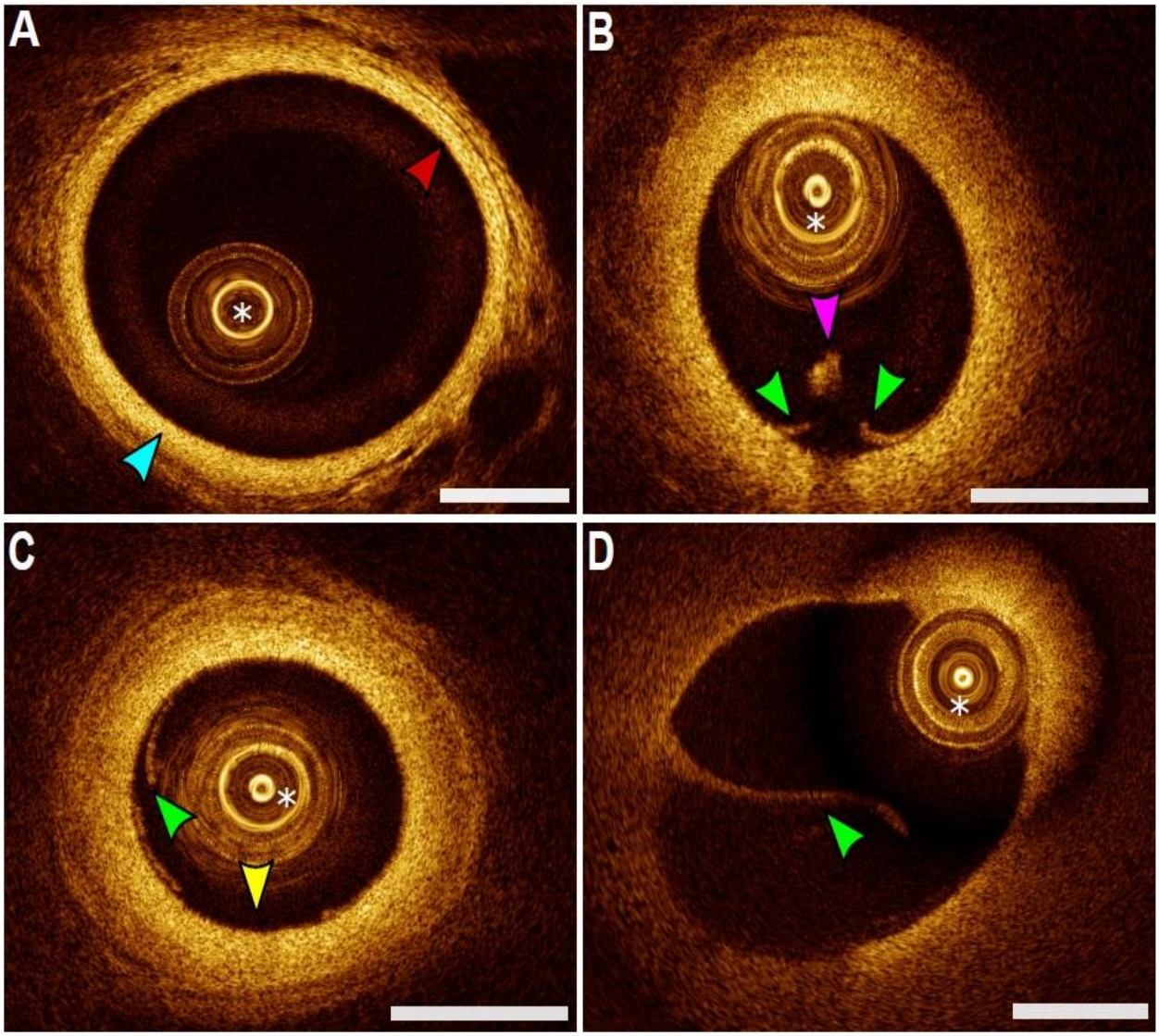

Figure 4-2: OCT Imaging of Normal and Damaged Swine Endothelium. (A) Normal swine vessel anatomy with thick tunica media occupying most of the vessel wall (blue arrow), with a thin layer of endothelial cells (red arrow). (**B)** Damaged endothelial layer (green arrows) elevated from the tunica media with intraluminal thrombus (pink arrow). (**C)** Elevated endothelium (green arrow) and denuded endothelium (yellow arrow). (**D)** Floating intima/media within the vessel lumen (green arrow). **Abbreviations**: OCT= optical coherence tomography. *OCT catheter. White bar length=1mm.

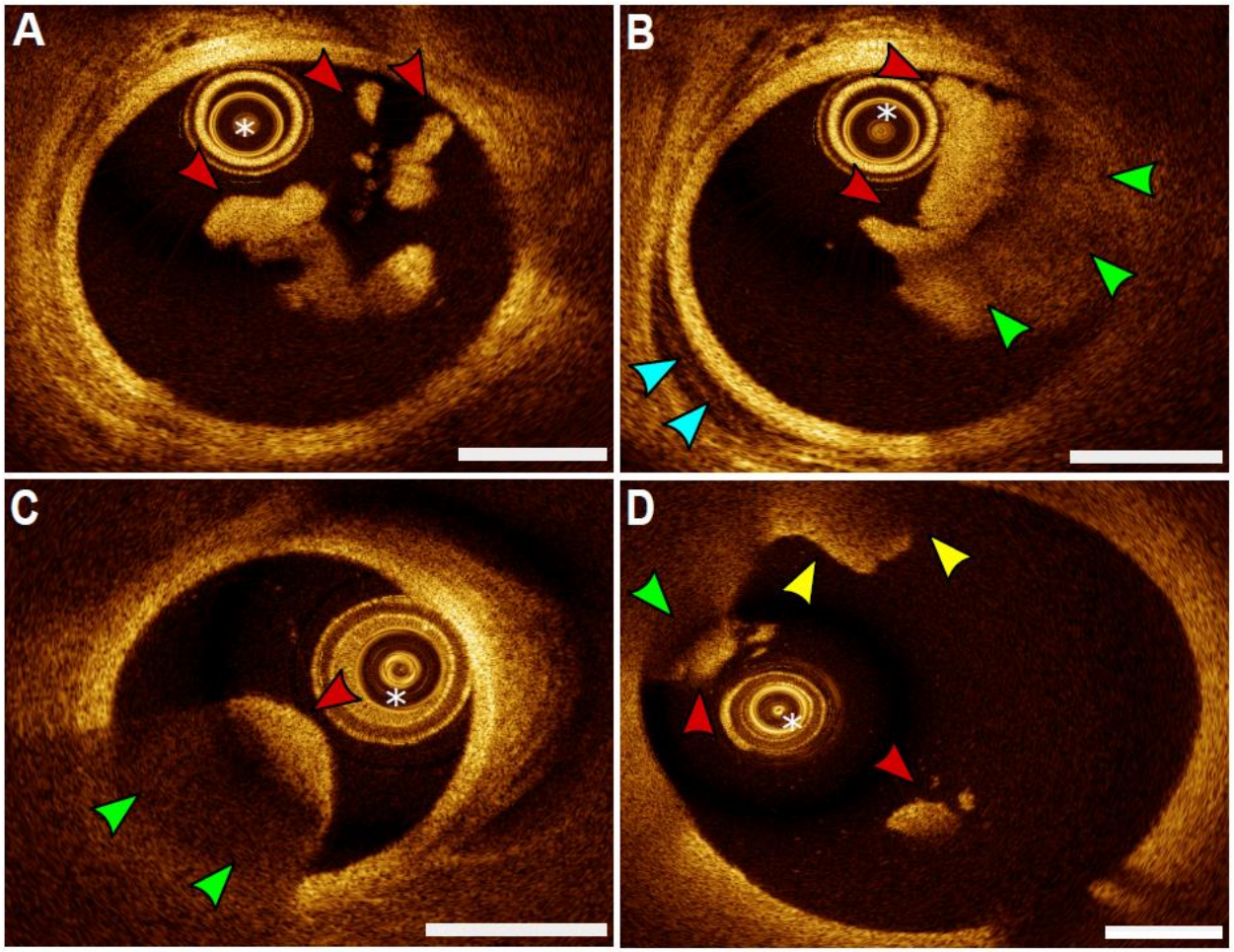

Figure 4-3: OCT Imaging Revealing Residual Thrombus. (**A-D)** Intraluminal residual thrombus (red arrows) with shadowing beyond the red thrombus (green arrows) despite TICI/AOL grade 3 revascularization. **(B)** Fluid and expansion observed within the tunica media (blue arrows). (**D)** Thrombus within the vessel wall (yellow arrows) extending into the lumen. **Abbreviations**: OCT= optical coherence tomography. *OCT catheter. White bar length=1mm.

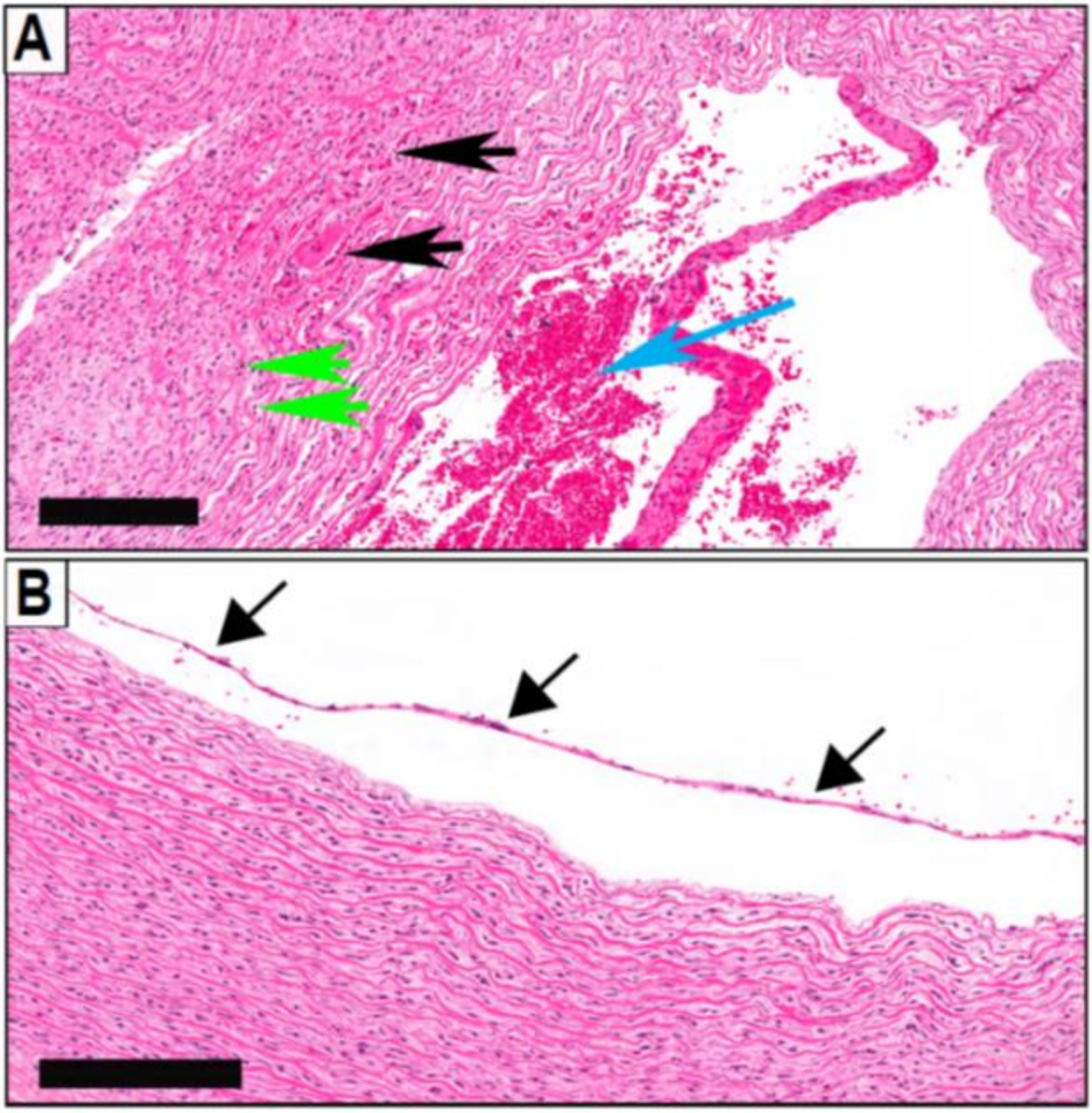

Figure 4-4: Histologic Analysis Showing Vessel Injury. (A) Vessel dissection (blue arrow), hemorrhage within the tunic media (black arrow), and neutrophil infiltration (green arrows). **(B)** Endothelial elevation (black arrows) from the tunica media. Scale bars=200μm.

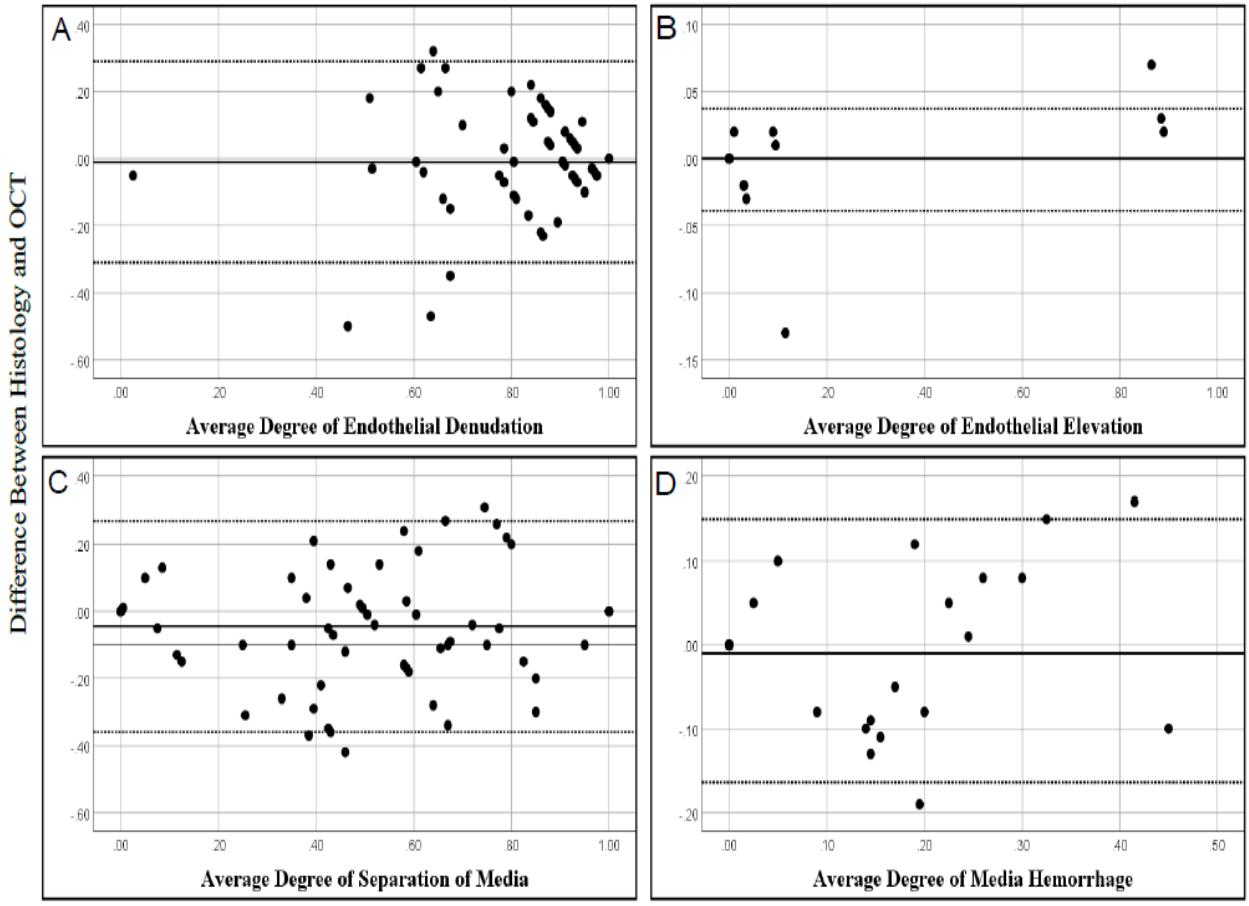

Figure 4-5: Bland-Altman Plots Comparing Histology and OCT. (A) Endothelial denudation with mean difference SD [1.96, -1.96] of 0.11 [0.29, -0.31]. **(B)** Endothelial elevation with a mean difference of 0.001 [0.04, -0.04]. **(C)** Separation of the media with a mean difference of 0.04 [0.27, -0.36]. **(D)** Hemorrhage of the media with a mean difference of 0.01 [0.15, -0.16].

	Endothelial Denudation	Endothelial Elevation	Separation of Media	Hemorrhage in Media	Dissection	Residual Thrombus
Histology						
Left SCA (1 Hour)	70 ± 10 %	3 ± 4 %	1 ± 2 %	0	No	Yes
Right ITA (3 Hours)	82 ± 15 %	0	43 ± 15 %	1 ± 3 %	No	Yes
Right SCA (6 Hours)	85 ± 28 %	8 ± 27%	72 ± 27 %	12 ± 40%	Yes	Yes
OCT						
Left SCA (1 Hour)	65 ± 16 %	7 ± 5 %	5 ± 15 %	0	No	6.2 ± 1
Right ITA (3 Hours)	87 ± 8 %	0	49 ± 11 %	0	No	4.3 ± 2
Right SCA (6 Hours)	93 ± 7 %	20 ± 15%	66 ± 18 %	21 ± 16%	Yes	9 ± 5

Table 4-1: Histologic and OCT Quantification of Vessel Wall Injury. Endothelial injury, residual thrombus, and separation/edema within the media were present in all vessels.

Abbreviations: SCA= superficial cervical artery, ITA= internal thoracic artery, OCT=optical coherence tomography.

4.4 Discussion

We describe for the first time a technique for in vivo imaging of the vessel wall and luminal environment after EVT using optical coherence tomography. Our findings include: 1) OCT imaging is technically feasible and can adequately quantify vessel wall injury, 2) Varying degrees of vessel injury occur after EVT, 3) Residual luminal thrombus can be present despite complete angiographic revascularization (TICI/AOL Grade 3), and 4) Prolonged direct vessel exposure to thrombus before EVT may increase vessel injury.

Endovascular thrombectomy has become the standard of care after several large randomized trials showed efficacy for patients with large vessel occlusion of the anterior circulation (Goyal, Menon et al. 2016). Yuki *et al*. and Gori *et al*. in 2013 first reported a novel animal model to evaluate iatrogenic arterial injury during mechanical thrombectomy by exposing the target arteries, implanting thrombus, performing mechanical thrombectomy, and conducting histologic assessment after harvesting the vessels (Gory et al. 2013, Yuki, Kan et al. 2013). These techniques have limitations, as the vessels need to be exposed and manipulated with a change in the surrounding soft tissue environment, and more importantly histologic analysis may be prone to processing artifacts. To circumvent this, Teng *et al*. in 2015 developed an in vitro live-cell platform to assess thrombectomy devices and allow direct visualization of the cell-device interaction (Teng, Pannell et al. 2015). Along with being in vitro, these platforms only examine endothelial injury and not the entire vessel wall.

Although histologic analysis remains the gold standard in the characterization of vascular injury, with spatial resolution of 10μm OCT is able to clearly define the different layers of the arterial wall and provide an assessment of the luminal environment without tissue preparation. We found OCT image acquisition to be feasible in all cases with our standardized protocol. Endothelial denudation was certainly quantifiable, along with the presence of luminal thrombus. Supporting this, Bland-Altman analysis confirmed acceptable agreement between histology and OCT for the varying degrees of vascular injury. It also appears that OCT can quantify endothelial elevation with increased specificity. We hypothesize that histologic specimens are ex-vivo and prone to subtle processing artifacts, and could underestimate the degree of endothelial elevation. Furthermore, this novel technique could address the deficiencies of prior models utilized to evaluate thrombectomy devices. Currently most devices are tested in silicon and glass phantom models to allow for direct visualization, and these models lack a biologically representative environment. OCT can specifically address this, and allow for observation of the interaction between the device and vessel wall in vivo.

The clinical significance of vessel wall injury during EVT remains unknown. The largest study investigating the relationship between vessel wall injury and clinical outcome was by Renu *et al*. in 2017 by means of MRVW imaging on a 1.5T scanner (Renu, Laredo et al. 2017). They found 34 patients (57%) had gadolinium vessel wall enhancement after EVT, which was associated with poor clinical outcome. The insufficient spatial resolution of MRVW imaging limits this modality to describing contrast enhancement or mural hemorrhage, and cannot adequately visualize varying degrees of injury. Direct evidence of vessel injury in humans was reported by Yin *et al*. who performed autopsies in 5 patients after EVT and found subintimal dissection

likely resulting from the procedure in one patient (Yin et al. 2010). We hypothesize that varying degrees of injury (endothelial denudation, intimal dissection, and edema of the media) will have varying clinical implications. OCT is able to quantify these degrees of injury in real-time.

An unexpected finding was the presence of residual luminal thrombus despite complete angiographic revascularization. Chueh *et al*. demonstrated that distal embolic showers with large (215-285 μm) and small fragments (23-37μm) occur during thrombectomy (Chueh et al. 2012). Although distal emboli have certainly been reported, there are no reports in the literature of residual luminal thrombus at the site of the target lesion in the presence of complete recanalization and reperfusion (TICI/AOL Grade 3). Gory *et al.* reported significant mural thrombus at the thrombectomy site; however these lesions were in the intimal layer causing no luminal narrowing (Gory, Bresson et al. 2013). The authors hypothesize that the observed thrombus is a combination of residual clot not captured by the stent retriever, along with new aggregation of platelets at the thrombectomy site due to exposed collagen from vessel wall injury. The clinical implications of residual thrombus after EVT remain unknown. The author's recent case series of three patients with basilar occlusion revealed significant residual thrombus after EVT adjacent to patent basilar perforators (Pasarikovski, Ramjist et al. 2019). The thrombus was not visible on cerebral angiography, CT angiography, or MR vessel wall imaging and could certainly cause ongoing strokes.

There are no reports evaluating endothelial injury at increasing time points to investigate the possible contribution of prolonged vessel wall exposure to thrombus in endothelial injury. Power *et al*. showed that thromboembolism alone can cause MRVW abnormalities in the absence of

EVT in 30% (3 patients) treated with medical therapy alone (Power, Matouk et al. 2014). They found patients undergoing EVT had significantly increased arterial wall abnormality compared to those treated with medical therapy alone, suggesting that iatrogenic injury occurs from the thrombectomy device. We observed increased endothelial injury and intimal edema in vessels undergoing EVT 6 hours after thrombus deposition. Components of the thrombus can affect endothelial function and morphology, and we also hypothesize that the clot may be more adherent to the vessel wall after increased time, causing more mechanical injury during retrieval (Jorgensen, Grothe et al. 1986).

There are several limitations to our model. First, swine extracranial arteries differ anatomically from human cerebral vessels. Swine blood vessels generally have thicker tunica media and a thinner intimal layer compared to humans (Yuki, Kan et al. 2013). Furthermore, swine vessels are more elastic compared to human vessels (van Andel et al. 2003). This can result in the swine model underestimating the degree of vessel wall injury due to stress and strain forces, as more elastic vessels can better tolerate these forces leading to decreased dissection and tears. However, OCT appears to be feasible in quantifying injury in the animal model, and should also be feasible in quantifying injury in humans. Second, we used erythrocyte rich thrombus in our model, which differs slightly from the cellular composition of thromboemboli and the clinical setting. Third, the swine vessels utilized in our model were non-tortuous and the vascular access was straightforward. The human intracranial circulation has significant tortuosity, particularly at the carotid siphon, and navigation of the OCT catheter may not be feasible for all patients. The distal tip of the OCT catheter is stiff due to the reflecting glass lens. In the author's own institutional experience, OCT image acquisition of the posterior circulation is straightforward. However,

overly tortuous carotid siphons are not easily traversed. Other authors have reported techniques for reliable navigation of tortuous carotid siphons (Guerrero et al. 2018, Martinez-Galdamez et al. 2019). Finally, the OCT catheter itself could also be a source of vascular injury. Large safety and feasibility studies reported in the interventional cardiology literature suggest that intravascular OCT is safe; however the intracranial vasculature is unique and specific investigations with respect to the intracranial circulation will need to be undertaken to ensure its safety(Yamaguchi et al. 2008).

4.5 Conclusion

Optical coherence tomography imaging after EVT is feasible in this pre-clinical study and can adequately quantify vessel wall injury in real time with histological accuracy. Varying degrees of vessel injury occur after EVT and residual luminal thrombus can be present despite complete angiographic revascularization.

Chapter 5: Endovascular Cerebral Venous Sinus Imaging with Optical Coherence Tomography

This chapter is based on the following work, with full reprint permission from *The American Journal of Neuroradiology.*

Pasarikovski, C. R., J. C. Ku, J. Keith, J. Ramjist, Y. Dobashi, S. M. Priola, L. da Costa and V. X. D. Yang (2020). Endovascular Cerebral Venous Sinus Imaging with Optical Coherence Tomography. *American Journal of Neuroradiology*: **41**(12): 2292-2297.

5.1 Introduction

The cerebral venous sinuses (CVS) are rigid structures located between the periosteal and meningeal layers of the dura matter (Mack et al. 2009). The sinuses act as reservoirs for collecting venous blood from both the deep and superficial venous system of the brain, and are lined with endothelium and elastic lamina (Vignes et al. 2007). They lack the smooth muscle layers found in most blood vessels and have no valves (Adeeb et al. 2012). Diseases of the CVS include dural arteriovenous fistulas (dAVF), cerebral venous sinus thrombosis (CVST), and idiopathic intracranial hypertension (IIH).

Imaging of the CVS has evolved considerably over the past two decades. Computed tomography venography (CTV) and magnetic resonance venography (MRV), with either 2-dimensional time-of-flight (2D TOF) or contrast enhanced (CE) MRV, are the current imaging modalities of choice for the diagnosis of CVST or venous sinus stenosis in IIH (Saposnik et al. 2011). However, large studies comparing the sensitivity and specificity of MRV for determining the degree of stenosis with digital subtraction angiography (DSA), which is the presumed gold standard for cerebral venous imaging, are lacking. Boddu *et al*. showed that CE-MRV significantly overestimated the size of sinus stenosis in patients with IIH when compared to intravascular ultrasound (IVUS), concluding that CE-MRV would be a poor modality for stent size selection (Boddu et al. 2018). Similarly, the accuracy of DSA has been questioned owing to the limitations of 2D planar imaging. Karmon *et al*. compared DSA with IVUS and reported that angiography was less sensitive in describing the luminal environment, frequently missing luminal thrombus, valves in the internal jugular vein, flaps and septations (Karmon et al. 2013).

Endovascular optical coherence tomography (OCT) is the highest resolution intravascular imaging modality available, utilizing near-infrared light with a wavelength of approximately 1300 nm and excellent spatial resolution of 10μm is achievable (Tearney, Regar et al. 2012). In comparison, IVUS has a spatial resolution of 100μm (approximately 10 times less resolution), and 3-Tesla MR vessel-wall imaging has a voxel size of 2.0 X 0.4 X 0.4mm. With near histologic resolution, OCT has been described as an optical biopsy modality (Tearney et al. 1997).

We hypothesize that endovascular OCT would enable superior characterization of the cerebral sinus luminal environment and visualize draining cortical veins and dural arteries. To our knowledge, endovascular OCT imaging of the human CVS has not been undertaken. The purpose of this research was to develop a proof of concept animal endovascular OCT cerebral venous sinus imaging model, and compare OCT imaging with histology. Doppler OCT images were also acquired.

5.2 Methods

All experiments were conducted according to the policies and standards established by the authors' institutional animal research ethics board. Four consecutive Yorkshire Swine weighing 40-45 kg were utilized for sinus imaging. There was no pre-screening imaging of venous anatomy for any animal. All procedures were carried out under general anesthetic with

continuous hemodynamic monitoring. The animals were fed standard diets at our facility for 2 weeks before the procedure.

Ultrasound guided right femoral punctures were performed and a 6 French (F) sheath was inserted into the right common femoral artery, and another into the right femoral vein. First, a 6-F Envoy guide catheter (Codman, Boston, MA) was used in conjunction with a 150cm Glidewire (Terumo, Somerset, NJ) to select the right ascending pharyngeal artery. The guide catheter was stationed before the rete mirabile. The C-Arm (Philips, Andover, MA) was then positioned in a true lateral view and cerebral angiography performed to visualize the sinus.

Next, a second 6-F Envoy was positioned in the right internal jugular (IJ) vein. Combined arterial pump injections from the ascending pharyngeal artery and venous hand injection, timed to the late venous phase of the arterial pump injection, were performed to visualize the internal jugular and sigmoid junction (Figure 5-1A). The connection between the internal jugular and the sigmoid sinus can be very small in calibre, and therefore both an arterial and venous run are required. A Transcend micro guidewire (Stryker, Kalamazoo, MI) was navigated into the superior sagittal sinus (SSS) via the sigmoid and transverse sinus under roadmap technique.

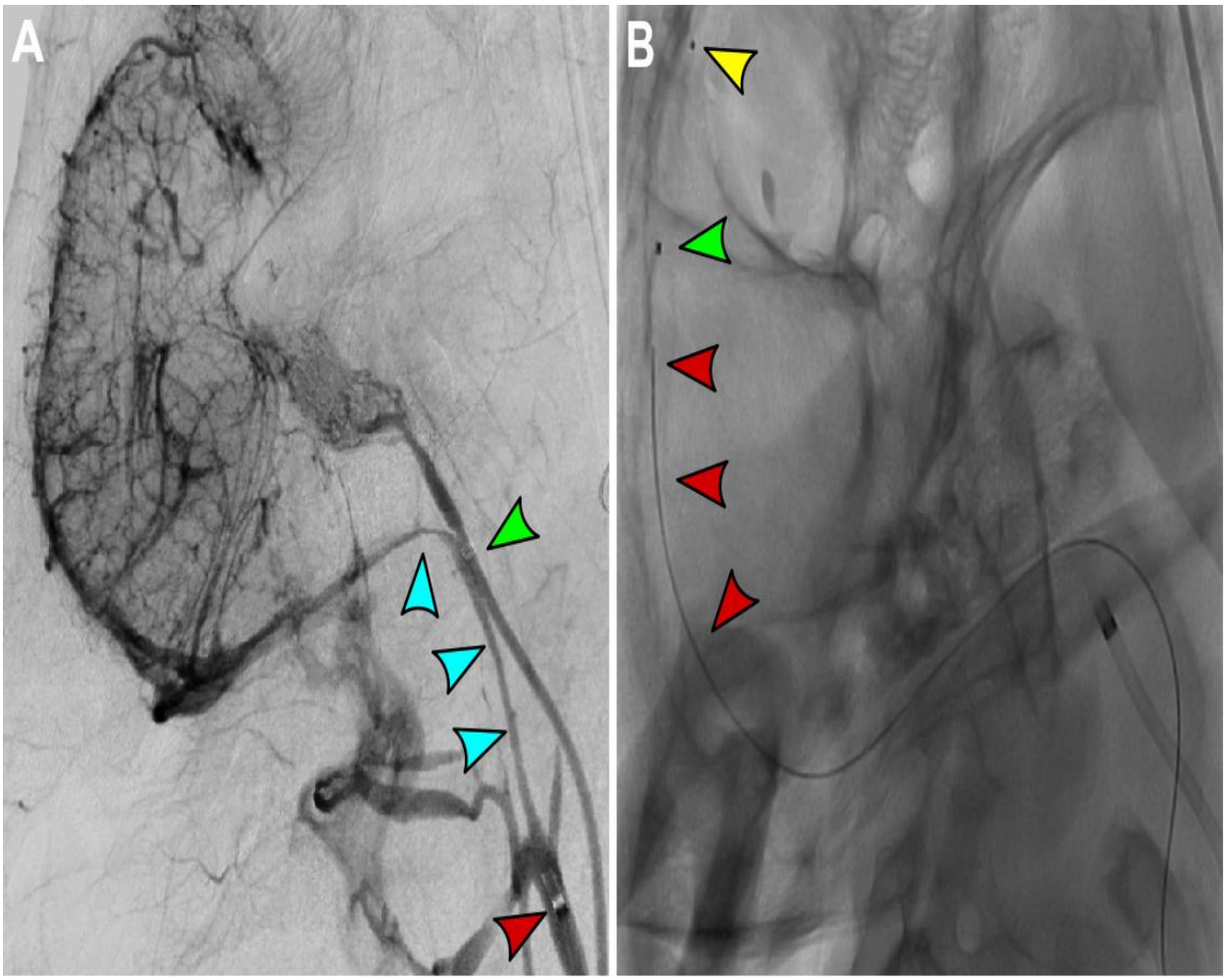

Figure 5-1: Swine Cerebral Venous Sinus. (**A)** Combined arterial and venous diagnostic angiography injections in lateral view via a guide catheter tip in the ascending pharyngeal artery (green arrow) and the internal jugular vein (red arrow) revealing the connection between the internal jugular vein and sigmoid sinus (blue arrows). (**B)** Optical coherence tomography (OCT) catheter in the superior sagittal sinus (SSS). The distal catheter marker (yellow arrow), lens marker (green arrow), and optical fiber (red arrows) are visible in the SSS.

Optical Coherence Tomography Imaging

The Dragonfly^{TM} OCT catheter (Abbott Vascular, Chicago, IL) was used for image acquisition. The following steps were sequentially followed for image acquisition: 1) Load an automated injection pump with 150 mL mixture of 50:50 contrast and saline. The pump is connected to the Envoy catheter in the ascending pharyngeal artery. This is used to clear the blood within the sinus lumen during OCT image acquisition, 2) Mount the OCT catheter on the Transcend micro guidewire and advance the device in a monorail fashion into the superior sagittal sinus, 3) Position the OCT catheter such that the optical lens radiopaque marker is in the anterior third of the sinus (Figure 1B), 4) Inject 3mL per second for 8 seconds total (24 mL total) via the pump, 5) Enable manual OCT pullback mode and initiate the pullback manually once the lumen begins to clear. The OCT catheter performs the motorized automated pullback of 54 mm total. OCT imaging frequency is 100 frames per second, with a total of 540 cross sectional images generated per pullback.

The technique for Doppler OCT (dOCT) image acquisition has been previously described by Vuong *et al.*(Vuong et al. 2014). Briefly, a split spectrum dOCT technique was utilized, to reduce phase noise without incorporating external bulk optical devices. During image acquisition an arterial injection of 2mL per second for 10 seconds (20 mL total) was done. Both OCT and dOCT images were reviewed independently by two physicians with extensive experience analyzing OCT images (CRP and VXDY).

Pathology

After OCT imaging and the sacrifice of the animal, craniotomy was performed and resection of the superior sagittal sinus beyond the torcula into the bilateral transverse sinuses, with 2 cm margins of adjacent dura along with preservation of draining cortical veins. The resected specimen segments were fixed in 10% neutral buffered formalin. Then the sinuses were sectioned coronally into 5 mm segments and submitted in total from anterior to posterior in tissue blocks for embedding in paraffin. One level through each of these tissue blocks were created, and 5 micrometer thick tissue sections were mounted on glass slides and stained with hematoxylin and eosin (H&E). H&E stained slides from each block of the sampled sinus were scanned by an Aperio AT Turbo slide scanner (Leica Biosystems, Buffalo Grove, Illinois) and the resulting digital histology images were examined using E-Slide Manager by an experienced Neuropathologist (JK).

For each digital histology image, the maximum diameter of the observed lumen of the superior sagittal sinus and/or transverse sinuses were measured digitally in μm, and the location and luminal diameter of the adjacent arterioles and venules were also recorded in μm. Digital photomicrographs were taken, with and without the annotated dimensions, and the digital photomicrographs were compared to the images obtained by structural OCT. For statistical analysis, Bland-Altman plots were generated using the mean difference between histology and OCT scores and a 1.96 standard deviation (SD) with respect to the various luminal characteristics. Histological processing artifacts can create 5-13% differences in vessel dimensions (Choy et al. 2005).

5.3 Results

Cerebral venous sinus access was successful in all animals, and successful OCT and dOCT images were acquired in 3/4 swine. In swine 2, access was gained into the SSS with the 0.014" microwire, however the OCT catheter could not traverse a suspected venous valve at the junction of the internal jugular vein and the sigmoid sinus, therefore no OCT or dOCT images were obtained. In the remaining 3 swine technically successful images were acquired. For image acquisition to be defined as successful, all the following criteria were all met: 1) Navigation of the OCT catheter to the appropriate location within the sinus, 2) Clearing of luminal blood with minimal artifact from red blood cells, 3) Capturing circumferential OCT images of the entire sinus lumen along the entire region of interest, 4) Identifying normal anatomic structures where present, 5) Identifying luminal lesions and vessel wall lesions when present.
The luminal environment could be characterized without ambiguity (Figure 5-2). Luminal diameter could readily be calculated, along with visualization of dural arteries and draining cortical veins (Figure 5-3). When present, luminal thrombus, likely secondary to micro guidewire manipulation, could be observed and characterized as red or white thrombus.

The average maximum diameter (Dmax) [95% confidence interval] of the sinus was 3.14mm [5.11 – 1.17]. The average diameter of adjacent dural arteries was 135 μm [211-60]. The average venule diameter was 260 μm [520-1]. Bland-Altman analysis demonstrated good agreement between histology (Figure 5-4) and OCT images across Dmax and arterial/venule diameter measurements (Figure 5-5). For Dmax, a mean difference with 1.96 and -1.96 SD (mean, [SD]) of 0.21 mm [3.62, -3.19] was observed, with 10% (2/20) of points outside the 95% confidence

interval (Figure 5-5). For dural arteriole diameter, a mean difference of -8µm [140, -157] was observed, with 10% (4/40) of points outside the 95% confidence interval (Figure 5-5). For venule diameter, a mean difference of -15µm [380, -411] was observed, with 8% (3/35) of points outside the 95% confidence interval (Figure 5-5).

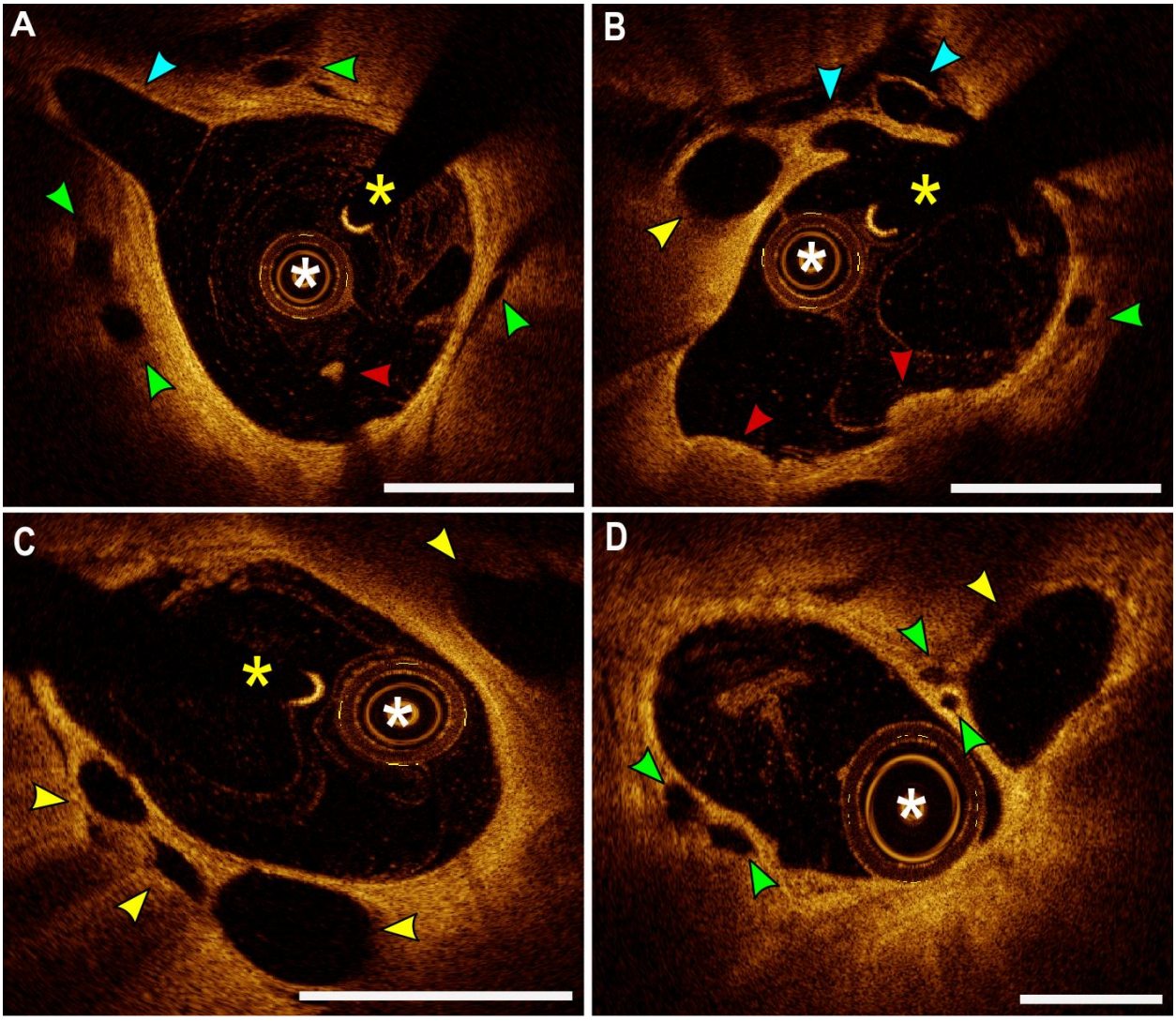

Figure 5-2: Cross sectional OCT imaging within the Superior Sagittal Sinus. (A-D) Large draining cortical veins can be observed entering the sinus (light blue arrow) with multiple adjacent dural arteries visible (green arrows), along with adjacent cortical veins outside the sinus lumen (yellow arrows). Small red thrombi (red arrows) also visible in certain sections, either free floating or attached to the sinus wall. White asterisk is the OCT lens and the yellow asterisk is the artifact from the wire. White bars = 2mm.

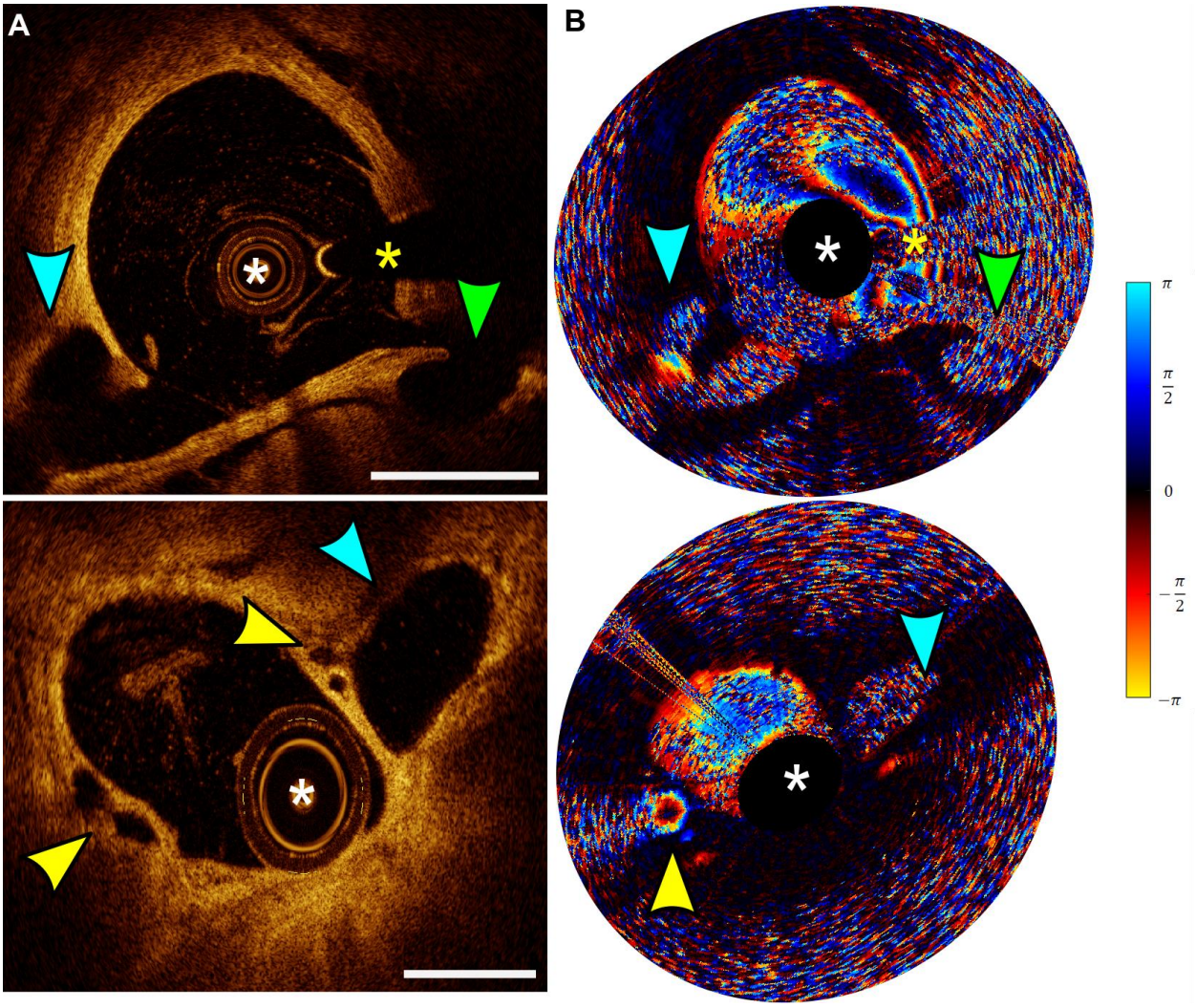

Figure 5-3: Corresponding Structural and Doppler OCT imaging. (A) Two separate structural images reveal large draining cortical veins (light blue and green arrows) along with dural arteries (yellow arrows) and **(B)** their corresponding doppler imaging with phase-shift colour map demonstrating flow in the sinus and dural arteries. White asterisk is the OCT lens and the yellow asterisk is the artifact from the wire. White bars = 2mm.

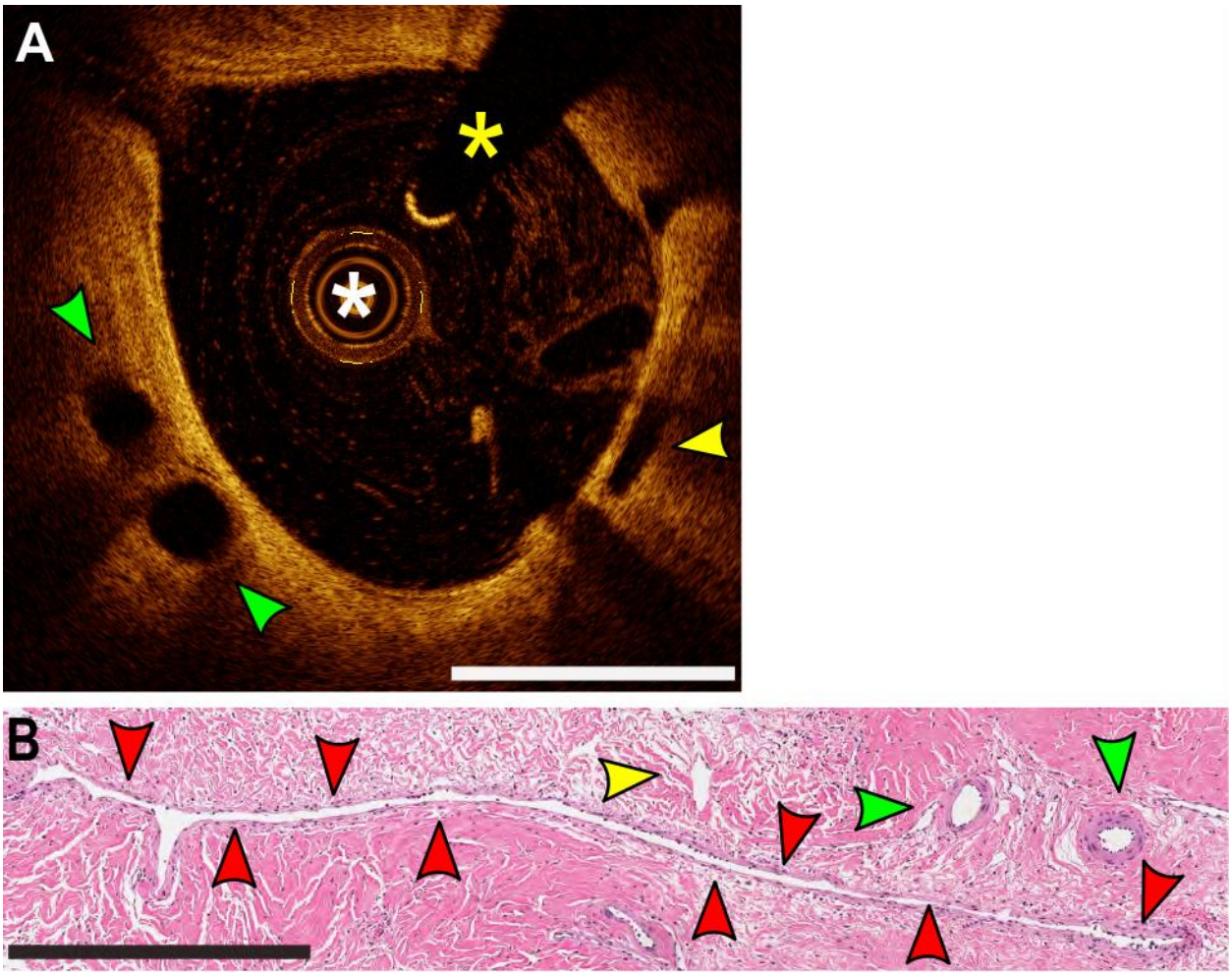

Figure 5-4: Structural OCT imaging and Corresponding Histological Section. (A) OCT showing two dural arteries (green arrows) and a dural venule (yellow arrow). **(B)** Histological cross section with H&E staining. The sinus is collapsed and the lumen outlined with red arrows, along with adjacent arterioles (green arrows) and a venule (yellow arrow). White asterisk is the OCT lens and the yellow asterisk is the artifact from the wire. White bars = 2mm. Black scale bar=500µm.

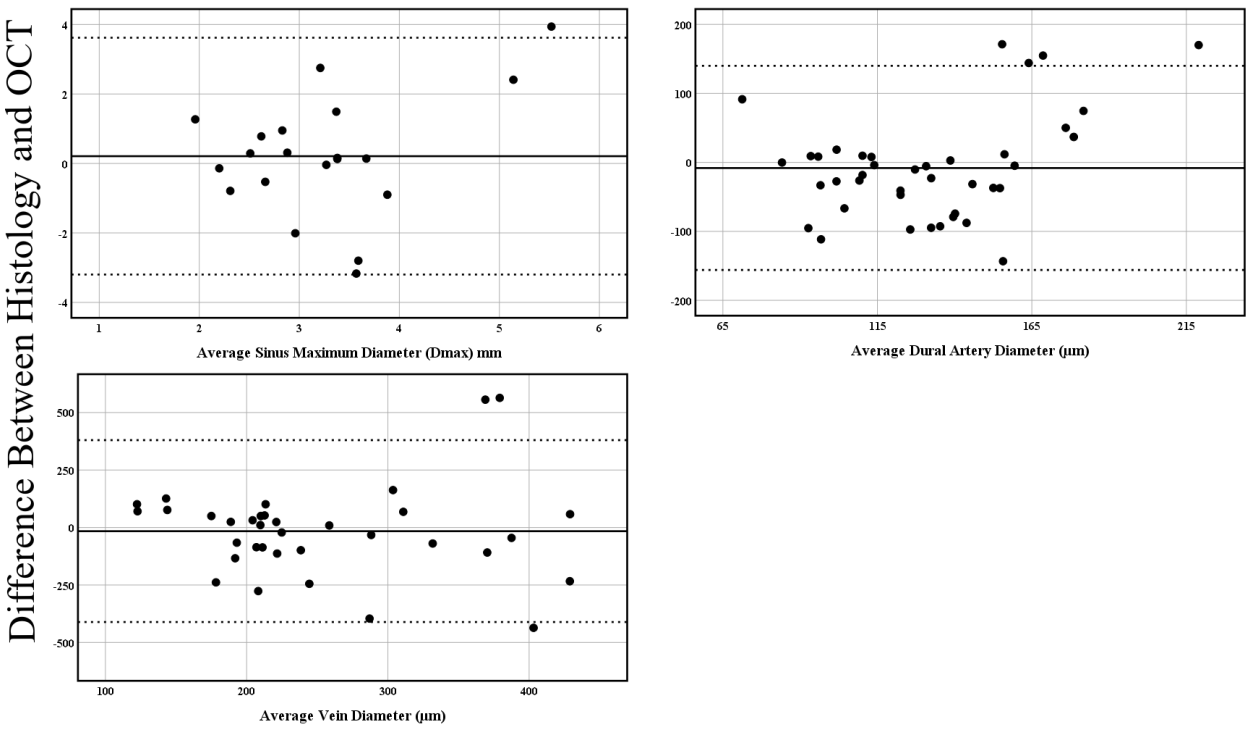

Figure 5-5: Bland Altman Plots Comparing OCT and Histology. (A) Sinus maximum diameter mean difference with 1.96 and -1.96 SD (mean, [SD]) of 0.21 mm [3.62, -3.19], and 10% (2/20) of points outside the 95% confidence interval. (**B)** Dural arteriole diameter with a mean difference of -8µm [140, -157], and 10% (4/40) of points outside the 95% confidence interval. **C)** Venule diameter with a mean difference of -15µm [380, -411], and 8% (3/35) of points outside the 95% confidence interval.

5.4 Discussion

The goal of this study was to test the hypothesis that endovascular optical coherence tomography can characterize the cerebral venous sinus luminal environment and visualize draining cortical veins and dural arteries with near histologic accuracy. In this pre-clinical swine study, OCT imaging was found to be technically feasible with luminal blood clearing through a single arterial injection, and accurate when compared to histology findings.

The first described use of intravascular imaging of the cerebral venous sinuses was by Tsumoto *et al.* in 2003. They described IVUS imaging in a patient with sigmoid sinus re-stenosis after stenting for venous hypertension, and identified intimal proliferation over the stent causing the stenosis (Tsumoto et al. 2003). Radvany *et al.* demonstrated for the first time using IVUS that transverse sinus stenosis in two patients with IIH was the result of intraluminal abnormalities (echogenic material within the sinus) and not extrinsic compression from raised intracranial pressure (Radvany et al. 2011). Several authors have since described the utilization of IVUS as a diagnostic tool and treatment adjunct for patients with IIH, particularly highlighting the inability of CTV/MRV or even DSA to differentiate thrombus and structural stenosis, and select proper stent sizes (Mokin et al. 2013, Buell et al. 2018, Yan et al. 2019).

To our knowledge, cerebral venous sinus imaging with OCT has not been previously reported in humans or in pre-clinical animal studies. Gounis *et al.* in 2018 described the utilization of optical coherence tomography in neurointerventional surgery (Gounis, Ughi et al. 2018). Current arterial applications of OCT include: visualizing stent-vessel interactions during carotid stenting and

flow-diversion for aneurysmal embolization, characterizing intracranial atherosclerotic disease, and after endovascular thrombectomy to assess for residual thrombus (Griessenauer, Gupta et al. 2017, Dohad, Zhu et al. 2018, Pasarikovski et al. 2019, Pasarikovski, Ramjist et al. 2019, Xu et al. 2020).

Optical coherence tomography has approximately 10 times the spatial resolution of IVUS, producing much higher quality images enabling improved visualization of the lumen, venous sinus wall, draining cortical veins, and dural arteries (Figure 5-6). This improved visualization has great potential with respect to aiding in the diagnosis and treatment of patients with cerebral venous pathology. Abnormalities such as sinus septations and luminal thrombus can be visualized readily. The potential applications of endovascular OCT in treating diseases of the CVS is boundless. For example, it is hypothesized that the near histologic accuracy of OCT in detecting and characterizing dural arteries could be used for image-guided ablation of arterial feeders in a dural AV fistula (Figure 5-7).

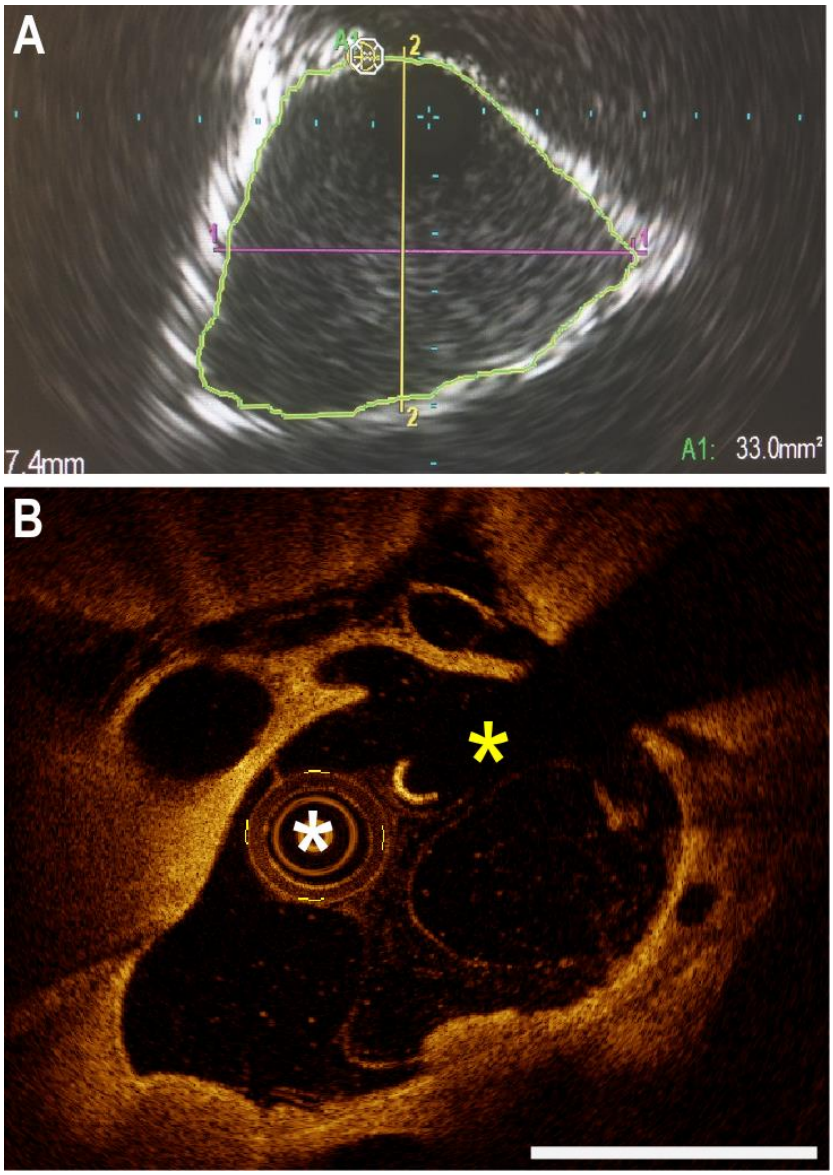

Figure 5-6: Comparision of IVUS and OCT in the Sagittal Sinus. Adapted from (Boddu, Gobin et al. 2018). **(A)** IVUS of human superior sagittal sinus imaging to determine maximal diameter and circumference, and **(B)** swine structural OCT imaging of the superior sagittal sinus. Although direct anatomic comparision cannot be made, OCT can clearly provide improved visualization of the sinus lumen and adjacent vessels. White asterisk is the OCT lens and the yellow asterisk is the artifact from the wire. White bars = 2mm.

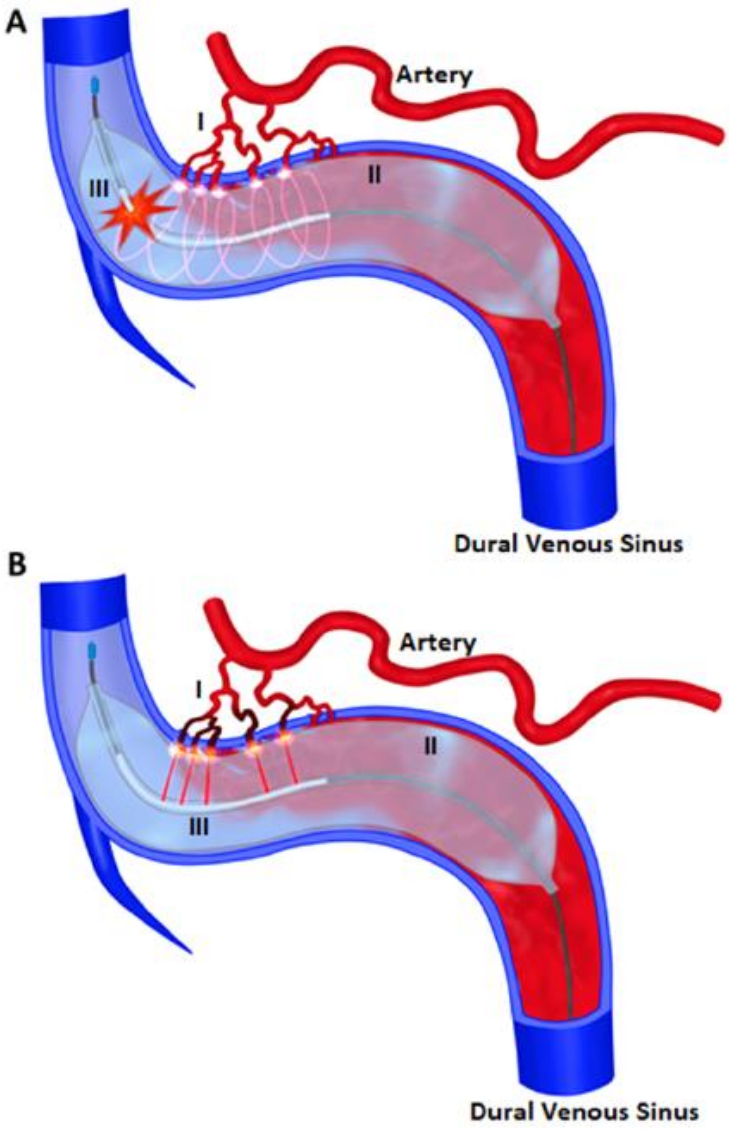

Figure 5-7: Dural Arteriovenous Fistula imaged and Treated using OCT. Adapted from (Pasarikovski, Cardinell et al. 2019)**. (A)** The OCT device is navigated into the dural venous sinus and through a transparent dual-lumen balloon **(II)**, optical imaging is undertaken **(III)** to identify the exact spatial position of arterial feeders **(I)** into the dural venous sinus. **(B)** Laser ablation of the arterial feeders is accomplished under image guidance through the saline-filled balloon. The arterial feeders **(I)** previously identified now undergo image-guided laser ablation **(III)** through the transparent dual lumen balloon **(II).**

In this swine model, clearing blood within the sinus lumen for OCT acquisition was achieved with an arterial injection. The authors could not place a large-gauge catheter (≥5 French) in the swine sinus (distal IJ or sigmoid) to try and clear luminal blood directly, as the swine sinus diameter is small. On the other hand, it is likely that in human imaging the sinus blood can be cleared with an intravenous injection through a guide catheter positioned in the sinus.

There are several limitations to this study. First, OCT was tested in swine whereas the human CVS are larger with the possibility of increased tortuosity, and therefore difficult navigation of the OCT catheter is possible in certain patients. Second, the safety of OCT in human imaging needs to be further studied. Although the OCT catheter is delivered via monorail technique over a 0.014" wire, venous perforation is possible via the stiff catheter tip.

5.5 Conclusions

Endovascular optical coherence tomography imaging was technically feasible in this pre-clinical swine study. Adoption of this imaging modality in the human cerebral venous sinus could help aid in the diagnosis, treatment, and understating of pathophysiology of dAVF, CVST, and IIH. Human safety and feasibility studies are needed.

Chapter 6: Mechanical Thrombectomy and Intravascular Imaging for Cerebral Venous Sinus Thrombosis: Preclinical Model

This chapter is based on the following work, with full reprint permission from *The Journal of Neurosurgery.*

Pasarikovski, C. R. *et al.* Mechanical thrombectomy and intravascular imaging for cerebral venous sinus thrombosis: a preclinical model. *Journal of neurosurgery*, 1-6, doi:10.3171/2020.6.JNS201795 (2020).

6.1 Introduction

Cerebral venous sinus thrombosis (CVST) is a rare type of stroke accounting for 1% of all strokes (Bousser and Ferro 2007). Anticoagulation remains the cornerstone of treatment for CVST (Saposnik, Barinagarrementeria et al. 2011). The majority of patients will clinically improve with systemic anticoagulation, however up to 13% experience ongoing morbidity and mortality (Ferro, Canhao et al. 2004). In 2015 Siddiqui *et al.* conducted the largest systematic review comprising 185 patients undergoing endovascular thrombectomy (EVT) for medically refractory CVST (Siddiqui, Dandapat et al. 2015). Overall 84% of patients had favourable outcome (modified Rankin scale (mRs) score 0-2), and 25% of patients had no/partial recanalization of the sinus (Siddiqui, Dandapat et al. 2015). In the analysis, the AngioJet rheolytic catheter (Boston Scientific, Marlborough, MA) was the most commonly used thrombectomy device in 40% of procedures. This device, along with several other devices used to treat CVST (AngioJet, Fogarty Embolectomy Device, Wires), have become less commonly utilized as the technology and techniques for EVT have evolved considerably over the past decade (Pierot and Derdeyn 2015).

Currently, there is limited data regarding recanalization rates and outcomes in patients with CVST undergoing thrombectomy with modern endovascular devices. The Society of Neurointerventional Surgery (SNIS) 2018 guidelines report insufficient evidence to recommend optimal endovascular devices/approaches (pharmacological thrombolysis, direct aspiration, stent retriever, balloon thrombectomy, balloon angioplasty/stenting) for medically refractory CVST (Lee, Mokin et al. 2018). The authors hypothesize that repurposed arterial thrombectomy devices

may not perform as expected in the cerebral venous sinus. Several anatomic differences exist between the cerebral venous sinus and arteries, including increased luminal diameter and vessel wall structure. The sinus wall is composed of endothelium and elastic lamina, lacking the smooth muscle found in arteries (Adeeb, Mortazavi et al. 2012). Furthermore, contrary to arterial stroke research, the preclinical models utilized to test various endovascular techniques and devices are lacking.

To the author's knowledge, there are no preclinical EVT models for CVST. The purpose of this research was to develop a reliable preclinical animal model for the testing of endovascular strategies to treat CVST. We describe a swine model of endovascular cerebral sinus thrombosis, subsequent endovascular thrombectomy, and intravascular imaging with optical coherence tomography (OCT) to assess the luminal environment after EVT. It was hypothesized that direct visualization of residual sinus thrombus, sinus injury, and bridging cortical vein thrombosis can be possible with OCT.

6.2 Methods

All experiments were conducted according to the policies and standards established by the author's institutional animal research ethics board. Five consecutive male Yorkshire Swine weighing 45 kg were utilized. There was no pre-screening imaging of venous anatomy for any animal. All procedures were carried out under general anesthetic with continuous hemodynamic monitoring.

A dedicated animal interventional radiology suite equipped with a single-plane C-Arm (Philips, Andover, MA) was used for all procedures. Ultrasound guided right femoral punctures were performed and a 6 French (F) sheath was inserted into the right common femoral artery, and another 6F sheath into the right femoral vein. A 6F Envoy (Codman, Boston, MA) guide catheter was navigated into the right ascending pharyngeal artery under roadmap technique, ensuring the guidewire does not enter the rete mirabile to avoid vasospasm of these vessels. A cerebral angiogram was performed demonstrating the venous drainage system. Next, a second 6F Envoy was navigated into the right internal jugular vein.

The cerebral venous drainage in swine is similar to humans; however the sinuses drain primarily via the spinal venous plexus and not the internal jugular vein (Fries et al. 1992). Therefore to reveal the connection between the internal jugular vein and sigmoid sinus, a simultaneous hand injection of contrast via the Envoy stationed in the right internal jugular vein was performed during the late venous phase pump injection from the ascending pharyngeal artery (Figure 6-1A). Under roadmap technique, a Transcend 0.014" microwire (Stryker, Kalamazoo, MI) was navigated into the superior sagittal sinus (Figure 6-1B).

Sinus Thrombosis

An SL-10 microcatheter (Stryker, Kalamazoo, MI) was navigated into the superior sagittal sinus using the Transcend wire. Super selective angiographic runs were performed via the SL-10 to reveal the sinus anatomy (Figure 6-2A). A HyperForm balloon (Medtronic, Minneapolis, Minnesota) was also navigated into the sinus under roadmap technique and stationed just

proximal to the SL-10 tip (Figure 6-2B). The balloon was inflated and contrast injections via the SL-10 confirmed occlusion of the sinus (Figure 6-2C/D). Following confirmation, swine thrombin (Sigma-Aldrich, St. Louis, Missouri) 150-200 units was slowly injected over 20 minutes through the SL-10 while the balloon remained inflated. After 20 minutes the balloon was deflated and removed. Arterial pump runs and super selective sinus runs confirmed the sinus thrombosis (Figure 6-3A/B). If insufficient thrombosis was achieved, the above steps were repeated.

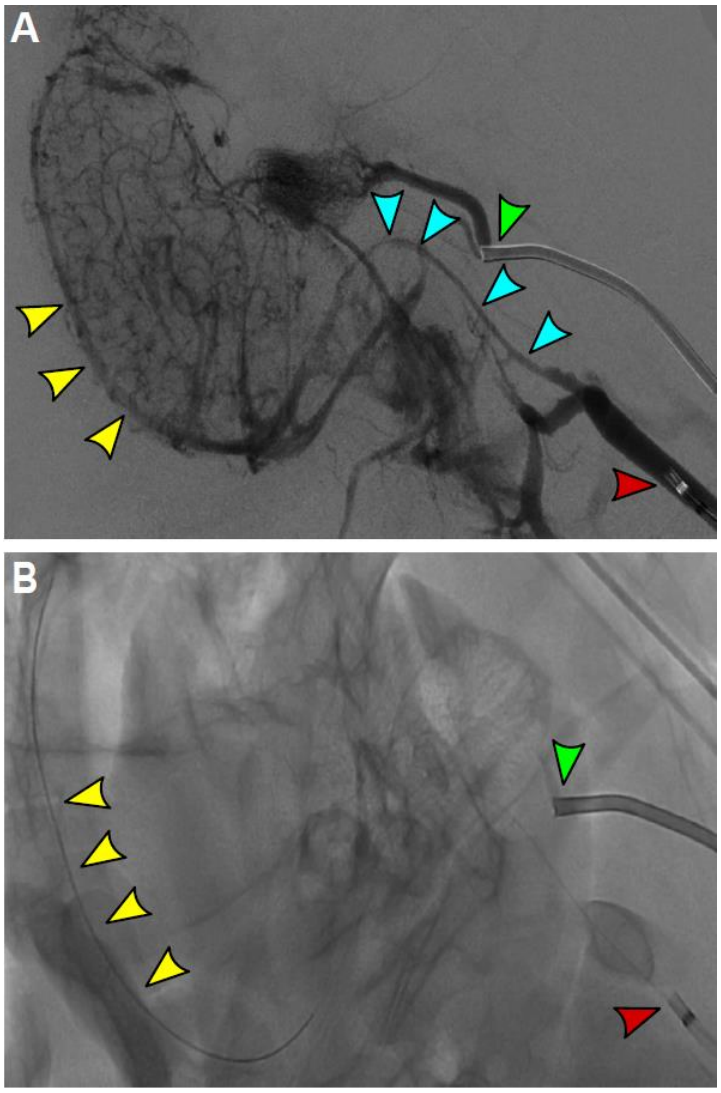

Figure 6-1: Swine Cerebral Venous Sinus. (A) Combined arterial and venous diagnostic angiography injections via a guide catheter in the ascending pharyngeal artery (green arrow) and the internal jugular vein (red arrow) revealing the connection between the internal jugular vein and sigmoid sinus (blue arrows) and the superior sagittal sinus (yellow arrows). **(B)** Transcend microwire stationed in the proximal third of the superior sagittal sinus (yellow arrows) via the right internal jugular (red arrow).

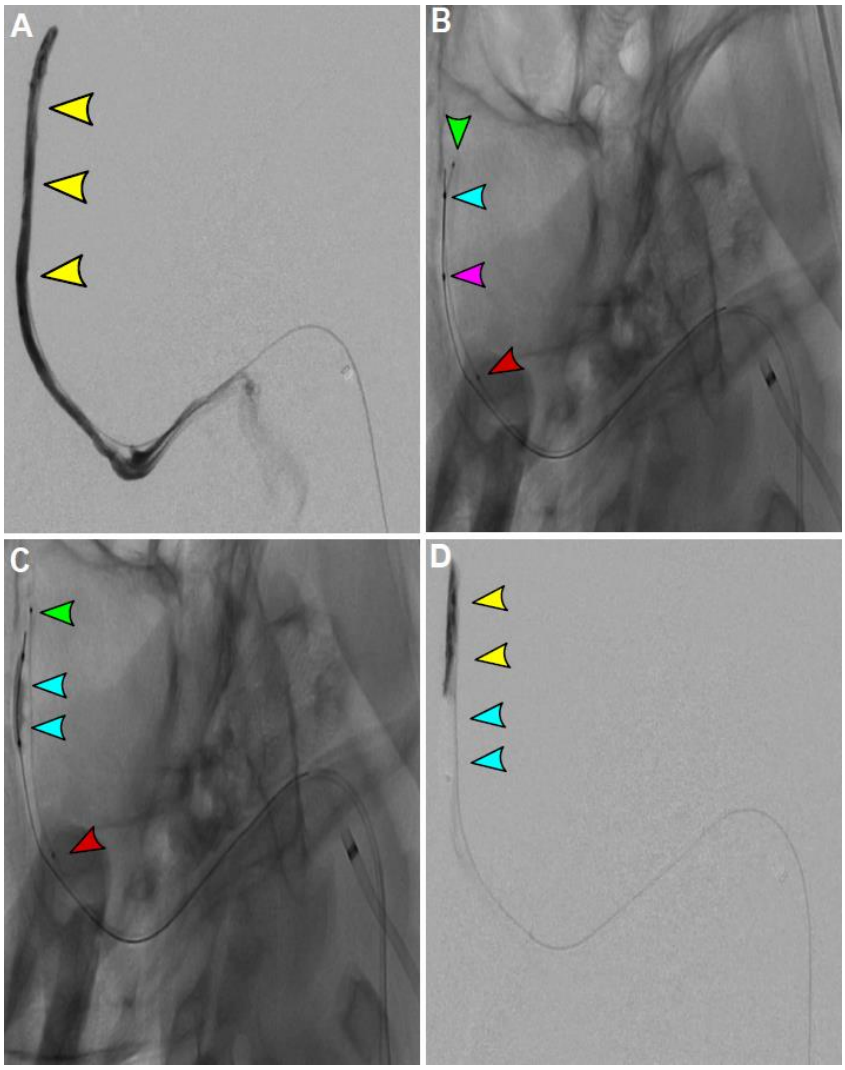

Figure 6-2: Swine Cerebral Venous Sinus Thrombosis. (A) Super selective microcatheter injection of the superior sagittal sinus (yellow arrows) outlining the sinus. **(B)** A HyperForm balloon deflated with proximal (purple arrow) and distal (blue arrow) markers visible, along with the proximal (red arrow) and distal (green arrow) markers of the SL-10. **(C)** Inflated HyperForm balloon (blue arrows) and proximal (red arrow) and distal (green arrow) markers of the SL-10. **(D)** Sinus occlusion confirmed with a microcatheter injection just proximal to the balloon occlusion (blue arrows) showing contrast pooling only proximal to the balloon (yellow arrows).

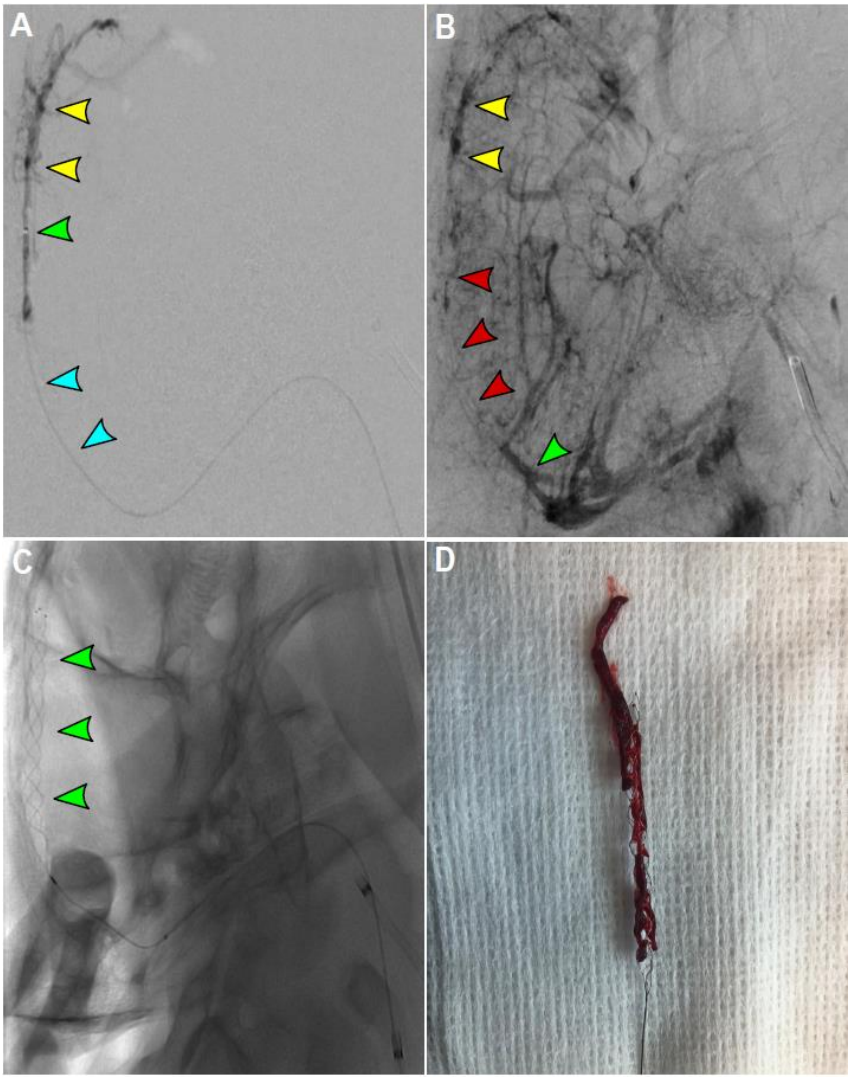

Figure 6-3: Endovascular Thrombectomy for Sinus Thrombosis. (A) The HyperForm balloon has been removed and microcatheter injection reveals filling of the proximal sinus (yellow arrows) and sinus occlusion. The distal SL-10 marker (green arrow) is visible along with the catheter outline (blue arrows). **(B)** Venous phase cerebral angiography injection via the ascending pharyngeal revealing the occluded sinus segment (red arrows) with ongoing filling of the proximal superior sagittal sinus (yellow arrows) and torcula (green arrow). **(C)** Second-generation stent retriever (green arrows) unsheathed in the sinus to perform endovascular thrombectomy of the occluded SSS. **(D)** The retrieved thrombus within the stent retriever.

Endovascular Thrombectomy

Endovascular thrombectomy was performed within 1 hour of sinus occlusion. A Trevo-18 microcatheter (Stryker, Kalamazoo, MI) was navigated into the sinus beyond the occlusion. A Trevo XP Stent Retriever (Stryker, Kalamazoo, MI) 6 X 25mm was deployed for 5 minutes (Figure 6-3C). The stent was subsequently retrieved into the Envoy and removed to examine for thrombus (Figure 6-3D). Repeated arterial pump injections were done to confirm successful thrombectomy (Figure 6-4A). Successful thrombectomy was defined as complete recanalization of the sinus using standard anterior/posterior and lateral angiography. If ongoing occlusion or residual thrombus remained, repeated attempts were made to remove the thrombus.

Optical Coherence Tomography Imaging

Intravascular OCT imaging was done before and immediately following thrombectomy. The Dragonfly^{TM} OCT catheter (Abbott Vascular, Chicago, IL) was used for image acquisition. The OCT catheter was navigated into the sinus via monorail technique over the Transcend microwire (Figure 6-4B). The following steps were sequentially followed for image acquisition: 1) Load an automated injection pump with 150 mL mixture of 50:50 contrast and saline. The pump is connected to the Envoy catheter in the ascending pharyngeal artery. This is used to clear the blood within the sinus lumen during OCT image acquisition, 2) Inject 3mL per second for 8 seconds total (24 mL total) via the pump, 3) Enable manual OCT pullback mode and initiate the pullback manually once the lumen begins to clear. The OCT catheter performs the motorized

automated pullback of 54 mm total. OCT imaging frequency is 100 frames per second, with a total of 540 cross sectional images generated per pullback.

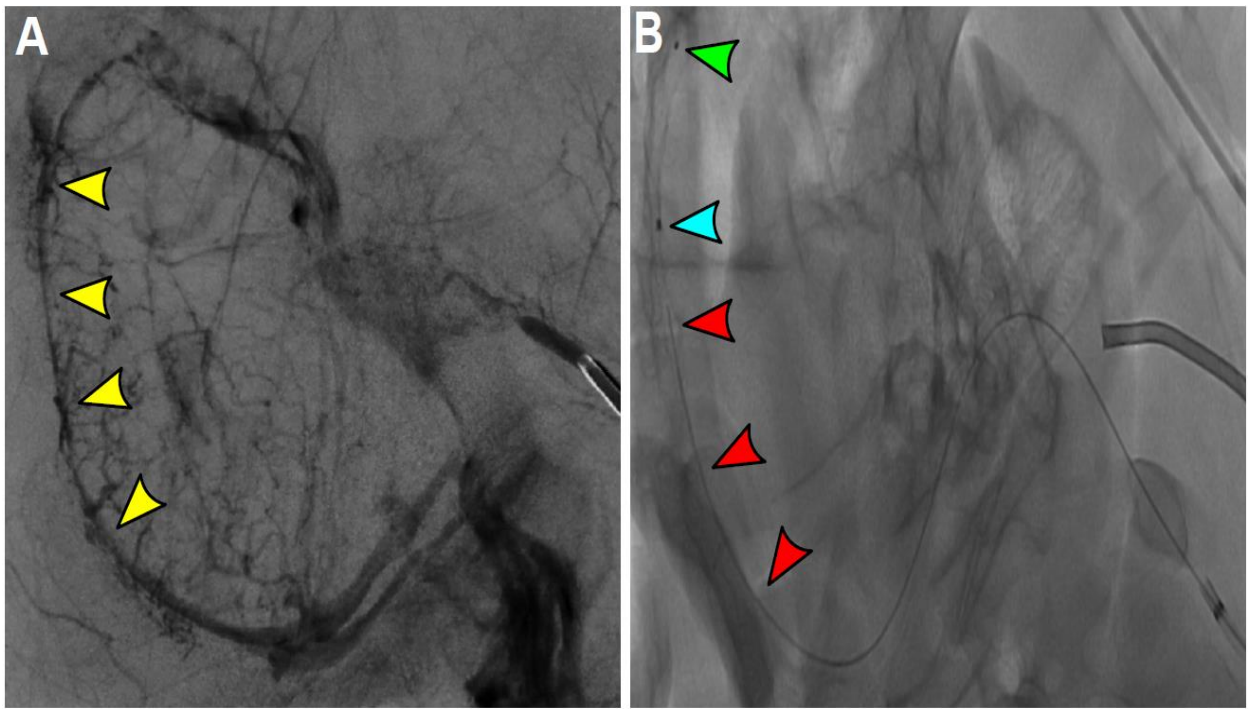

Figure 6-4: Post Thrombectomy imaging with Angiography and OCT. (A) Angiography demonstrating patency of the sinus (yellow arrows) after thrombectomy. **(B)** Optical coherence tomography catheter navigated into the sinus via monorail technique over a 0.014" wire. The distal marker (green arrow), lens marker (blue arrow), and fiber optic wire (red arrows) are visible.

6.3 Results

Thrombosis of superior sagittal sinus, mechanical thrombectomy, and subsequent OCT imaging was technically successful in 4/5 swine. In swine 3 there were suspected valves in the bilateral internal jugular veins that could not be crossed with either a microwire or microcatheter. Various techniques and attempts including venous injections with saline to collapse the valves were unsuccessful. In the remaining 4 swine access into the sinus was straightforward. Thrombosis was induced in 3/4 swine with a single thrombin injection, and one swine required a second injection of 100 units over 20 minutes. Recanalization of the sinus with a second-generation stent retriever was successful after one attempt in all swine. OCT imaging after thrombectomy revealed regions of normal sinus anatomy (Figure 6-5A). A thin layer of endothelium over dense connective tissue was observed, with bridging cortical veins draining into the sinus (Figure 6-5A). In addition, regions of residual sinus luminal thrombus were observed despite complete angiographic recanalization (Figure 6-5B). Thrombosed bridging cortical veins were also observed (Figure 6-5C/D) before draining into the sinus.

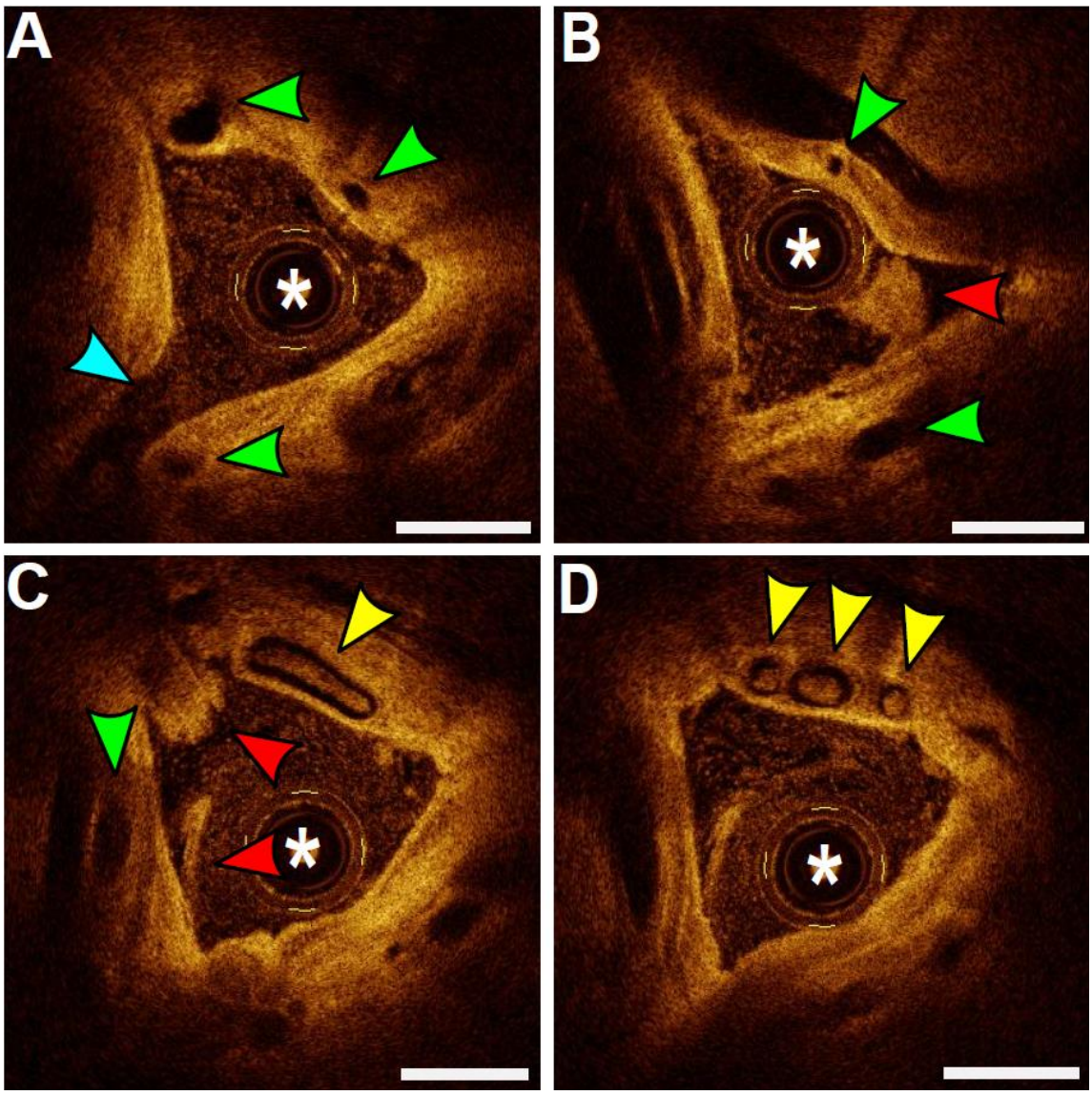

Figure 6-5: OCT imaging of the Superior Sagittal Sinus after Thrombectomy. (A) OCT imaging before mechanical thrombectomy showing the normal sinus anatomy. Draining cortical veins (blue arrow) into the sinus and bridging cortical veins adjacent to the sinus (green arrows) are visible. **(B-D)** OCT imaging after thrombectomy showing evidence of residual sinus luminal thrombus (red arrows), patent cortical veins (green arrows), and evidence of ongoing thrombosed bridging cortical veins (yellow arrows). White bar = 2mm. Asterisk (*) is OCT lens artifact.

6.4 Discussion

The authors describe the first preclinical animal model for cerebral venous sinus thrombosis and mechanical thrombectomy. In addition, using intravascular optical coherence tomography the luminal environment can be visualized after thrombectomy to assess the efficacy of the endovascular technique and devices utilized for recanalization. With this study, we were able to confirm the presence of ongoing thrombosis of bridging cortical veins despite recanalization of the cerebral venous sinus, as one putative reason for poor patient outcome despite a successful procedure.

The goals of management of CVST include treating the underlying thrombophilia, controlling raised intracranial pressure when present, halting the propagation of venous thrombosis, and recanalizing the sinus. Two randomized trials have shown that the initiation of early anticoagulation with unfractionated heparin (UFH) or low molecular weight heparin (LMWH) appears to be safe and is associated with a decreased risk of morbidity and mortality (Einhaupl et al. 1991, de Bruijn and Stam 1999). The authors hypothesize that in patients presenting with CVST without severe neurological deficits, and therefore unlikely to have high burden of venous congestion and raised intracranial pressure, halting the progression of sinus thrombus with anticoagulation should allow the circulatory system time to remove the thrombus physiologically. The majority (approximately 87%) of patients will fall in this category and have good outcomes (Ferro, Canhao et al. 2004). However, a portion of patients will present in either a comatose state or continue to deteriorate clinically despite early anticoagulation. In these patients, it is likely that the burden of sinus and bridging cortical vein thrombus has exceeded the

brains ability to compensate, leading to significant compromise of venous drainage, venous infarcts, and raised intracranial pressure. In these cases, along with treating the underlying thrombophilia, timely thrombolysis (not merely halting propagation of sinus thrombus with anticoagulation) may be beneficial.

Several authors have described endovascular thrombolysis in this group of patients who deteriorate despite anticoagulation or present with coma, altered mental status, intracranial hemorrhage, or deep venous thrombosis (Stam et al. 2008, Siddiqui et al. 2014). These small case series may be subject to publication bias. The only proposed randomized controlled trial by Coutinho *et al.* to assess if endovascular thrombolysis improves the functional outcome of patients with a severe form of CVST was halted in 2017 for futility (Coutinho et al. 2013).

We suggest that before this important clinical question is assessed in a trial, reliable preclinical testing of techniques and devices must be undertaken. Considering CVST's unique pathophysiology and large clot burden, the simple repurposing of arterial thrombectomy techniques and devices does not seem to work as intended. CVST is its own disease and may require a tailored approach. The literature describing device testing for arterial stroke is vast and comprehensive, and it is likely the same level of innovation will be required to refine devices and techniques for CVST treatment (Herrmann et al. 2019). For example, venous clot shape, composition, total burden, and the interaction with devices, sinus wall anatomy, and overall dimensions may differ significantly from arterial stroke models.

Furthermore, in this study evidence of residual sinus luminal thrombus was observed along with ongoing thrombosis of bridging cortical veins despite recanalization. This was seen on intravascular OCT but not apparent on cerebral angiography. Mechanical thrombectomy with a stent retriever may be able to recanalize the sinus but will not be effective addressing thrombus in adjacent bridging cortical veins. Modern devices cannot access cortical veins safely, and the risk of perforation is likely high. The authors' hypothesize that if bridging cortical vein thrombus is observed after mechanical thrombectomy, direct intra-sinus chemical thrombolysis may be warranted to dissolve the remaining clot. Patency of the sinus without patency of bridging veins (particularly if the vein drains an eloquent or large portion of the cerebral cortex) is unlikely to be beneficial. In addition, residual thrombus within the sinus may lead to re-occlusion. These findings highlight the utility of intravascular imaging to visualize the luminal environment after thrombectomy (Pasarikovski, Ramjist et al. 2019, Pasarikovski, Keith et al. 2020).

The majority of previously published animal CVST models surgically expose the superior sagittal sinus and produce sinus thrombosis via either surgical ligation, injection of thrombotic material directly into the sinus, or topical application of ferric chloride. Wang *et al*. in 2010 are the only group to describe a transvenous technique to occlude the sinus (Wang, Tan et al. 2010). They described pre-screening swine with cerebral angiography and performed occlusion of the sinus in specimens with favorable anatomy, found in half of their animals. As the techniques and endovascular devices have improved over the past decade, the authors here describe a technique to reliably thrombose the sinus and perform thrombectomy without pre-screening. We acknowledge that primate anatomy most closely resembles the human cerebral venous drainage, however there are significant limitations to access to primates, and it is difficult to justify primate

experiments for device/technique testing. Furthermore, this preclinical model was utilized to examine the efficacy of a second-generation stent retriever with respect to sinus recanalization. Other thrombectomy devices such as aspiration catheters, balloons, and combination techniques can be tested given the relatively straightforward access into the sinus. Pharmacologic therapy with thrombolytics could also be assessed. If large-bore devices are tested, larger swine may be needed to accommodate the catheters.

There are several limitations to this preclinical model. The proposed preclinical CVST model describes sinus occlusion and subsequent thrombectomy and intravascular imaging. Although sinus recanalization is an important metric in the treatment of CVST, its use as a surrogate for clinical outcome is limited. Future studies are needed to evaluate which patients would benefit most from endovascular treatment for CVST based on neurological outcome. The thrombus in the swine sinus did not occur spontaneously, and therefore the thrombus may have different composition and mechanical properties compared to spontaneous human thrombus. Furthermore, to conduct the experiments at minimum a C-Arm with roadmap capabilities is required, along with an experienced neurointerventionalist.

6.5 Conclusion

We describe a preclinical model to assess endovascular techniques and devices for the treatment of cerebral venous sinus thrombosis. Repurposed devices from arterial stroke may not perform as expected given the unique features of venous sinus thrombosis. Residual bridging cortical vein thrombus and residual sinus thrombus, visualized on intravascular OCT, may be present despite

complete sinus recanalization on angiography, and this may be the etiology of poor clinical outcome despite technical success. This model may be helpful in developing and testing a new generation of devices designed specifically for CVST treatment.

Chapter 7: Optical Coherence Tomography Imaging after Endovascular Thrombectomy for Basilar Artery Occlusion

This chapter is based on the follow work, with full reprint permission from *The Journal of Neurosurgery.*

Pasarikovski, C. R., Ramjist, J., da Costa, L., Black, S. E. & Yang, V. Optical coherence tomography imaging after endovascular thrombectomy for basilar artery occlusion: report of 3 cases. *Journal of neurosurgery*, 133:1141–1146, 2020.

7.1 Introduction

Endovascular thrombectomy (EVT) has become the standard of care for eligible patients with acute ischemic stroke secondary to proximal large vessel occlusion (Powers, Rabinstein et al. 2018). Second-generation stent retrievers have emerged as the preferred endovascular tool for revascularization (Pierot, Soize et al. 2015). These devices produce shear and stress forces on the vessel wall during clot retrieval, and the endothelial layer in direct contact with the device is particularly vulnerable to injury. Studies evaluating for endothelial damage after EVT have been done by means of retrieved human clot, magnetic resonance vessel-wall (MRVW) imaging, and animal histopathologic studies (Gounis, Wakhloo et al. 2013, Singh, Doostkam et al. 2013, Power, Matouk et al. 2014). These techniques all have limitations, as MRVW imaging has insufficient spatial resolution to directly visualize endothelial injury, and histopathologic examinations are *ex-vivo* and unable to provide real-time patterns of injury (Teng, Pannell et al. 2015).

Endovascular optical coherence tomography (OCT) imaging is the highest-resolution intravascular imaging modality currently available. This technology has traditionally been utilized in interventional cardiology, and more recently applied in neurointerventional surgery (Gounis, Ughi et al. 2018). OCT utilizes near-infrared light with a wavelength of approximately 1.3μm and excellent intraluminal spatial resolution of 10-20 μm is achievable (Tearney, Regar et al. 2012).

Understanding the mechanism of endothelial injury after EVT is vital, as the blood vessel endothelium is known to play a pivotal role in regulating inflammatory pathways, permeability of the blood-brain barrier, and thrombosis (Pearson 1999). In an attempt to investigate for endothelial injury, our first objective was conducting an animal feasibility study of intraluminal imaging after EVT using OCT at one, three, and six hours after vessel occlusion with thrombus. This design allowed for *in-vivo* real-time imaging of the lumen immediately after EVT, while evaluating whether prolonged arterial exposure to thrombus increases endothelial injury. We utilized a swine stroke model, and found that revascularization and OCT imaging was feasible for all 9 vessels tested (Chapter 4) . Endothelial denudation was present in 65 ±16%, 87 ±8%, and 93 ±7% of the vessel surface 1, 3, and 6 hours after thrombus deposition and subsequent EVT, respectively. Residual intraluminal thrombus was present in vessels at all time intervals despite complete angiographic revascularization. Bland-Altman plots showed excellent agreement between OCT and histologic analysis with respect to the degree of endothelial denudation and elevation, separation of the media, and hemorrhage within the media. OCT appears to be more specific in detecting endothelial elevation.

Next, with the aim of examining for evidence of endothelial injury in real-time, we report three consecutive cases of *in-vivo* OCT imaging immediately after EVT for acute ischemic stroke.

7.2 Methods

Patient History

Three consecutive patients underwent OCT imaging. Patient one was a 52 year-old male found to have BAO after presenting to a local hospital with diplopia, ataxia and vertigo. He was transferred emergently and on arrival was National Institutes of Stroke Scale (NIHSS) score 3. He was not an IVT candidate, as he was outside the 4.5 hour time window. Given low NIHSS score and the likelihood for worsening ischemia, he underwent EVT with time to puncture of 440 minutes (7.3 hours). He underwent EVT with a stent retriever with thrombolysis in cerebral infarction (TICI) grade 3 reperfusion, and arterial occlusive lesion (AOL) recanalization score of 3 achieved on the first attempt.

Patient two was a 71 year-old male with initial NIHSS score of 7. Although symptom onset was >24 hours, given the apparent perfusion dependence with worsening symptoms when upright, he was taken emergently for EVT with time to puncture of 1510 minutes (25.2 hours). He underwent EVT with aspiration device with TICI/AOL score 3 achieved on the first attempt. Patient three was an 87 year-old male presenting 5h after symptom onset with NIHSS score 14. He was found to have a partial distal basilar occlusion and complete proximal right posterior cerebral artery (PCA) occlusion. He was taken emergently for EVT with time to puncture of 330 minutes. He underwent EVT with stent retriever device with TICI/AOL score 3 achieved on the first attempt.

Optical Coherence Tomography Image Acquisition

Immediately after the EVT procedure is completed and flow restored, OCT images were obtained. The Dragonfly^{TM} OCT catheter (St. Jude Medical, Minneapolis, MN) was used for image acquisition. The following steps were sequentially followed for image acquisition: 1) Load an automated injection pump with 150 cc of heparinized saline. This is used to clear the blood within the lumen during image acquisition, 2) A 5 French distal access catheter was stationed in the right distal vertebral artery, 3) Mount the catheter on a rapid exchange guidewire and position the device such that the optical lens radiopaque marker is distal to the basilar segment with previous thrombus, 4) Infuse 4cc per second for 6 seconds via the automated pump. The OCT catheter automatically detects luminal blood-clearing and performs the motorized automated pullback of 54mm total. This was repeated a second time for each patient.

7.3 Results

Technically successful images were obtained for each patient. There were no complications (vessel dissection, perforation, or vasospasm) associated with image acquisition. In patient one the distal basilar artery beyond the previously thrombosed region appeared normal with intima, media and adventitia all discernible. The internal and external elastic lamina was also visible (Figure 7-1A). More proximally, thick concentric plaque fibrosis was present with loss of the internal and external lamina (Figure 7-2B). At the thrombectomy site, significant intraluminal residual thrombus remained (Figure 7-2C-D). The clot was predominately red clot, with high backscattering and signal attenuation. Similar findings of atherosclerotic disease and residual thrombus were present for patient two (Figure 7-3B-D). There was thrombosis of one basilar

perforator next to patent perforators (Figure 7-3B, C). Patient three did not have any evidence of residual thrombus in the basilar artery, with normal intima, media and adventitia (Figure 7-4A-B). CT angiography done within 24 hours of EVT displayed no luminal filling defects (Figure 7-5A, C). MRVW imaging done within 24 hours revealed basilar artery enhancement that was eccentric for patient one (Figure 7-5B) and concentric (Figure 7-5D) for patient two. There was no evidence of luminal thrombus present.

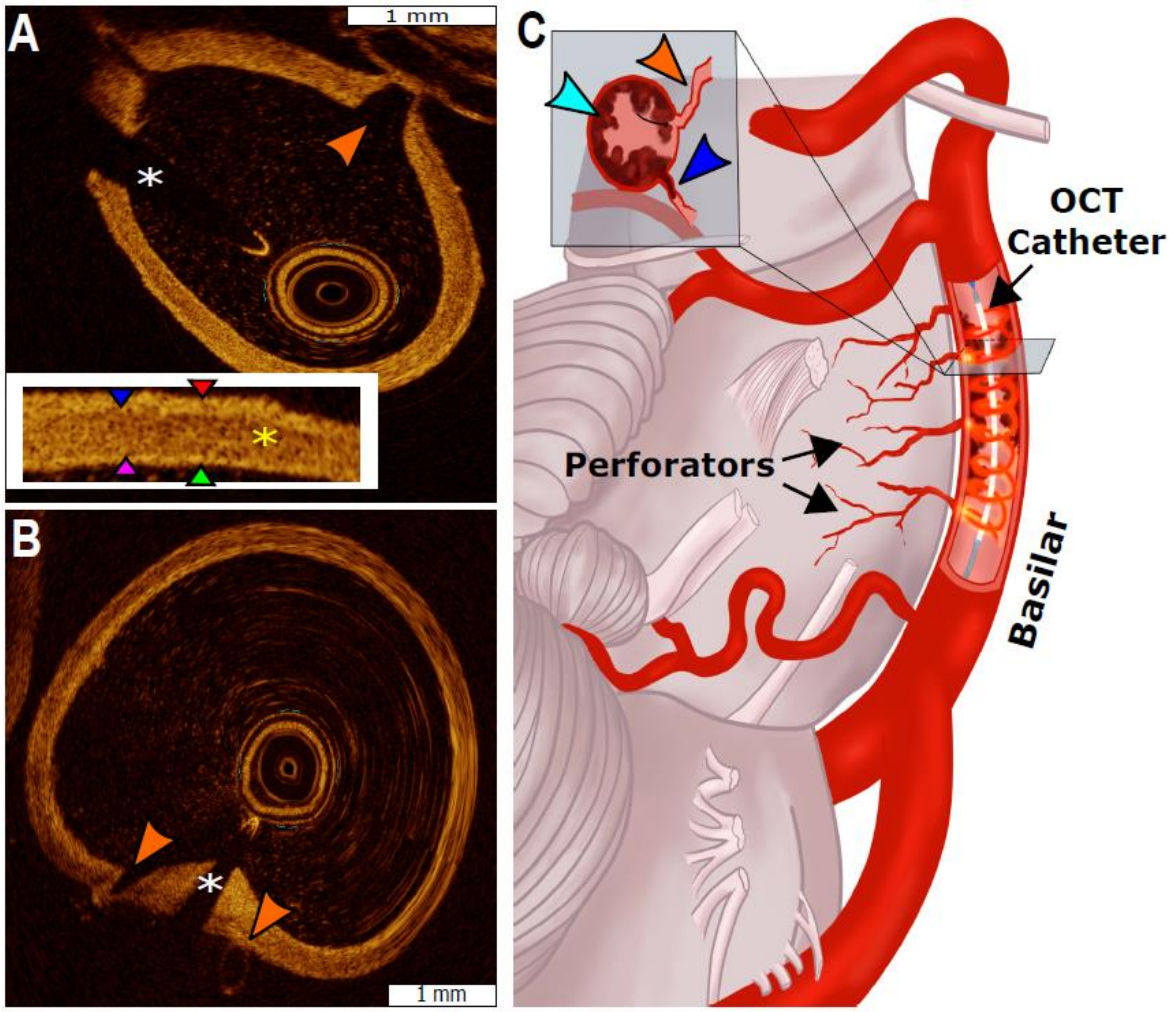

Figure 7-1: OCT Imaging of the Basilar Artery. (A) Distal basilar of patient one appearing normal with intima (green arrow head), media (yellow asterisk) and adventitia (red arrow head) all discernible. The internal (purple arrow head) and external elastic lamina (blue arrow head) was also visible. A perforator is also visible (orange arrow). **(B)** Distal basilar of patient two appearing normal with visible perforators (orange arrow head). **(C)** The OCT catheter positioned in the basilar artery such the optical lens marker is beyond the arterial region of interest. A cross section is shown depicting residual thrombus (light blue arrow), patent perforator (orange arrow), and thrombosed perforator (dark blue arrow). **Abbreviations**: OCT=optical coherence tomography. White asterisk (*) denotes the wire and the shadow produced from the wire.

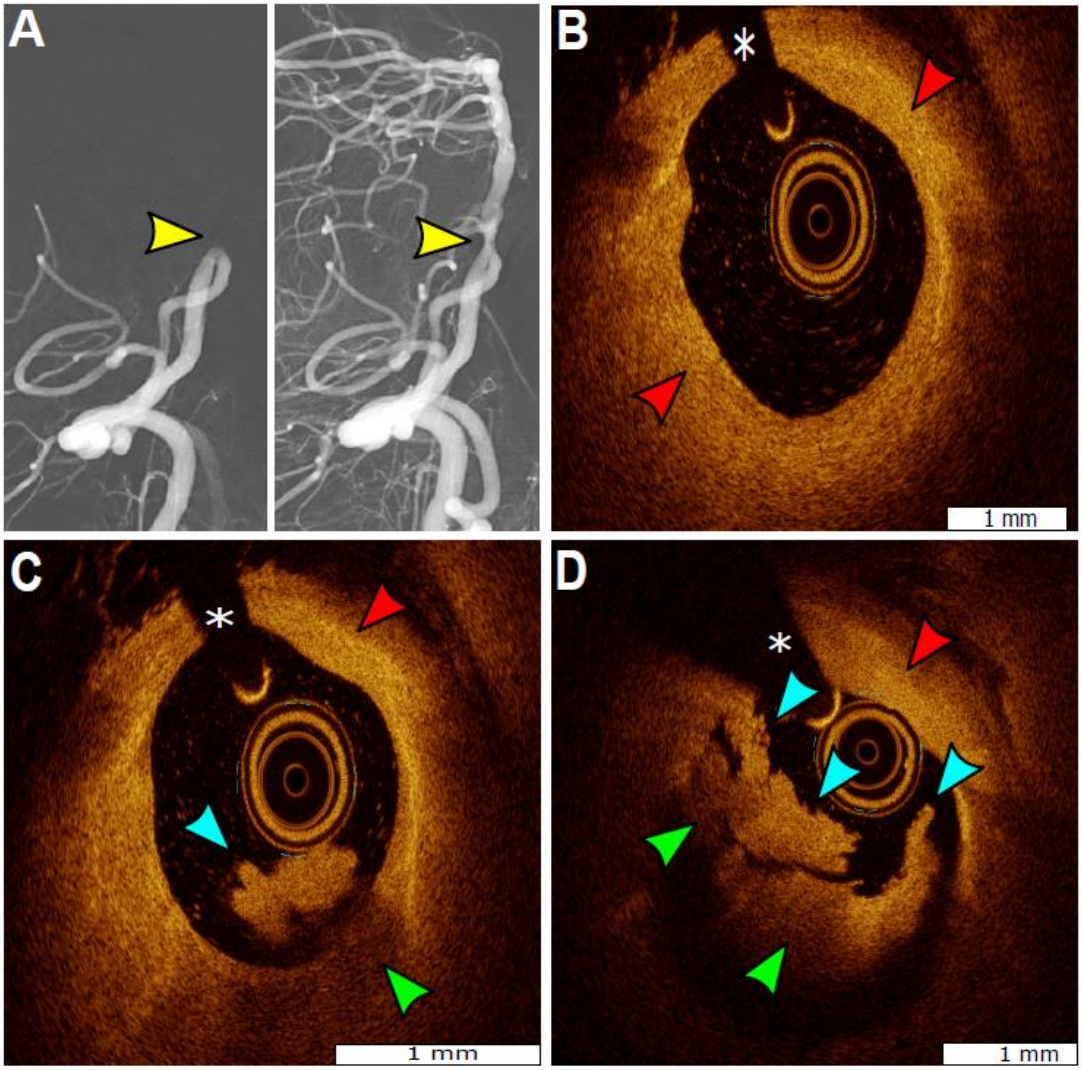

Figure 7-2: Patient 1 Angiographic and OCT imaging. (A) Angiogram demonstrating complete basilar occlusion (yellow arrow) and TICI 3 reperfusion after thrombectomy**. (B)** Thick plaque fibrosis was present (red arrows) causing concentric outward remodelling and loss of normal vessel architecture, and no internal and external lamina**. (C-D)** Significant intraluminal red thrombus (light blue arrows) causing signal attenuation (green arrows) beyond the clot. Concentric fibrous plaque throughout the vessel wall (red arrows). **Abbreviations**: OCT=optical coherence tomography, TICI=thrombosis in cerebral infarction. White asterisk (*) denotes the wire and the shadow produced from the wire.

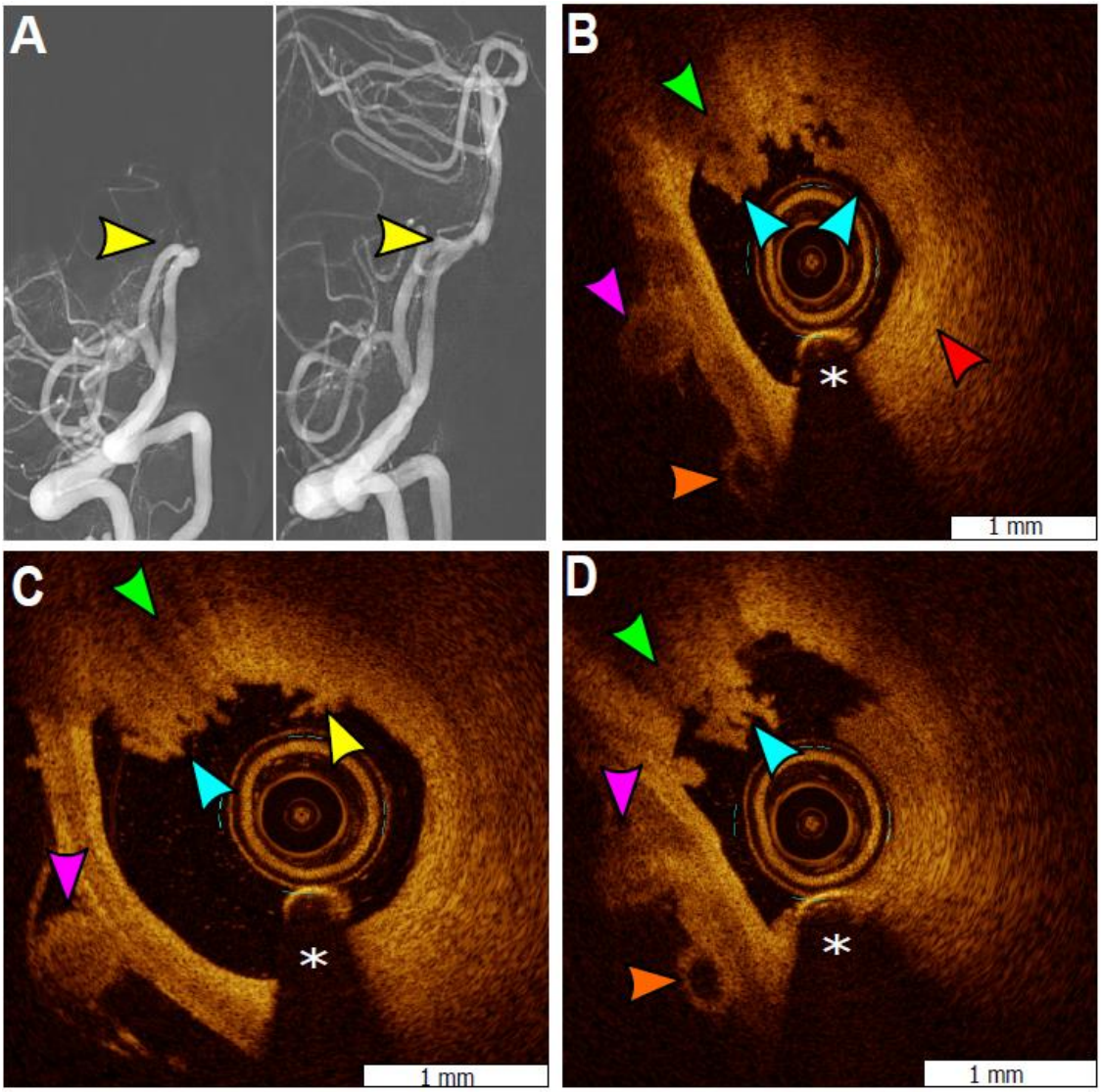

Figure 7-3: Patient Two Angiographic and OCT imaging. (**A)** Angiogram demonstrating complete proximal basilar occlusion (yellow arrow) and TICI 3 reperfusion after thrombectomy. **(B-D)** Residual red thrombus (light blue arrows) with signal attenuation (green arrows) and white thrombus (yellow arrow) without signal attenuation. Thrombosed perforators (purple arrows) and open perforator (orange arrow) visible. Fibrous plaque present throughout (red arrows). **Abbreviations**: OCT=optical coherence tomography, TICI=thrombosis in cerebral infarction. White asterisk (*) denotes the wire and the shadow produced from the wire.

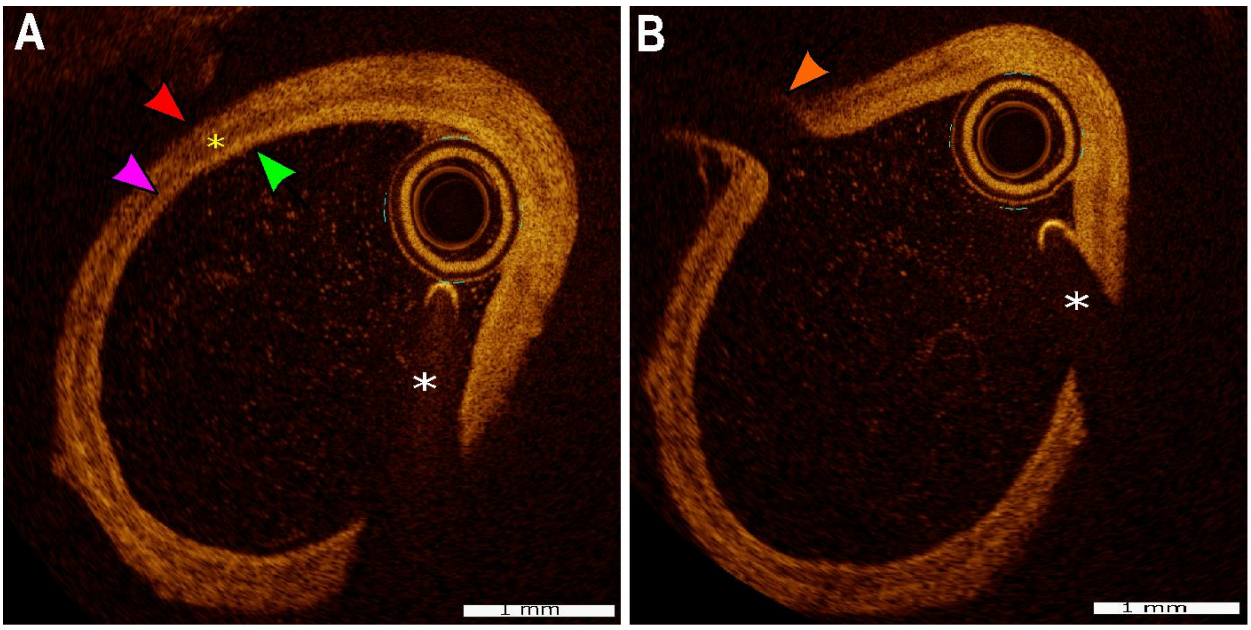

Figure 7-4: Case Three OCT imaging. (A-B) Basilar artery of patient three appearing normal with intima (green arrow head), media (yellow asterisk), adventitia (red arrow head), and internal elastic lamina (purple arrow head) all discernible. A perforator is also visible (orange arrow). **Abbreviations**: OCT=optical coherence tomography. White asterisk (*) denotes the wire and the shadow produced from the wire.

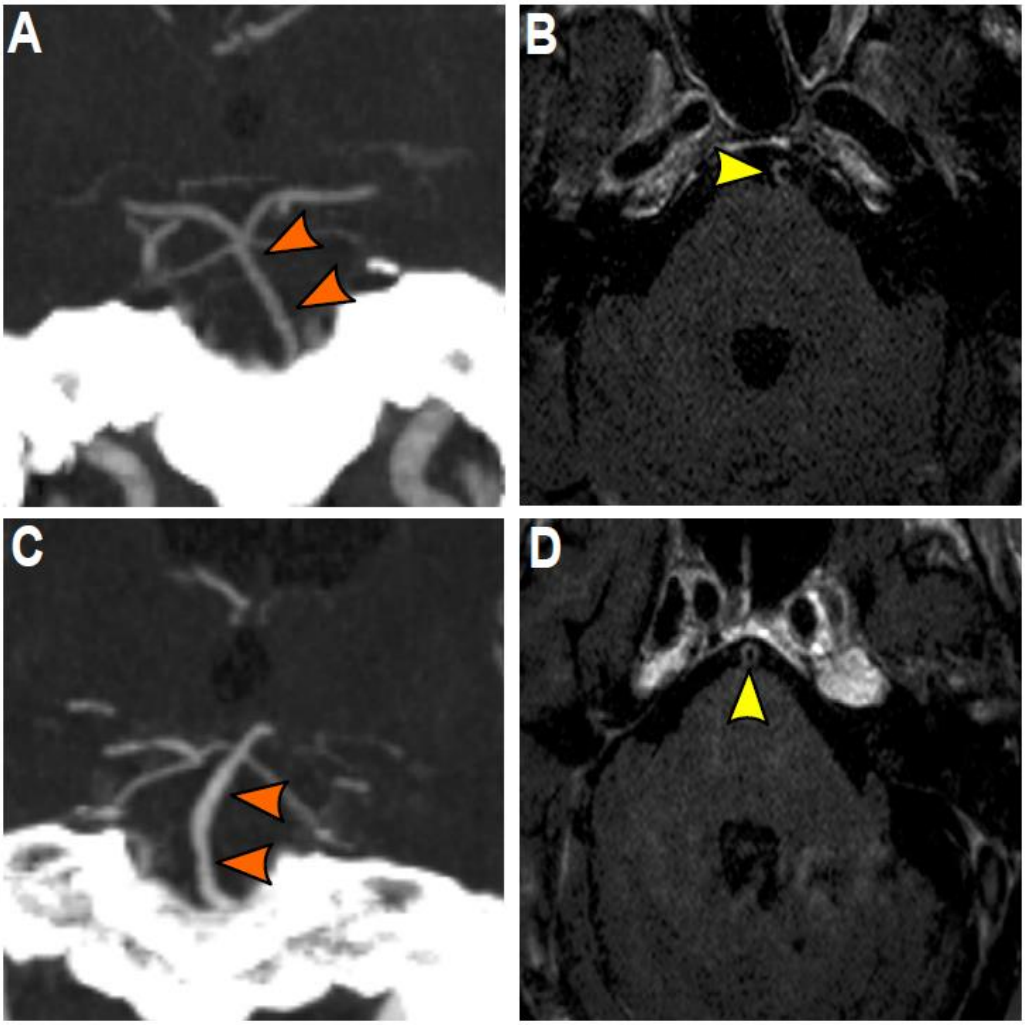

Figure 7-5: Case One/Two CTA and MRVW imaging. (A) Patient one coronal CTA of the basilar artery (orange arrows) displaying revascularization of the vessel with no luminal filling defect. **(B)** Patient one axial T1-weighted blood/CSF suppression sequence with gadolinium displaying eccentric enhancement of the basilar artery (yellow arrow). **(C)** Patient two coronal CTA of the basilar artery (orange arrows) again displaying revascularization of the vessel with no luminal filling defect. **(D)** Patient two axial T1-weighted blood/CSF suppression sequence with gadolinium administration displaying more concentric enhancement of the basilar artery (yellow arrow). **Abbreviations**: CTA= CT angiography, MRVW= magnetic resonance vessel wall.

Clinical Course and Antithrombotic Management

Given the extent of residual thrombus as observed on OCT for patients one and two, both were thought to be at significant risk for additional strokes, particularly to adjacent basilar perforators. Both patients were loaded with Aspirin (ASA) 325mg PO immediately after EVT and maintained on ASA 81mg daily. They were also maintained on a full-dose unfractionated heparin (UFH) infusion immediately after EVT. Both were discharged on low-molecular weight heparin and ASA. Patient three was started on ASA 81 mg daily 24 hours after EVT.

Patient one remained in hospital for 6 days post EVT and was discharged with mRS 1. Patient two remained in hospital for 5 days and was discharged with mRS 1. Both patients were assessed 4 weeks after discharged and continued to improve clinically with no further stroke/TIA like symptoms. Follow-up imaging revealed no intracranial hemorrhage. Patient three required ongoing assistance ambulating, and was discharged to a rehabilitation facility after 2 weeks with mRS 4.

7.4 Discussion

To our knowledge, we describe for the first time intravascular OCT imaging after EVT for acute ischemic stroke secondary to large vessel occlusion. Our findings include: 1) OCT imaging in acute BAO was safe and feasible in three consecutive patients, 2) Residual luminal thrombus can be present despite complete angiographic revascularization, and this thrombus was not visible on

CT angiography or MRVW imaging, and 3) Intracranial atherosclerotic remodelling appears to grow outward, with minimal luminal narrowing and concentric intimal thickening.

Gao *et al*. in 2018 described *in-vivo* OCT imaging of the basilar artery 18 months after EVT in a patient with suspected basilar dissection. Angiographic findings were ambiguous, and they utilized OCT to adequately reveal the double lumen, thus enabled the accurate diagnosis of dissection (Gao et al. 2018). With the aim of assessing for endothelial injury in real-time after EVT, we interestingly observed that significant residual thrombus can exist at the thrombectomy site despite patients having TICI grade/AOL score of 3. Distal emboli released downstream during thrombectomy have certainly been described, but to our knowledge there are no reports in the literature of residual thrombus at the site of the target lesion in the presence of complete recanalization and reperfusion (Chueh, Wakhloo et al. 2012). Furthermore, the residual thrombus was also not visible on CT angiography or MRVW imaging done within 24 hours of EVT. The two possible reasons for this are that the thrombus either migrated or dissolved at the time of CT/MRVW imaging, or endovascular OCT is better at detecting small thrombi given the superior spatial resolution.

We also observed significant concentric intimal thickening of the basilar with loss of normal vessel architecture. The remodelling appears to grow outward, with minimal luminal narrowing. This is in keeping with the findings of Roth *et al*, who conducted a histopathological study in 194 autopsy individuals and found that posterior circulation arteries had greater concentric intimal thickening and outward remodelling compared to the anterior circulation (Roth et al. 2017).

Limited information exists regarding the role of antithrombotics post revascularization. The AHA/ASA guidelines until 2018 recommended against anticoagulation within 24 hours due to concerns of increased risk of hemorrhage, and currently report the risk as uncertain (Powers, Rabinstein et al. 2018). The only study examining early (<24h) antithrombotics most interestingly found that of all treatment subgroups, patients undergoing EVT benefited most from early antithrombotics regarding functional outcome (Jeong et al. 2016). They did not find an increase in intracranial hemorrhage with administration of early antithrombotics after EVT. We hypothesize that their conclusion could be an illustration of the protective effect of early antithrombotics in the setting of residual intraluminal thrombus after EVT. Certainly, the risk of intracranial hemorrhage needs to be weighed against the benefit of early anticoagulation in the setting of residual thrombus, and prospective studies are needed to determine if there is a role for early antithrombotics after EVT. The utility of OCT imaging after EVT has great promise. We demonstrate that the micron-scale spatial resolution of OCT enables detection of residual luminal thrombus and ongoing thrombosis of basilar perforators. The current standard of reporting reperfusion after EVT using the TICI scale may not adequately capture the luminal environment after EVT. OCT could theoretically provide clinicians with added information and possibly guide antithrombotic management after EVT. In this study, we utilized OCT in the posterior circulation due to the less tortuous anatomy compared to the anterior circulation. The stiffness of the current catheter prevents reliable navigation beyond the carotid siphon, and this technology needs to innovate before becoming feasible in the anterior circulation.

7.5 Conclusion

We have shown for the first time that despite complete revascularization, significant residual thrombus exists after endovascular thrombectomy. The thrombus was not visible with other imaging modalities due to lack of spatial resolution. This unique application of optical coherence tomography has provided the first-peak within the blood vessel lumen after restoring flow in stroke patients. This residual thrombus could cause ongoing function-limiting strokes with occlusion of vital basilar perforators. Prior prospective studies and randomized trials underway with variable post revascularization antithrombotic management in the setting of residual thrombus may not strictly be comparing intravenous thrombolysis and endovascular thrombectomy. This may lead to an understated conclusion regarding the role of endovascular thrombectomy in basilar artery occlusion. The role of early post revascularization anticoagulation should be considered after endovascular thrombectomy.

Chapter 8: General Discussion, Conclusions, and Future Work

The goal of this research was to attempt to advance the field of neurointerventional surgery with the application of intravascular imaging. We broadly hypothesized that intravascular imaging could be used as both a diagnostic tool and as an adjunct during treatment for various cerebrovascular diseases. The general scientific approach employed to test this broad hypothesis was the development of preclinical cerebrovascular animal models to demonstrate if intravascular imaging was feasible. If feasibility could be established, we would proceed to human investigations.

Briefly, endovascular optical coherence tomography imaging is the highest-resolution intravascular imaging modality currently available. OCT has traditionally been utilized in interventional cardiology, and more recently applied in neurointerventional surgery (Gounis, Ughi et al. 2018). OCT utilizes near-infrared light with a wavelength of approximately 1.3μm and excellent intraluminal spatial resolution of 10-20 μm is achievable (Tearney, Regar et al. 2012). For these specific reasons, OCT was chosen as the intravascular imaging modality of choice for this research.

Within the scope of cerebrovascular disease, the specific pathologies selected to test the feasibility of endovascular OCT were those with suboptimal clinical outcomes despite the use of modern endovascular techniques and devices for diagnosis and treatment. The pathologies

investigated in this thesis were arterial ischemic stroke and cerebral venous stroke. The relationship between them is that they all fall under the umbrella of stroke; however the main linkage as it pertains to this thesis is the suboptimal clinical outcomes in each disease, for which we hypothesized, could be improved with intravascular imaging. Therefore, the common theme is cerebrovascular diseases in which the diagnosis and treatment can be improved with the incorporation of endovascular OCT imaging. This general discussion will follow the format in chapter three, with discussions of each specific disease discussed sequentially.

8.1 Acute Ischemic Stroke

Our research began with the investigation of iatrogenic vascular injury during endovascular thrombectomy (EVT). We hypothesized that iatrogenic vascular injury occurs during EVT, and that there are varying degrees of vascular injury. These include: endothelial denudation, intimal dissection, and edema of the tunica media. The variable degrees of injury will likely have varying clinical implications (such as increased total area of ischemia) for patients and need to first be characterized. This has not been accomplished previously. Furthermore, we hypothesized that increased duration of thrombosis will cause increased vascular injury during thrombectomy, due to the toxic effects of the thrombus adjacent to the vessel endothelium.

To test our hypothesis, a preclinical swine study of OCT imaging after EVT at one, three, and six hours after vessel occlusion with thrombus was performed. This design allowed for in-vivo real-time imaging of the lumen immediately after EVT, while evaluating whether prolonged arterial exposure to thrombus increases endothelial injury. We found that revascularization and OCT

imaging was feasible for all 9 vessels tested. Endothelial denudation was present in 65 ±16%, 87 ±8%, and 93 ±7% of the vessel surface 1, 3, and 6 hours after thrombus deposition and subsequent EVT, respectively. Residual intraluminal thrombus was present in vessels at all time intervals despite complete angiographic revascularization. Bland-Altman plots showed excellent agreement between OCT and histologic analysis with respect to the degree of endothelial denudation and elevation, separation of the media, and hemorrhage within the media. OCT appeared to be more specific in detecting endothelial elevation.

This preclinical study confirmed our hypothesis that iatrogenic injury during thrombectomy occurs, and that there are varying degrees of vascular injury. Furthermore, prolonged direct vessel exposure to thrombus before EVT increased vessel injury, which we also hypothesized. Endovascular OCT was an excellent tool to evaluate this injury, even outperforming histology. In hindsight, one may argue that this finding is predictable, that in-vivo imaging immediately after thrombectomy would outperform traditional histologic processing which is ex-vivo and prone to processing artifacts.

The clinical significance of vessel wall injury during EVT remains unknown. The goal of the preclinical animal study conducted was to determine if varying degrees of injury occur, and if the injury could be characterised with OCT. Therefore no conclusions could be drawn with respect to the possible clinical implications of this vascular injury. The largest study investigating the relationship between vessel wall injury and clinical outcome was by Renu *et al*. in 2017 by means of MRVW imaging on a 1.5T scanner (Renu, Laredo et al. 2017). They found 34 patients

(57%) had gadolinium vessel wall enhancement after EVT, which was associated with poor clinical outcome. The insufficient spatial resolution of MRVW imaging limits this modality to describing contrast enhancement or mural hemorrhage, and cannot adequately visualize varying degrees of injury. Direct evidence of vessel injury in humans was reported by Yin *et al*. who performed autopsies in 5 patients after EVT and found subintimal dissection likely resulting from the procedure in one patient (Yin, Benavides et al. 2010).

An unexpected finding during this study, and something we did not deliberately investigate for, was the presence of residual luminal thrombus despite complete angiographic revascularization. We did not hypothesize that we would find extensive residual thrombus after EVT. Chueh *et al*. demonstrated that distal embolic showers with large (215-285 μm) and small fragments (23-37μm) occur during thrombectomy (Chueh, Wakhloo et al. 2012). Although distal emboli have certainly been reported, there are no reports in the literature of residual luminal thrombus at the site of the target lesion in the presence of complete recanalization and reperfusion (thrombolysis in cerebral infarction (TICI) reperfusion grade 3 and arterial occlusive lesion (AOL) Grade 3). Gory *et al.* reported significant mural thrombus at the thrombectomy site; however these lesions were in the intimal layer causing no luminal narrowing (Gory, Bresson et al. 2013). This observed thrombus was likely a combination of residual clot not captured by the stent retriever, along with new aggregation of platelets at the thrombectomy site due to exposed collagen from vessel wall injury.

Our original aim was that if endovascular OCT was feasible in the preclinical animal model with excellent correlation with histology, we would proceed to human imaging in patients with basilar thrombosis to investigate the luminal environment for evidence of basilar endothelial injury or ongoing perforator thrombosis. Patients with basilar stroke were chosen because contrary to the findings in the anterior circulation, large multicenter observational studies have demonstrated poor clinical outcome despite successful recanalization of the basilar artery (Singer, Berkefeld et al. 2015). Others have found no correlation between favourable outcome and time to recanalization (van Houwelingen, Luijckx et al. 2016). One notable criticism of these studies is the potential inclusion of patients with established infarcts of the brainstem for which revascularization will be futile, owing to difficulty determining the extent of ischemic core in the brainstem (Lindsberg and Strbian 2015). Nonetheless, the etiology of the difference in outcomes between the anterior and posterior circulation remains unknown. Our unexpected finding of residual thrombus provided even more motivation to utilize OCT in patients with basilar stroke.

Institutional research ethics board (REB) approval was obtained for endovascular OCT imaging after EVT for patients with basilar thrombosis. Endovascular OCT is Health Canada approved for coronary imaging/intervention only, and REB approval is required for any neurointerventional imaging. Patients with acute basilar artery occlusions (BAO) undergoing EVT were imaged with OCT after clot retrieval.

To our knowledge, we describe for the first time endovascular OCT imaging after EVT for acute ischemic stroke secondary to large vessel occlusion. Our findings include: 1) OCT imaging in

acute BAO was safe and feasible in four consecutive patients, 2) Residual luminal thrombus can be present despite complete angiographic revascularization, and this thrombus was not visible on CT angiography or MRVW imaging, and 3) Intracranial atherosclerotic remodelling appears to grow outward, with minimal luminal narrowing and concentric intimal thickening.

Although our original aim was examining for endothelial injury in real-time after EVT, we remarkably again (just as in the preclinical animal model) observed that significant residual thrombus can exist at the thrombectomy site despite patients having TICI grade/AOL score of 3. Furthermore, the residual thrombus was also not visible on CT angiography or MRVW imaging done within 24 hours of EVT. The two possible reasons for this are that the thrombus either migrated or dissolved at the time of CT/MRVW imaging, or endovascular OCT is better at detecting small thrombi given the superior spatial resolution.

The Basilar Artery International Cooperation Study (BASIC) prospective registry cast doubt on the common assumption that intra-arterial thrombolysis (IAT) was superior to intravenous thrombolysis (IVT) for patients with BAO (Schonewille et al. 2009). Others have shown higher rates of revascularization in patients undergoing IAT compared to IVT, without improved functional outcome (Lindsberg and Mattle 2006). The study protocol regarding antithrombotic management of patients after IAT was not provided, and not included in the protocol for the current two ongoing RCTs investigating the efficacy of EVT in BAO (van der Hoeven et al. 2013, Liu et al. 2017). We hypothesize that the reason for the unexpected finding that improved revascularization did not translate into improved functional outcome is the presence of residual

thrombus after EVT. Floating thrombus adjacent to vital basilar perforators could cause ongoing ischemic infarcts to brainstem structures after successful recanalization. No conventional imaging modality at the time could have detected the residual thrombus.

We further hypothesize that prior studies, with variable antithrombotic management between patients undergoing IVT and IAT, have not accounted for the confounding effect of residual thrombus after IAT. Commonly, institutions treat patients with both IVT and full-dose UFH after the exclusion of intracranial hemorrhage (Strbian et al. 2014). Antithrombotic treatment is well known to decrease the risk of stroke secondary to thromboembolism. If the majority of patients in the IAT arm of previous trials did not receive post recanalization antithrombotic medication, while patients in the IVT arm commonly received antithrombotic medication, one could make a conclusion while not accounting for the effect of antithrombotic treatment on residual thrombus. A possible cause for the finding of non-superiority of EVT could be ongoing clinically impactful infarcts secondary to residual thrombus, occurring in the absence of antithrombotic management.

Similar findings of non-superiority of EVT do not exist in the anterior circulation. The posterior circulation and particularly the basilar artery are distinct in several aspects. Basilar artery thrombus may not be as compact as in the anterior circulation, allowing for residual fragments to be left behind after EVT (Lindsberg et al. 2015). Even small perforator infarcts due to residual thrombus in the brainstem could have catastrophic consequences compared to small cortical infarcts from residual anterior circulation clot. Our findings also shed light on the shared empirical observation that reocclusion is common after EVT in BAO. Given the degree of

residual thrombus observed, one could imagine growth of the residual thrombus leading to complete reocclusion.

Limited information exists regarding the role of antithrombotics post revascularization. The AHA/ASA guidelines until 2018 recommended against anticoagulation within 24 hours due to concerns of increased risk of hemorrhage, and currently report the risk as uncertain (Powers, Rabinstein et al. 2018). The only study examining early (<24h) antithrombotics most interestingly found that of all treatment subgroups, patients undergoing EVT benefited most from early antithrombotics regarding functional outcome (Jeong, Kim et al. 2016). We hypothesize that their conclusion is an illustration of the protective effect of antithrombotics in the setting of residual intraluminal thrombus after EVT. Regarding our two study patients, we initiated immediate antiplatelet therapy and full-dose UFH infusion to decrease the risk of ongoing brainstem strokes. Both patients experienced no further stroke-like symptoms and follow-up imaging revealed no intracranial hemorrhage.

The novelty of these findings cannot be overstated. Since becoming the standard of care for eligible patients, endovascular thrombectomy clinical outcomes are compared to angiographic revascularization for all major trials published in the world's top journals. Angiographic revascularization does not capture the presence of residual thrombus, which has likely gone undetected. A new technology (OCT) has now shown that despite complete angiographic revascularization, the vessel lumen may still have a significant thrombus burden. In the future

directions section below, we expand on what we hypothesize the clinical implications of these findings are and future studies to test these hypotheses.

8.1.1 Conclusions

In summary, the initiation of this thesis began with a preclinical swine model establishing the feasibility of OCT imaging after EVT examining for iatrogenic vascular injury. We found varying degrees of vascular injury, and more interestingly residual thrombus despite complete angiographic revascularization. Next, we proceeded with human endovascular OCT imaging after EVT with patients with basilar stroke. The purpose of this was to investigate the apparent dichotomy regarding the benefit of revascularization with EVT between the anterior and posterior circulation. The novel discovery of this work is that significant residual intraluminal thrombus exists after EVT. This residual thrombus could certainly cause ongoing function-limiting strokes with occlusion of vital basilar perforators after EVT. Prior prospective studies and RCTs underway with variable post revascularization antithrombotic management in the setting of residual thrombus may not strictly be comparing IVT and EVT. This may lead to an understated/false conclusion regarding the role of EVT in BAO. Furthermore, the only study evaluating the role of post revascularization antithrombotic showed specifically that patients undergoing EVT benefited most from early antithrombotics. The role of post revascularization anticoagulation should be assessed in a prospective trail.

8.2 Cerebral Venous Sinus Thrombosis

After investigating iatrogenic vascular injury and residual thrombus in arterial ischemic stroke animal and human studies, we proceeded to investigate the etiology of poor clinical outcomes in patients undergoing endovascular thrombectomy of the cerebral venous sinuses. We broadly assumed that the successes of endovascular OCT imaging of the arterial system could be expanded to the venous system. Contrary to arterial anatomy, the sinuses act as reservoirs for collecting venous blood from both the deep and superficial venous system, and are lined with endothelium and elastic lamina. They lack the smooth muscle layers found in most blood vessels and have no valves.

We hypothesized that a preclinical animal model utilizing swine can be used for intravascular imaging and creating an endovascular venous thrombosis model to test various devices and techniques. Modern endovascular techniques should allow for the catheterization of the sinus with subsequent imaging, imagine-guided thrombosis, and treatment. Furthermore, we hypothesized that intravascular imaging can identify regions of ongoing cortical vein thrombosis as a possible etiology for poor clinical outcomes.

We quickly found that there were no preclinical endovascular swine thrombosis models. Modern thrombectomy devices have been exclusively designed for arterial thrombectomy and are not tested in the venous system, where the venous sinus wall anatomically differs considerably. Most animal CVST models surgically expose the superior sagittal sinus and thrombose the sinus via either surgical ligation, injection of thrombotic material directly into the sinus, or topical

application of ferric chloride. To our knowledge, Wang *et al*. in 2010 are the only group to describe a transvenous technique to occlude the SSS in a swine model, however this was done before the era of endovascular thrombectomy and they did not test techniques or devices for thrombectomy (Wang, Tan et al. 2010).

As endovascular techniques and devices evolve, the role of mechanical thrombectomy in the treatment of CVST must be evaluated. Reliable preclinical animal models are necessary to evaluate current/new devices to help determine which are most effective in removing thrombus and safe for venous sinus mechanical thrombectomy. Modern thrombectomy devices such as second-generation stent retrievers and aspiration catheters are designed for arterial thrombectomy, and may behave differently in the venous sinuses given the anatomical differences described above.

Therefore, our first aim was designing a preclinical animal model for cerebral venous sinus catheterization and subsequent endovascular OCT imaging of the sinus and bridging cortical veins, comparing OCT findings with histology.

Baboons have the most anatomically similar cerebral venous system, however experiments done on primates are difficult to justify from both an ethical and cost standpoint. Swine also have similar venous system and therefore four consecutive Yorkshire Swine weighing 40-45 kg were selected. Technically successful OCT images were obtained in 3/4 swine. The luminal environment, along with visualization of dural arteries and draining cortical veins were

characterized. The average maximum diameter of the sinus, dural arteries, and cortical veins was 3.14mm, 135 μm, and 260 μm respectively. Bland-Altman analysis demonstrated excellent agreement between histology and OCT images. Endovascular OCT imaging was feasible in this preclinical animal study. Adoption of this imaging modality in the human cerebral venous sinus could help aid in the diagnosis, treatment, and understating of the pathophysiology of various diseases of the sinus

Our next aim was to proceed to a model of sagittal sinus thrombosis, subsequent endovascular thrombectomy, and OCT imaging. Five consecutive male Yorkshire swine weighing 45Kg were utilized. Thrombosis of the superior sagittal sinus was induced with bovine thrombin injection via a microcatheter under distal balloon occlusion for 15 minutes. Combined arterial injections and super selective sinus injections confirmed the extent of thrombosis. Endovascular thrombectomy was subsequently performed with a second generation stent retriever, followed by endovascular OCT imaging to assess the luminal environment after thrombectomy.

Thrombosis of superior sagittal sinus, endovascular thrombectomy, and subsequent OCT imaging was technically successful in 4/5 swine. Recanalization of the sinus with a second-generation stent retriever was successful after one attempt in ¾ (75%) swine, and one swine required 2 attempts. OCT imaging after thrombectomy revealed regions of residual sinus luminal thrombus despite complete angiographic recanalization. Thrombosed bridging cortical veins were also observed before draining into the sinus, along with patent cortical veins.

As was observed in arterial stroke OCT imaging, we similarly observed that ongoing thrombosis of cortical veins could be present. This was observed on OCT but not apparent on cerebral angiography. Mechanical thrombectomy with a stent retriever may be able to recanalize the sinus but will not be effective addressing thrombus in adjacent bridging cortical veins. Modern devices cannot access cortical veins safely, and the risk of perforation is likely high. We hypothesize that if bridging cortical vein thrombus is observed after mechanical thrombectomy, direct intra-sinus chemical thrombolysis may be warranted to dissolve the remaining clot. Patency of the sinus without patency of bridging veins (particularly if the vein drains an eloquent or large portion of the cerebral cortex) is unlikely to be beneficial. In addition, residual thrombus within the sinus may lead to re-occlusion. These findings further highlight the utility of intravascular imaging to visualize the luminal environment after thrombectomy (Pasarikovski, Ramjist et al. 2019, Pasarikovski, Keith et al. 2020). This finding of sinus recanalization and ongoing cortical vein thrombosis is a finding and may be the etiology of poor clinical outcome despite technical success.

Our preclinical model of sinus thrombosis, subsequent thrombectomy and endovascular OCT imaging is entirely novel. A preclinical model designed to assess endovascular techniques and devices for the treatment of CVST has not previously been established. Repurposed devices from arterial stroke may not perform as expected given the unique features of venous sinus thrombosis. This model may be helpful in developing and testing a new generation of devices designed specifically for CVST treatment.

8.2.1 Conclusions

We describe the first preclinical animal model for cerebral venous sinus thrombosis and mechanical thrombectomy. In addition, using endovascular optical coherence tomography the luminal environment can be visualized after thrombectomy to assess the efficacy of the endovascular technique and devices utilized for recanalization. With this study, we were able to confirm the presence of ongoing thrombosis of bridging cortical veins despite recanalization of the cerebral venous sinus, as one putative reason for poor patient outcome despite a successful procedure.

8.3 Limitations

The application of endovascular optical coherence tomography in cerebrovascular disease has several limitations. Endovascular OCT is only FDA and Health Canada approved for use in the diagnosis and treatment of cardiac disease. The device used in this research was designed to navigate and image coronary vessels, and not the cerebral vasculature. The repurposing of a device, from coronary to cerebral imaging, will inherently come with limitations.

The first limitation is the field-of-view of the OCT device. Given that the diameters of coronary arteries are generally similar to those in the brain, the OCT cross sectional images translate well for cerebral arteries. However, imaging of the human venous sinus could prove difficult. At an estimated average diameter of 7mm, the current OCT device may not capture the entire cerebral

venous sinus lumen. This could lead to missing important anatomic details and pathology. Also, placing a stent without visualizing the entire lumen may not be feasible.

The second limitation is the reliable navigation of the device. The coronary vasculature is not particularly tortuous, and hence cardiologists have minimal difficulty navigating the catheter. The cerebral vasculature is the most tortuous in the human body. Specifically, the internal carotid artery at the carotid siphon can make multiple 180 degree turns in a short segment. Therefore the stiffness of the OCT catheter may preclude navigation and hence imaging of a tortuous carotid siphon. In this work we showed that OCT imaging of the common carotid artery and basilar artery were feasible. These segments are relatively straight and therefore we cannot claim that OCT is feasible in the setting of the tortuous anatomy in the anterior circulation.

Finally, another OCT limitation is the depth of penetration of the current OCT device. An inherent limitation of the detection of single-scattered infrared light limits tissue depth penetration to approximately 3mm. This limited penetration may not capture the entire vessel wall pathology, such as in intracranial atherosclerotic disease or the entire aneurysm sac or dome. This would limit imaging of the aneurysm to the parent vessel, neck, and a portion of the dome only. To address the issues listed above, researchers have developed a new endovascular OCT device which is designed specifically for use in neurointerventional surgery. The device is currently in the preclinical animal testing phase. The advent of a neuro-dedicated device may change the way we diagnose and treat cerebrovascular diseases.

There are also inherent limitations to preclinical animal models. With respect to the cerebral venous sinus imaging and thrombectomy model, clinical outcomes were not assessed. The thrombus in the swine sinus did not occur spontaneously, and therefore the thrombus may have different composition and mechanical properties compared to spontaneous human thrombus. The safety of OCT in human venous imaging needs to be further studied. Although the OCT catheter is delivered via monorail technique over a 0.014” wire, venous perforation is possible via the stiff catheter tip, and this was not assessed in our model.

With respect to arterial OCT imaging, similar to the swine venous sinus, swine extracranial arteries differ anatomically from human cerebral vessels. Swine blood vessels generally have thicker tunica media and a thinner intimal layer compared to humans. This can result in the swine model underestimating the degree of vessel wall injury due to stress and strain forces, as more elastic vessels can better tolerate these forces leading to decreased dissection and tears. Second, we used erythrocyte rich thrombus in our model, which differs slightly from the cellular composition of thromboemboli and the clinical setting.

8.4 Future Directions

8.4.1 Arterial Ischemic Stroke

It is apparent that OCT imaging after EVT has great promise. We demonstrate that the micron-scale spatial resolution of OCT enables detection of residual luminal thrombus and ongoing thrombosis of basilar perforators. The current standard of reporting reperfusion after EVT using the TICI scale (which is used in all major stroke trials) may not adequately capture the luminal environment after EVT. OCT could theoretically provide clinicians with added information and possibly guide antithrombotic management after EVT.

The presence of this residual thrombus adjacent to vital basilar perforators could have major implications, and we believe investigating this further is a priority to help shed light on the poor outcomes observed in basilar stroke patients. Although intuitively we would suspect that residual thrombus could be harmful, the clinical significance of this residual thrombus remains unknown. Furthermore, it is unclear what portion of patients will have residual thrombus despite complete radiographic revascularization. Therefore, for our future work, we have proposed the following prospective observational safety and feasibility study of optical coherence tomography imaging in a larger cohort of patients with basilar artery occlusion. Given this is a new application of an existing cardiology technology, safety and feasibility must first be established in the cerebral vasculature, and that is the goal of this proposal.

Objectives

1. Primary Technical Success Outcome (Feasibility)

Device technical success definition: 1) Navigation of the OCT catheter to the appropriate location within the vessel, 2) Clearing of luminal blood with minimal artifact from red blood cells, 3) Capturing circumferential OCT images of the entire arterial lumen along the entire region of interest, 4) Identifying normal anatomic structures (intima, media, adventitia, and internal/external elastic lamina) where present, 5) Identifying interatrial and vessel wall lesions when present. For the image acquisition to be defined as successful, all above criteria must be met.

2. Primary Safety Outcome

OCT device Related Complications: Defined as any vessel dissection, perforation, vasospasm, or device detachment. Complications may arise during the EVT procedure itself (without OCT imaging) and these complications include vessel dissection, vasospasm and perforation. Perforation, vasospasm and dissection can be immediately appreciated during the procedure, and diagnostic runs before OCT imaging will be done to ensure differentiation between vessel dissection/perforation/vasospasm caused by the EVT procedure and OCT imaging.

Note: This proposal is underpowered to detect any meaningful differences in clinical outcomes between patients with vs. without residual thrombus. We will collect, observe, and report on outcome data only. Our primary objective is the feasibility of obtaining images in a safe fashion, and we believe a sample size of 25 is adequate for this preliminary safety and feasibility study.

Study Design

This proposal is a single-center, prospective observational safety and feasibility study to assess the technical success and safety of endovascular OCT after EVT (Figure 9-1). The goal is to enroll 25 patients over 2 years.

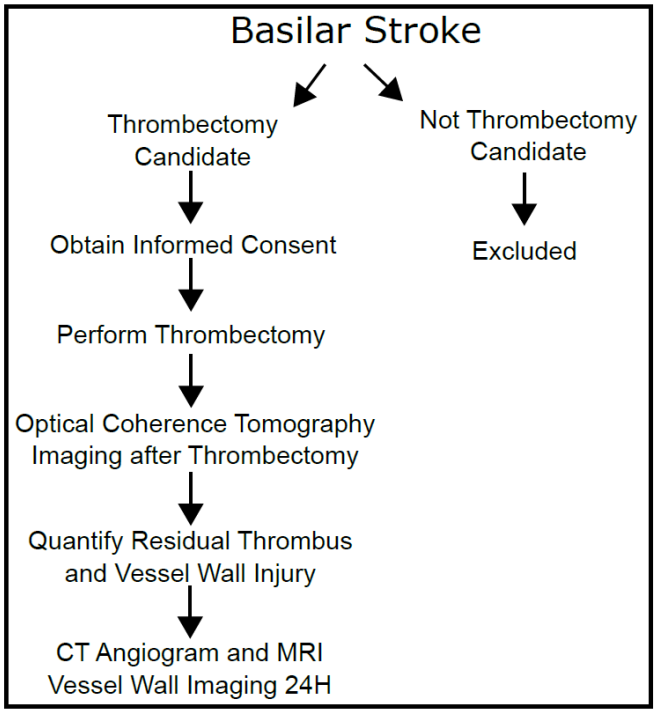

Figure 8-1: Proposed Basilar Stroke OCT study. Graphical representation of the overall proposal structure. All patients who are candidates for basilar stroke thrombectomy will be considered for optical coherence tomography imaging.

We believe that OCT image acquisition will be technically feasible and safe in the vast majority of patients. This is based on our experience in four patients imaged after EVT, and our general use of OCT in carotid atherosclerotic disease and intracranial aneurysms. We expect to find that a significant number of patients will have residual thrombus despite complete angiographic revascularization. We further hypothesize that patients with OCT confirmed residual thrombus will have worse functional outcomes compared to those who do not have residual thrombus. This is predicated on the hypothesis that residual thrombus will not be clinically dormant, but an important cause of new/worsening stroke or reocclusion after EVT. Floating thrombus adjacent to vital basilar perforators could cause ongoing ischemic infarcts to brainstem structures after successful recanalization. We hypothesize this may play a role in the poor outcomes observed in basilar stroke patients.

Our ultimate goal will be to use OCT to guide rational antithrombotic management for patients with confirmed residual thrombus after EVT for BAO; however we must first determine if OCT imaging is safe and feasible. The next step would be establishing if the presence of OCT confirmed residual thrombus is clinically relevant before even suggesting treating the thrombus with antithrombotics that carry risk of intracranial hemorrhage.

If it is shown that patients with OCT confirmed residual thrombus have worse clinical outcome compared to patients without residual thrombus, this would pave the way for a pilot study of early antithrombotics in patients with residual thrombus. Limited information exists regarding the role of antithrombotics post revascularization. The AHA/ASA guidelines until 2018 recommended against anticoagulation within 24 hours due to concerns of increased risk of

hemorrhage, and currently report the risk as uncertain (Powers, Rabinstein et al. 2018). The only study examining early (<24h) antithrombotics most interestingly found that of all treatment subgroups, patients undergoing EVT benefited most from early antithrombotics regarding functional outcome (Jeong, Kim et al. 2016). We hypothesize that their conclusion is an illustration of the protective effect of early antithrombotics in the setting of residual intraluminal thrombus after EVT. Certainly, the risk of intracranial hemorrhage needs to be weighed against the benefit of early anticoagulation in the setting of residual thrombus, and prospective studies are needed to determine if there is any role for early antithrombotics after EVT.

If the presence of residual thrombus as shown using OCT causes new/worse function-limiting strokes with occlusion of vital basilar perforators after EVT, it would shed light on a potentially treatable contributor of the poor outcomes in basilar occlusion. As described above, with this knowledge we could design and conduct a pilot study of early antithrombotics in patients with OCT confirmed residual thrombus. OCT guided antithrombotic treatment would be completely novel. This may lead to improved functional outcome in one of the most devastating medical diseases with mortality above 90% in cases of failed recanalization. Furthermore, our proposal is the first ever OCT stroke study. Our ultimate goal will be to use OCT to guide rational antithrombotic management for patients with confirmed residual thrombus after EVT for BAO as described above.

8.4.2 Cerebral Aneurysms

The prevalence of intracranial aneurysms in the population is approximately 3.2% (Vernooij et al. 2007). A brain aneurysm forms when there is a weak point within the wall of a blood vessel, causing an outpouching of a segment of the blood vessel. The cause of the weakness in the blood vessel wall leading to aneurysm formation remains an area of great research interest. Hemodynamic stress, inflammation, and extracellular matrix deficits are all believed to play an important role in aneurysmal formation (Jung 2018). The shapes of aneurysms vary, but they are broadly described as saccular, fusiform or dissecting (Figure 9-2).

With respect to the management of cerebral aneurysms, there has been a revolution in the way we treat aneurysms after the ISAT trial in 2005 (Molyneux, Kerr et al. 2005). Most ruptured aneurysms in the United States and Canada are now are treated endovascularly (Smith et al. 2011). Different techniques for endovascular aneurysmal embolization are utilized including: coiling, stent-assisted coiling, and flow-diverting stents. Although endovascular treatment has improved patient care, aneurysm recurrence rates due to coil compaction/recanalization can approach 20% (Ferns et al. 2009).

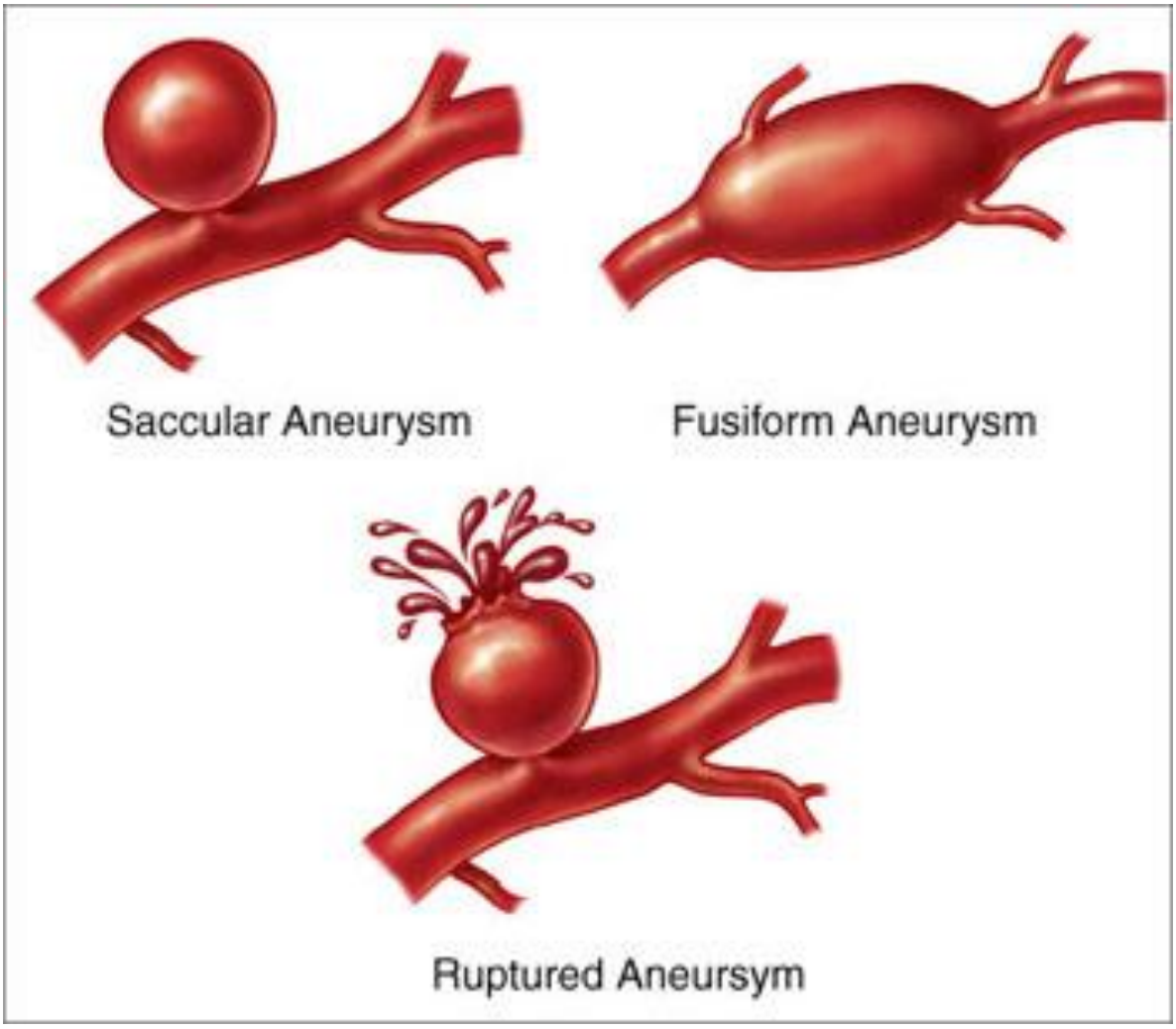

Figure 8-2: Cerebral Aneurysm Morphology. The morphology of cerebral aneurysms can be generally defined as either saccular or fusiform. Most aneurysms are saccular in shape.

Among these treatment options, flow diversion for aneurysmal embolization has emerged as a safe and widely utilized endovascular treatment option (Kallmes et al. 2015). The exact mechanism of aneurysmal healing after flow diversion remains unknown. The two main proposed mechanisms of healing include: 1) Altered hemodynamics causing subsequent aneurysmal thrombosis, and 2) Endothelialization over the device stent-struts occluding the aneurysm neck.

Studies supporting each as the primary mechanism exist. In 2014 Kadirvel *et al*. shed light on the cellular events associated with aneurysmal healing after showing that occlusion was present only when complete endothelialization was observed across the aneurysm neck (Kadirvel et al. 2014). The endothelial cells were derived from the adjacent parent artery and used the stent-struts as a scaffold. Conversely, Cebral *et al.* in 2014 showed using computational fluid dynamics (CFD) in a rabbit aneurysmal model that slow-flow induced thrombosis in the aneurysm dome may be the primary healing mechanism (Cebral et al. 2014). A subsequent study also showed that smaller inflow rates after flow diversion resulted in decreased aneurysmal occlusion time (Chung et al. 2015).

Understanding the dominance or relative importance, and sequence of events for each mechanism in aneurysmal healing could have significant implications, including identifying patients whose aneurysms are likely to recur after flow diversion. Furthermore, the duration of antiplatelet therapy after treatment is controversial, owing to lack of understanding of timing of stent endothelialization. Designing and improving future devices will require a basic understanding of aneurysmal healing following flow diversion.

A future project to improve our understanding of aneurysmal healing after flow diversion treatment is needed. To accomplish this, we propose utilizing a novel endovascular technique for simultaneous structural imaging and hemodynamic analysis *in-vivo* in a rabbit aneurysm model. Doppler Optical Coherence Tomography (dOCT) will enable real-time intravascular examination of endothelialization over stent-struts, and hemodynamic conditions within the aneurysm sac.

We suspect that flow diversion will initially cause decrease flow within the aneurysm leading to regions of thrombosis, beginning in the dome of the aneurysm. Simultaneously endothelialization over the stent-struts will begin in regions where the stent is in direct contact with the parent vessel wall. This endothelialization will continue toward the neck of the aneurysm, in conjunction with progressive increase in thrombus formation and subsequent further decreased flow within the aneurysm as the sac progressively thrombosis.

We suspect that decreased flow into the aneurysm will allow for a better environment for endothelialization of the aneurysm neck. We hypothesize that depending on aneurysmal size, morphology, and wall anatomy that the degree of thrombosis in the aneurysm will vary, hence leading to inconsistent endothelialization and ultimate none-obliteration of the aneurysm.

The uniqueness of this future work lies in the integration of structural and doppler OCT simultaneously. To our knowledge, this has not been undertaken as our group is the only group to have intravascular doppler OCT. This was developed in 2014 by a graduate student of Dr. Yang working in conjunction with the original LightLab OCT team that subsequently became the modern Dragonfly catheter.

Structural OCT alone has been utilized previously to examine for endothelialization after flow diversion for aneurysmal embolization with great success (King et al. 2018, Matsuda et al. 2018). OCT utilizes near-infrared light with a wavelength of approximately 1300 nm and excellent blood vessel wall spatial resolution of 10-20 μm is achievable (Tearney, Regar et al. 2012). It is the highest resolution intravascular imaging modality currently available. With respect to hemodynamic studies, computational fluid dynamic (CFD) analysis after flow diversion has several limitations. For example, most models apply boundary conditions rather than patient-specific characteristics, and assume rigidity of the vessel wall (Kallmes 2012). Outputs of these models can vary by 50% depending on whether CT angiography or rotational 3D angiography is used for geometric estimation (Geers et al. 2011). Doppler OCT would provide real-time *in-vivo* hemodynamics with particularly improved velocity spatial resolution.

Chapter 9: References

Adeeb, N., M. M. Mortazavi, R. S. Tubbs and A. A. Cohen-Gadol (2012). "The cranial dura mater: a review of its history, embryology, and anatomy." Childs Nerv Syst **28**(6): 827-837.

Berkhemer, O. A., P. S. Fransen, D. Beumer, L. A. van den Berg, H. F. Lingsma, A. J. Yoo, W. J. Schonewille, J. A. Vos, P. J. Nederkoorn, M. J. Wermer, M. A. van Walderveen, J. Staals, J. Hofmeijer, J. A. van Oostayen, G. J. Lycklama a Nijeholt, J. Boiten, P. A. Brouwer, B. J. Emmer, S. F. de Bruijn, L. C. van Dijk, L. J. Kappelle, R. H. Lo, E. J. van Dijk, J. de Vries, P. L. de Kort, W. J. van Rooij, J. S. van den Berg, B. A. van Hasselt, L. A. Aerden, R. J. Dallinga, M. C. Visser, J. C. Bot, P. C. Vroomen, O. Eshghi, T. H. Schreuder, R. J. Heijboer, K. Keizer, A. V. Tielbeek, H. M. den Hertog, D. G. Gerrits, R. M. van den Berg-Vos, G. B. Karas, E. W. Steyerberg, H. Z. Flach, H. A. Marquering, M. E. Sprengers, S. F. Jenniskens, L. F. Beenen, R. van den Berg, P. J. Koudstaal, W. H. van Zwam, Y. B. Roos, A. van der Lugt, R. J. van Oostenbrugge, C. B. Majoie, D. W. Dippel and M. C. Investigators (2015). "A randomized trial of intraarterial treatment for acute ischemic stroke." N Engl J Med **372**(1): 11-20.

Boddu, S. R., P. Gobin, C. Oliveira, M. Dinkin and A. Patsalides (2018). "Anatomic measurements of cerebral venous sinuses in idiopathic intracranial hypertension patients." PLoS One **13**(6): e0196275.

Bouma, B. E., M. Villiger, K. Otsuka and W. Y. Oh (2017). "Intravascular optical coherence tomography [Invited]." Biomed Opt Express **8**(5): 2660-2686.

Bousser, M. G. and J. M. Ferro (2007). "Cerebral venous thrombosis: an update." Lancet Neurol **6**(2): 162-170.

Brott, T. G., R. W. Hobson, 2nd, G. Howard, G. S. Roubin, W. M. Clark, W. Brooks, A. Mackey, M. D. Hill, P. P. Leimgruber, A. J. Sheffet, V. J. Howard, W. S. Moore, J. H. Voeks, L. N. Hopkins, D. E. Cutlip, D. J. Cohen, J. J. Popma, R. D. Ferguson, S. N. Cohen, J. L. Blackshear, F. L. Silver, J. P. Mohr, B. K. Lal, J. F. Meschia and C. Investigators (2010). "Stenting versus endarterectomy for treatment of carotid-artery stenosis." N Engl J Med **363**(1): 11-23.

Buell, T. J., D. M. S. Raper, I. J. Pomeraniec, D. Ding, C. J. Chen, D. G. Taylor and K. C. Liu (2018). "Transient resolution of venous sinus stenosis after high-volume lumbar puncture in a patient with idiopathic intracranial hypertension." J Neurosurg **129**(1): 153-156.

Campbell, B. C., P. J. Mitchell, T. J. Kleinig, H. M. Dewey, L. Churilov, N. Yassi, B. Yan, R. J. Dowling, M. W. Parsons, T. J. Oxley, T. Y. Wu, M. Brooks, M. A. Simpson, F. Miteff, C. R. Levi, M. Krause, T. J. Harrington, K. C. Faulder, B. S. Steinfort, M. Priglinger, T. Ang, R. Scroop, P. A. Barber, B. McGuinness, T. Wijeratne, T. G. Phan, W. Chong, R. V. Chandra, C. F. Bladin, M. Badve, H. Rice, L. de Villiers, H. Ma, P. M. Desmond, G. A. Donnan, S. M. Davis and E.-I. Investigators (2015). "Endovascular therapy for ischemic stroke with perfusion-imaging selection." N Engl J Med **372**(11): 1009-1018.

Cebral, J. R., F. Mut, M. Raschi, S. Hodis, Y. H. Ding, B. J. Erickson, R. Kadirvel and D. F. Kallmes (2014). "Analysis of hemodynamics and aneurysm occlusion after flow-diverting treatment in rabbit models." AJNR Am J Neuroradiol **35**(8): 1567-1573.

Choy, J. S., O. Mathieu-Costello and G. S. Kassab (2005). "The effect of fixation and histological preparation on coronary artery dimensions." Ann Biomed Eng **33**(8): 1027-1033.

Chueh, J. Y., A. K. Wakhloo and M. J. Gounis (2012). "Effectiveness of mechanical endovascular thrombectomy in a model system of cerebrovascular occlusion." AJNR Am J Neuroradiol **33**(10): 1998-2003.

Chung, B., F. Mut, R. Kadirvel, R. Lingineni, D. F. Kallmes and J. R. Cebral (2015). "Hemodynamic analysis of fast and slow aneurysm occlusions by flow diversion in rabbits." J Neurointerv Surg **7**(12): 931-935.

Coutinho, J. M., J. M. Ferro, S. M. Zuurbier, M. S. Mink, P. Canhao, I. Crassard, C. B. Majoie, J. A. Reekers, E. Houdart, R. J. de Haan, M. G. Bousser and J. Stam (2013). "Thrombolysis or anticoagulation for cerebral venous thrombosis: rationale and design of the TO-ACT trial." Int J Stroke **8**(2): 135-140.

Coutinho, J. M., S. M. Zuurbier, M. G. Bousser, X. Ji, P. Canhao, Y. B. Roos, I. Crassard, A. P. Nunes, M. Uyttenboogaart, J. Chen, B. J. Emmer, S. D. Roosendaal, E. Houdart, J. A. Reekers, R. van den Berg, R. J. de Haan, C. B. Majoie, J. M. Ferro, J. Stam and T.-A. investigators (2020). "Effect of Endovascular Treatment With Medical Management vs Standard Care on Severe Cerebral Venous Thrombosis: The TO-ACT Randomized Clinical Trial." JAMA Neurol **77**(8): 966-973.

de Bruijn, S. F. and J. Stam (1999). "Randomized, placebo-controlled trial of anticoagulant treatment with low-molecular-weight heparin for cerebral sinus thrombosis." Stroke **30**(3): 484-488.

Dohad, S., A. Zhu, S. Krishnan, F. Wang, S. Wang, J. Cox and T. D. Henry (2018). "Optical coherence tomography guided carotid artery stent procedure: technique and potential applications." Catheter Cardiovasc Interv **91**(3): 521-530.

Einhaupl, K. M., A. Villringer, W. Meister, S. Mehraein, C. Garner, M. Pellkofer, R. L. Haberl, H. W. Pfister and P. Schmiedek (1991). "Heparin treatment in sinus venous thrombosis." Lancet **338**(8767): 597-600.

Ferns, S. P., M. E. Sprengers, W. J. van Rooij, G. J. Rinkel, J. C. van Rijn, S. Bipat, M. Sluzewski and C. B. Majoie (2009). "Coiling of intracranial aneurysms: a systematic review on initial occlusion and reopening and retreatment rates." Stroke **40**(8): e523-529.

Ferro, J. M., P. Canhao, J. Stam, M. G. Bousser, F. Barinagarrementeria and I. Investigators (2004). "Prognosis of cerebral vein and dural sinus thrombosis: results of the International Study on Cerebral Vein and Dural Sinus Thrombosis (ISCVT)." Stroke **35**(3): 664-670.

Fries, G., T. Wallenfang, J. Hennen, M. Velthaus, A. Heimann, H. Schild, A. Perneczky and O. Kempski (1992). "Occlusion of the pig superior sagittal sinus, bridging and cortical veins: multistep evolution of sinus-vein thrombosis." J Neurosurg **77**(1): 127-133.

Gao, P., L. Gui, B. Yang, T. Krings and L. Jiao (2018). "Optical Coherence Tomography of Spontaneous Basilar Artery Dissection in a Patient With Acute Ischemic Stroke." Front Neurol **9**: 858.

Geers, A. J., I. Larrabide, A. G. Radaelli, H. Bogunovic, M. Kim, H. A. Gratama van Andel, C. B. Majoie, E. VanBavel and A. F. Frangi (2011). "Patient-specific computational hemodynamics of intracranial aneurysms from 3D rotational angiography and CT angiography: an in vivo reproducibility study." AJNR Am J Neuroradiol **32**(3): 581-586.

Gory, B., D. Bresson, I. Kessler, M. L. Perrin, A. Guillaudeau, K. Durand, S. Ponsonnard, C. Couquet, C. Yardin and C. Mounayer (2013). "Histopathologic evaluation of arterial wall response to 5 neurovascular mechanical thrombectomy devices in a swine model." AJNR Am J Neuroradiol **34**(11): 2192-2198.

Gounis, M. J., G. J. Ughi, M. Marosfoi, D. K. Lopes, D. Fiorella, H. G. Bezerra, C. W. Liang and A. S. Puri (2018). "Intravascular Optical Coherence Tomography for Neurointerventional Surgery." Stroke: STROKEAHA118022315.

Gounis, M. J., A. K. Wakhloo and J. Y. Chueh (2013). "Preclinical investigations for thrombectomy devices--does it translate to humans?" Stroke **44**(6 Suppl 1): S7-S10.

Goyal, M., A. M. Demchuk, B. K. Menon, M. Eesa, J. L. Rempel, J. Thornton, D. Roy, T. G. Jovin, R. A. Willinsky, B. L. Sapkota, D. Dowlatshahi, D. F. Frei, N. R. Kamal, W. J. Montanera, A. Y. Poppe, K. J. Ryckborst, F. L. Silver, A. Shuaib, D. Tampieri, D. Williams, O. Y. Bang, B. W. Baxter, P. A. Burns, H. Choe, J. H. Heo, C. A. Holmstedt, B. Jankowitz, M. Kelly, G. Linares, J. L. Mandzia, J. Shankar, S. I. Sohn, R. H. Swartz, P. A. Barber, S. B. Coutts, E. E. Smith, W. F. Morrish, A. Weill, S. Subramaniam, A. P. Mitha, J. H. Wong, M. W. Lowerison, T. T. Sajobi, M. D. Hill and E. T. Investigators (2015). "Randomized assessment of rapid endovascular treatment of ischemic stroke." N Engl J Med **372**(11): 1019-1030.

Goyal, M., B. K. Menon, W. H. van Zwam, D. W. Dippel, P. J. Mitchell, A. M. Demchuk, A. Davalos, C. B. Majoie, A. van der Lugt, M. A. de Miquel, G. A. Donnan, Y. B. Roos, A. Bonafe, R. Jahan, H. C. Diener, L. A. van den Berg, E. I. Levy, O. A. Berkhemer, V. M. Pereira, J. Rempel, M. Millan, S. M. Davis, D. Roy, J. Thornton, L. S. Roman, M. Ribo, D. Beumer, B. Stouch, S. Brown, B. C. Campbell, R. J. van Oostenbrugge, J. L. Saver, M. D. Hill, T. G. Jovin and H. collaborators (2016). "Endovascular thrombectomy after large-vessel ischaemic stroke: a meta-analysis of individual patient data from five randomised trials." Lancet **387**(10029): 1723-1731.

Griessenauer, C. J., R. Gupta, S. Shi, A. Alturki, R. Motiei-Langroudi, N. Adeeb, C. S. Ogilvy and A. J. Thomas (2017). "Collar Sign in Incompletely Occluded Aneurysms after Pipeline Embolization: Evaluation with Angiography and Optical Coherence Tomography." AJNR Am J Neuroradiol **38**(2): 323-326.

Guerrero, B. P., C. D. Pacheco, A. Saied, K. Joshi, C. Rodriguez, M. Martinez-Galdamez and D. K. Lopes (2018). "First Human Evaluation of Endothelial Healing after a Pipeline Flex Embolization Device with Shield Technology Implanted in Posterior Circulation Using Optical Coherence Tomography." Neurointervention **13**(2): 129-132.

Herrmann, A. M., S. Meckel, M. J. Gounis, L. Kringe, E. Motschall, C. Mulling and J. Boltze (2019). "Large animals in neurointerventional research: A systematic review on models, techniques and their application in endovascular procedures for stroke, aneurysms and vascular malformations." J Cereb Blood Flow Metab **39**(3): 375-394.

Hopkins, L. N. and R. D. Ecker (2008). "Cerebral endovascular neurosurgery." Neurosurgery **62**(6 Suppl 3): 1483-1501; discussion 1501-1482.

Huang, D., E. A. Swanson, C. P. Lin, J. S. Schuman, W. G. Stinson, W. Chang, M. R. Hee, T. Flotte, K. Gregory, C. A. Puliafito and et al. (1991). "Optical coherence tomography." Science **254**(5035): 1178-1181.

Jeong, H. G., B. J. Kim, M. H. Yang, M. K. Han, H. J. Bae and S. H. Lee (2016). "Stroke outcomes with use of antithrombotics within 24 hours after recanalization treatment." Neurology **87**(10): 996-1002.

Jorgensen, L., A. G. Grothe, T. Larsen, R. L. Kinlough-Rathbone and J. F. Mustard (1986). "Injury to cultured endothelial cells by thrombin-stimulated platelets." Lab Invest **54**(4): 408-415.

Jovin, T. G., A. Chamorro, E. Cobo, M. A. de Miquel, C. A. Molina, A. Rovira, L. San Roman, J. Serena, S. Abilleira, M. Ribo, M. Millan, X. Urra, P. Cardona, E. Lopez-Cancio, A. Tomasello, C. Castano, J. Blasco, L. Aja, L. Dorado, H. Quesada, M. Rubiera, M. Hernandez-Perez, M. Goyal, A. M. Demchuk, R. von Kummer, M. Gallofre, A. Davalos and R. T. Investigators (2015). "Thrombectomy within 8 hours after symptom onset in ischemic stroke." N Engl J Med **372**(24): 2296-2306.

Jung, K. H. (2018). "New Pathophysiological Considerations on Cerebral Aneurysms." Neurointervention **13**(2): 73-83.

Kadirvel, R., Y. H. Ding, D. Dai, I. Rezek, D. A. Lewis and D. F. Kallmes (2014). "Cellular mechanisms of aneurysm occlusion after treatment with a flow diverter." Radiology **270**(2): 394-399.

Kallmes, D. F. (2012). "Point: CFD--computational fluid dynamics or confounding factor dissemination." AJNR Am J Neuroradiol **33**(3): 395-396.

Kallmes, D. F., R. Hanel, D. Lopes, E. Boccardi, A. Bonafe, S. Cekirge, D. Fiorella, P. Jabbour, E. Levy, C. McDougall, A. Siddiqui, I. Szikora, H. Woo, F. Albuquerque, H. Bozorgchami, S. R. Dashti, J. E. Delgado Almandoz, M. E. Kelly, R. t. Turner, B. K. Woodward, W. Brinjikji, G. Lanzino and P. Lylyk (2015). "International retrospective study of the pipeline embolization device: a multicenter aneurysm treatment study." AJNR Am J Neuroradiol **36**(1): 108-115.

Karmon, Y., R. Zivadinov, B. Weinstock-Guttman, K. Marr, V. Valnarov, K. Dolic, C. L. Kennedy, D. Hojnacki, E. M. Carl, J. Hagemeier, L. N. Hopkins, E. I. Levy and A. H. Siddiqui (2013). "Comparison of intravascular ultrasound with conventional venography for detection of extracranial venous abnormalities indicative of chronic cerebrospinal venous insufficiency." J Vasc Interv Radiol **24**(10): 1487-1498 e1481.

King, R. M., O. W. Brooks, E. T. Langan, J. Caroff, F. Clarencon, T. Tamura, J. M. Wainwright, M. J. Gounis, M. Marosfoi and A. S. Puri (2018). "Communicating malapposition of flow diverters assessed with optical coherence tomography correlates with delayed aneurysm occlusion." J Neurointerv Surg **10**(7): 693-697.

Kreitzer, N., P. Khatri, O. Adeoye, T. Abruzzo, A. Grossman, A. Ringer and J. Broderick (2016). "Abstract TP2: Heparin Use Across Major Endovascular Trials." Stroke **47**(suppl_1): ATP2-ATP2.

Lee, S. K., M. Mokin, S. W. Hetts, J. T. Fifi, M. G. Bousser, J. F. Fraser and S. Society of NeuroInterventional (2018). "Current endovascular strategies for cerebral venous thrombosis: report of the SNIS Standards and Guidelines Committee." J Neurointerv Surg **10**(8): 803-810.

Lindsberg, P. J. and H. P. Mattle (2006). "Therapy of basilar artery occlusion: a systematic analysis comparing intra-arterial and intravenous thrombolysis." Stroke **37**(3): 922-928.

Lindsberg, P. J., J. Pekkola, D. Strbian, T. Sairanen, H. P. Mattle and G. Schroth (2015). "Time window for recanalization in basilar artery occlusion: Speculative synthesis." Neurology **85**(20): 1806-1815.

Lindsberg, P. J. and D. Strbian (2015). "Recanalization of basilar artery occlusion." Ann Neurol **78**(5): 832-833.

Liu, X., G. Xu, Y. Liu, W. Zhu, M. Ma, Y. Xiong, W. Zi, Q. Dai, T. Leung, B. Yan, S. Davis, D. S. Liebeskind, V. M. Pereira, R. G. Nogueira and B. T. Investigators (2017). "Acute basilar artery occlusion: Endovascular Interventions versus Standard Medical Treatment (BEST) Trial-Design and protocol for a randomized, controlled, multicenter study." Int J Stroke **12**(7): 779-785.

Mack, J., W. Squier and J. T. Eastman (2009). "Anatomy and development of the meninges: implications for subdural collections and CSF circulation." Pediatr Radiol **39**(3): 200-210.

Martinez-Galdamez, M., J. Escartin, B. Pabon, C. Diaz, R. Martin-Reyes, A. Hermosin, E. Crespo, C. Rodriguez, G. Monedero, K. Joshi and D. K. Lopes (2019). "Optical coherence tomography: Translation from 3D-printed vascular models of the anterior cerebral circulation to the first human images of implanted surface modified flow diverters." Interv Neuroradiol **25**(2): 150-156.

Matsuda, Y., J. Chung and D. K. Lopes (2018). "Analysis of neointima development in flow diverters using optical coherence tomography imaging." J Neurointerv Surg **10**(2): 162-167.

Maus, V., A. Brehm, I. Tsogkas, S. Henkel and M. N. Psychogios (2019). "Stent retriever placement in embolectomy: the choice of the post-bifurcational trunk influences the first-pass reperfusion result in M1 occlusions." J Neurointerv Surg **11**(3): 237-240.

Mokin, M., P. Kan, A. A. Abla, T. Kass-Hout, K. V. Snyder, E. I. Levy and A. H. Siddiqui (2013). "Intravascular ultrasound in the evaluation and management of cerebral venous disease." World Neurosurg **80**(5): 655 e657-613.

Molyneux, A. J., R. S. Kerr, L. M. Yu, M. Clarke, M. Sneade, J. A. Yarnold, P. Sandercock and G. International Subarachnoid Aneurysm Trial Collaborative (2005). "International subarachnoid aneurysm trial (ISAT) of neurosurgical clipping versus endovascular coiling in 2143 patients with ruptured intracranial aneurysms: a randomised comparison of effects on survival, dependency, seizures, rebleeding, subgroups, and aneurysm occlusion." Lancet **366**(9488): 809-817.

Nogueira, R. G., A. P. Jadhav, D. C. Haussen, A. Bonafe, R. F. Budzik, P. Bhuva, D. R. Yavagal, M. Ribo, C. Cognard, R. A. Hanel, C. A. Sila, A. E. Hassan, M. Millan, E. I. Levy, P. Mitchell, M. Chen, J. D. English, Q. A. Shah, F. L. Silver, V. M. Pereira, B. P. Mehta, B. W. Baxter, M. G. Abraham, P. Cardona, E. Veznedaroglu, F. R. Hellinger, L. Feng, J. F. Kirmani, D. K. Lopes, B. T. Jankowitz, M. R. Frankel, V. Costalat, N. A. Vora, A. J. Yoo, A. M. Malik, A. J. Furlan, M. Rubiera, A. Aghaebrahim, J. M. Olivot, W. G. Tekle, R. Shields, T. Graves, R. J. Lewis, W. S. Smith, D. S. Liebeskind, J. L. Saver, T. G. Jovin and D. T. Investigators (2018). "Thrombectomy 6 to 24 Hours after Stroke with a Mismatch between Deficit and Infarct." N Engl J Med **378**(1): 11-21.

Pasarikovski, C. R., J. Cardinell and V. X. D. Yang (2019). "Perspective review on applications of optics in cerebral endovascular neurosurgery." J Biomed Opt **24**(3): 1-7.

Pasarikovski, C. R., L. da Costa, V. M. Pereira, J. Ramjist, Y. Dobashi and V. X. D. Yang (2019). "Optical coherence tomography–guided flow diversion for aneurysmal treatment." Neurology: Clinical Practice: 10.1212/CPJ.0000000000000729.

Pasarikovski, C. R., J. Keith, L. da Costa, J. Ramjist, Y. Dobashi, S. E. Black and V. X. D. Yang (2020). "Optical coherence tomography imaging after endovascular thrombectomy: a novel method for evaluating vascular injury in a swine model." J Neurosurg: 1-8.

Pasarikovski, C. R., J. C. Ku, J. Keith, J. Ramjist, Y. Dobashi, S. M. Priola, L. da Costa, A. Kumar and V. X. D. Yang (2020). "Mechanical thrombectomy and intravascular imaging for cerebral venous sinus thrombosis: a preclinical model." J Neurosurg: 1-6.

Pasarikovski, C. R., J. C. Ku, J. Keith, J. Ramjist, Y. Dobashi, S. M. Priola, L. da Costa and V. X. D. Yang (2020). "Endovascular Cerebral Venous Sinus Imaging with Optical Coherence Tomography." AJNR Am J Neuroradiol **41**(12): 2292-2297.

Pasarikovski, C. R., J. C. Ku, S. M. Priola, L. da Costa and V. X. D. Yang (2020). "Endovascular optical coherence tomography imaging in cerebrovascular disease." J Clin Neurosci **80**: 30-37.

Pasarikovski, C. R., J. Ramjist, L. da Costa, S. E. Black, J. Cardinell and V. X. Yang (2020). "Optical Coherence Tomography as an Adjunct During Carotid Artery Stenting for Carotid Atherosclerotic Disease." Clin Neuroradiol **30**(3): 503-509.

Pasarikovski, C. R., J. Ramjist, L. da Costa, S. E. Black and V. Yang (2019). "Optical coherence tomography imaging after endovascular thrombectomy for basilar artery occlusion: report of 3 cases." J Neurosurg: 1-6.

Patel, R. A. and C. J. White (2011). "Acute ischemic stroke treatment: State of the art." Vasc Med **16**(1): 19-28.

Pearson, J. D. (1999). "Endothelial cell function and thrombosis." Baillieres Best Pract Res Clin Haematol **12**(3): 329-341.

Perren, F., O. Kargiotis, J. M. Pignat and V. M. Pereira (2018). "Hemodynamic Changes May Indicate Vessel Wall Injury After Stent Retrieval Thrombectomy for Acute Stroke." J Neuroimaging **28**(4): 412-415.

Peschillo, S., F. Diana, J. Berge and P. Missori (2017). "A comparison of acute vascular damage caused by ADAPT versus a stent retriever device after thrombectomy in acute ischemic stroke: a histological and ultrastructural study in an animal model." J Neurointerv Surg **9**(8): 743-749.

Pierot, L. and C. Derdeyn (2015). "Interventionalist perspective on the new endovascular trials." Stroke **46**(6): 1440-1446.

Pierot, L., S. Soize, A. Benaissa and A. K. Wakhloo (2015). "Techniques for endovascular treatment of acute ischemic stroke: from intra-arterial fibrinolytics to stent-retrievers." Stroke **46**(3): 909-914.

Power, S., C. Matouk, L. K. Casaubon, F. L. Silver, T. Krings, D. J. Mikulis and D. M. Mandell (2014). "Vessel wall magnetic resonance imaging in acute ischemic stroke: effects of embolism and mechanical thrombectomy on the arterial wall." Stroke **45**(8): 2330-2334.

Powers, W. J., A. A. Rabinstein, T. Ackerson, O. M. Adeoye, N. C. Bambakidis, K. Becker, J. Biller, M. Brown, B. M. Demaerschalk, B. Hoh, E. C. Jauch, C. S. Kidwell, T. M. Leslie-Mazwi, B. Ovbiagele, P. A. Scott, K. N. Sheth, A. M. Southerland, D. V. Summers, D. L. Tirschwell and C. American Heart Association Stroke (2018). "2018 Guidelines for the Early Management of Patients With Acute Ischemic Stroke: A Guideline for Healthcare Professionals From the American Heart Association/American Stroke Association." Stroke **49**(3): e46-e110.

Prati, F., D. Capodanno, T. Pawlowski, V. Ramazzotti, M. Albertucci, A. La Manna, M. Di Salvo, R. J. Gil and C. Tamburino (2010). "Local delivery versus intracoronary infusion of abciximab in patients with acute coronary syndromes." JACC Cardiovasc Interv **3**(9): 928-934.

Radvany, M. G., J. Gomez and P. Gailloud (2011). "Intravascular ultrasound of the transverse sinus in two patients with pseudotumor cerebri: technical note." J Neurointerv Surg **3**(4): 379-382.

Reil, T. D., W. S. Moore, V. S. Kashyap, S. S. Nene, H. A. Gelabert and W. J. Quinones-Baldrich (2000). "The effects of thrombus, thrombectomy and thrombolysis on endothelial function." Eur J Vasc Endovasc Surg **19**(2): 162-168.

Renu, A., C. Laredo, A. Lopez-Rueda, L. Llull, R. Tudela, L. San-Roman, X. Urra, J. Blasco, J. Macho, L. Oleaga, A. Chamorro and S. Amaro (2017). "Vessel Wall Enhancement and Blood-Cerebrospinal Fluid Barrier Disruption After Mechanical Thrombectomy in Acute Ischemic Stroke." Stroke **48**(3): 651-657.

Roth, W., S. Morgello, J. Goldman, J. P. Mohr, M. S. Elkind, R. S. Marshall and J. Gutierrez (2017). "Histopathological Differences Between the Anterior and Posterior Brain Arteries as a Function of Aging." Stroke **48**(3): 638-644.

Saposnik, G., F. Barinagarrementeria, R. D. Brown, Jr., C. D. Bushnell, B. Cucchiara, M. Cushman, G. deVeber, J. M. Ferro, F. Y. Tsai, C. American Heart Association Stroke, E. the Council on and Prevention (2011). "Diagnosis and management of cerebral venous thrombosis: a statement for healthcare professionals from the American Heart Association/American Stroke Association." Stroke **42**(4): 1158-1192.

Saver, J. L., M. Goyal, A. Bonafe, H. C. Diener, E. I. Levy, V. M. Pereira, G. W. Albers, C. Cognard, D. J. Cohen, W. Hacke, O. Jansen, T. G. Jovin, H. P. Mattle, R. G. Nogueira, A. H. Siddiqui, D. R. Yavagal, B. W. Baxter, T. G. Devlin, D. K. Lopes, V. K. Reddy, R. du Mesnil de Rochemont, O. C. Singer, R. Jahan and S. P. Investigators (2015). "Stent-retriever thrombectomy after intravenous t-PA vs. t-PA alone in stroke." N Engl J Med **372**(24): 2285-2295.

Schonewille, W. J., C. A. Wijman, P. Michel, C. M. Rueckert, C. Weimar, H. P. Mattle, S. T. Engelter, D. Tanne, K. W. Muir, C. A. Molina, V. Thijs, H. Audebert, T. Pfefferkorn, K. Szabo, P. J. Lindsberg, G. de Freitas, L. J. Kappelle, A. Algra and B. s. group (2009). "Treatment and outcomes of acute basilar artery occlusion in the Basilar Artery International Cooperation Study (BASICS): a prospective registry study." Lancet Neurol **8**(8): 724-730.

Shindo, S., K. Fujii, M. Shirakawa, K. Uchida, Y. Enomoto, T. Iwama, M. Kawasaki, Y. Ando and S. Yoshimura (2015). "Morphologic Features of Carotid Plaque Rupture Assessed by Optical Coherence Tomography." AJNR Am J Neuroradiol **36**(11): 2140-2146.

Siddiqui, F. M., C. Banerjee, S. M. Zuurbier, Q. Hao, C. Ahn, G. L. Pride, M. Wasay, C. B. Majoie, D. Liebeskind, M. Johnson and J. Stam (2014). "Mechanical thrombectomy versus intrasinus thrombolysis for cerebral venous sinus thrombosis: a non-randomized comparison." Interv Neuroradiol **20**(3): 336-344.

Siddiqui, F. M., S. Dandapat, C. Banerjee, S. M. Zuurbier, M. Johnson, J. Stam and J. M. Coutinho (2015). "Mechanical thrombectomy in cerebral venous thrombosis: systematic review of 185 cases." Stroke **46**(5): 1263-1268.

Singer, O. C., J. Berkefeld, C. H. Nolte, G. Bohner, H. P. Haring, J. Trenkler, K. Groschel, W. Muller-Forell, K. Niederkorn, H. Deutschmann, T. Neumann-Haefelin, C. Hohmann, M. Bussmeyer, A. Mpotsaris, A. Stoll, A. Bormann, J. Brenck, M. U. Schlamann, S. Jander, B. Turowski, G. C. Petzold, H. Urbach, D. S. Liebeskind and E. S. Group (2015). "Mechanical

recanalization in basilar artery occlusion: the ENDOSTROKE study." Ann Neurol **77**(3): 415-424.

Singh, P., S. Doostkam, M. Reinhard, V. Ivanovas and C. A. Taschner (2013). "Immunohistochemical analysis of thrombi retrieved during treatment of acute ischemic stroke: does stent-retriever cause intimal damage?" Stroke **44**(6): 1720-1722.

Smith, G. A., P. Dagostino, M. G. Maltenfort, A. S. Dumont and J. K. Ratliff (2011). "Geographic variation and regional trends in adoption of endovascular techniques for cerebral aneurysms." J Neurosurg **114**(6): 1768-1777.

Stam, J., C. B. Majoie, O. M. van Delden, K. P. van Lienden and J. A. Reekers (2008). "Endovascular thrombectomy and thrombolysis for severe cerebral sinus thrombosis: a prospective study." Stroke **39**(5): 1487-1490.

Strbian, D., T. Sairanen, H. Silvennoinen, O. Salonen and P. J. Lindsberg (2014). "Intravenous thrombolysis of basilar artery occlusion: thrombus length versus recanalization success." Stroke **45**(6): 1733-1738.

Tearney, G. J., M. E. Brezinski, B. E. Bouma, S. A. Boppart, C. Pitris, J. F. Southern and J. G. Fujimoto (1997). "In vivo endoscopic optical biopsy with optical coherence tomography." Science **276**(5321): 2037-2039.

Tearney, G. J., E. Regar, T. Akasaka, T. Adriaenssens, P. Barlis, H. G. Bezerra, B. Bouma, N. Bruining, J. M. Cho, S. Chowdhary, M. A. Costa, R. de Silva, J. Dijkstra, C. Di Mario, D. Dudek, E. Falk, M. D. Feldman, P. Fitzgerald, H. M. Garcia-Garcia, N. Gonzalo, J. F. Granada, G. Guagliumi, N. R. Holm, Y. Honda, F. Ikeno, M. Kawasaki, J. Kochman, L. Koltowski, T. Kubo, T. Kume, H. Kyono, C. C. Lam, G. Lamouche, D. P. Lee, M. B. Leon, A. Maehara, O. Manfrini, G. S. Mintz, K. Mizuno, M. A. Morel, S. Nadkarni, H. Okura, H. Otake, A. Pietrasik, F. Prati, L. Raber, M. D. Radu, J. Rieber, M. Riga, A. Rollins, M. Rosenberg, V. Sirbu, P. W. Serruys, K. Shimada, T. Shinke, J. Shite, E. Siegel, S. Sonoda, M. Suter, S. Takarada, A. Tanaka, M. Terashima, T. Thim, S. Uemura, G. J. Ughi, H. M. van Beusekom, A. F. van der Steen, G. A. van Es, G. van Soest, R. Virmani, S. Waxman, N. J. Weissman, G. Weisz and T. International Working Group for Intravascular Optical Coherence (2012). "Consensus standards for acquisition, measurement, and reporting of intravascular optical coherence tomography studies: a report from the International Working Group for Intravascular Optical Coherence Tomography Standardization and Validation." J Am Coll Cardiol **59**(12): 1058-1072.

Teng, D., J. S. Pannell, R. C. Rennert, J. Li, Y. S. Li, V. W. Wong, S. Chien and A. A. Khalessi (2015). "Endothelial trauma from mechanical thrombectomy in acute stroke: in vitro live-cell platform with animal validation." Stroke **46**(4): 1099-1106.

Tereshchenko, A. S., V. M. Mironov, E. V. Merculov and A. N. Samko (2013). "[Basic principles of optical coherence tomography in interventional cardiology]." Vestn Rentgenol Radiol(6): 67-72.

Tsumoto, T., T. Miyamoto, M. Shimizu, Y. Inui, K. Nakakita, S. Hayashi and T. Terada (2003). "Restenosis of the sigmoid sinus after stenting for treatment of intracranial venous hypertension: case report." Neuroradiology **45**(12): 911-915.

Uemura, S., K. Ishigami, T. Soeda, S. Okayama, J. H. Sung, H. Nakagawa, S. Somekawa, Y. Takeda, H. Kawata, M. Horii and Y. Saito (2012). "Thin-cap fibroatheroma and microchannel findings in optical coherence tomography correlate with subsequent progression of coronary atheromatous plaques." Eur Heart J **33**(1): 78-85.

van Andel, C. J., P. V. Pistecky and C. Borst (2003). "Mechanical properties of porcine and human arteries: implications for coronary anastomotic connectors." Ann Thorac Surg **76**(1): 58-64; discussion 64-55.

van der Hoeven, E. J., W. J. Schonewille, J. A. Vos, A. Algra, H. J. Audebert, E. Berge, A. Ciccone, M. Mazighi, P. Michel, K. W. Muir, V. Obach, V. Puetz, C. A. Wijman, A. Zini, J. L. Kappelle and B. S. Group (2013). "The Basilar Artery International Cooperation Study (BASICS): study protocol for a randomised controlled trial." Trials **14**: 200.

van Houwelingen, R. C., G. J. Luijckx, A. Mazuri, R. P. Bokkers, O. S. Eshghi and M. Uyttenboogaart (2016). "Safety and Outcome of Intra-Arterial Treatment for Basilar Artery Occlusion." JAMA Neurol **73**(10): 1225-1230.

Vernooij, M. W., M. A. Ikram, H. L. Tanghe, A. J. Vincent, A. Hofman, G. P. Krestin, W. J. Niessen, M. M. Breteler and A. van der Lugt (2007). "Incidental findings on brain MRI in the general population." N Engl J Med **357**(18): 1821-1828.

Vignes, J. R., A. Dagain, J. Guerin and D. Liguoro (2007). "A hypothesis of cerebral venous system regulation based on a study of the junction between the cortical bridging veins and the superior sagittal sinus. Laboratory investigation." J Neurosurg **107**(6): 1205-1210.

Vuong, B., H. Genis, R. Wong, J. Ramjist, J. Jivraj, H. Farooq, C. Sun and V. X. Yang (2014). "Evaluation of flow velocities after carotid artery stenting through split spectrum Doppler optical coherence tomography and computational fluid dynamics modeling." Biomed Opt Express **5**(12): 4405-4416.

Wang, J., H. Q. Tan, M. H. Li, X. J. Sun, C. M. Fu, Y. Q. Zhu, B. Zhou, H. W. Xu, W. Wang and B. Xue (2010). "Development of a new model of transvenous thrombosis in the pig superior sagittal sinus using thrombin injection and balloon occlusion." J Neuroradiol **37**(2): 109-115.

Wengrovitz, M., D. A. Healy, R. R. Gifford, R. G. Atnip and B. L. Thiele (1995). "Thrombolytic therapy and balloon catheter thrombectomy in experimental femoral artery thrombosis: effect on arterial wall morphology." J Vasc Interv Radiol **6**(2): 205-210.

Writing Group, M., D. Mozaffarian, E. J. Benjamin, A. S. Go, D. K. Arnett, M. J. Blaha, M. Cushman, S. R. Das, S. de Ferranti, J. P. Despres, H. J. Fullerton, V. J. Howard, M. D. Huffman, C. R. Isasi, M. C. Jimenez, S. E. Judd, B. M. Kissela, J. H. Lichtman, L. D. Lisabeth, S. Liu, R. H. Mackey, D. J. Magid, D. K. McGuire, E. R. Mohler, 3rd, C. S. Moy, P. Muntner, M. E. Mussolino, K. Nasir, R. W. Neumar, G. Nichol, L. Palaniappan, D. K. Pandey, M. J. Reeves, C.

J. Rodriguez, W. Rosamond, P. D. Sorlie, J. Stein, A. Towfighi, T. N. Turan, S. S. Virani, D. Woo, R. W. Yeh, M. B. Turner, C. American Heart Association Statistics and S. Stroke Statistics (2016). "Executive Summary: Heart Disease and Stroke Statistics--2016 Update: A Report From the American Heart Association." Circulation **133**(4): 447-454.

Xu, X., M. Li, R. Liu, Q. Yin, X. Shi, F. Wang, J. Gao, G. Xu, R. Ye and X. Liu (2020). "Optical coherence tomography evaluation of vertebrobasilar artery stenosis: case series and literature review." J Neurointerv Surg.

Yamaguchi, T., M. Terashima, T. Akasaka, T. Hayashi, K. Mizuno, T. Muramatsu, M. Nakamura, S. Nakamura, S. Saito, M. Takano, T. Takayama, J. Yoshikawa and T. Suzuki (2008). "Safety and feasibility of an intravascular optical coherence tomography image wire system in the clinical setting." Am J Cardiol **101**(5): 562-567.

Yan, F., G. Rajah, Y. Ding, Y. Hua, H. Zhang, L. Jiao, G. Li, M. Ren, R. Meng, F. Lin and X. Ji (2019). "Safety and efficacy of intravascular ultrasound as an adjunct to stenting for cerebral venous sinus stenosis-induced idiopathic intracranial hypertension: a pilot study." J Neurosurg: 1-6.

Yin, N. S., S. Benavides, S. Starkman, D. S. Liebeskind, J. A. Saver, N. Salamon, R. Jahan, G. R. Duckwiler, S. Tateshima, F. Vinuela, P. M. Vespa, D. J. Chute and H. V. Vinters (2010). "Autopsy findings after intracranial thrombectomy for acute ischemic stroke: a clinicopathologic study of 5 patients." Stroke **41**(5): 938-947.

Yuki, I., I. Kan, A. Golshan, J. Sohn, Y. Murayama, H. V. Vinters and F. Vinuela (2013). "A swine model to analyze arterial structural changes induced by mechanical thrombectomy." AJNR Am J Neuroradiol **34**(8): E87-90.